INVESTIGATION ON HEAT TRANSFER IN CONICAL COILED HEAT EXCHANGERS

Thesis

submitted for the award of the degree

of

Doctor of Philosophy

By

Mr. Purandare Pramod Shripad
Registration No: 950908018

Under the guidance of

Dr. Raj Kumar Gupta
Associate Professor,
Department of Chemical Engineering
Thapar University, Patiala
Patiala- 147004

Dr. Mandar M. Lele
Professor
Department of Mechanical Engineering
MIT College of Engineering
Pune- 411038

DEPARTMENT OF MECHANICAL ENGINEERING

THAPAR UNIVERSITY, PATIALA

PATIALA - 147004, INDIA

CERTIFICATE

This is to certify that thesis entitled **"Investigation on Heat Transfer in Conical Coiled Heat Exchangers"**, being submitted by Mr. Purandare Pramod Shripad, to the Department of Mechanical Engineering, Thapar University, Patiala, in partial fulfillment for award of the degree of **Doctor of Philosophy**, is a record of bonafide research work carried out by him. Mr. Purandare Pramod Shripad has worked under our guidance and supervision and has fulfilled the requirements for the submission of this thesis, which to our knowledge has reached the requisite standards.

The results embodied in the thesis have not been submitted in the part of full to any other university or institute for the award of any diploma or degree.

Dr. Raj Kumar Gupta
Associate Professor,
Department of Chemical Engineering
Thapar University, Patiala
Patiala- 147004

Dr. Mandar M. Lele
Professor
Department of Mechanical Engineering
MIT College of Engineering
Pune- 411038

ACKNOWLEDGEMENT

I would like to express my deepest gratitude to my mentors and academic advisors **Dr. Mandar M. Lele** and **Dr. Raj Kumar Gupta** for their valuable guidance and support. I am thankful for all the time and effort they spent to guide me during this study. I appreciate their continued encouragement and valuable insights during my doctoral program. Their support during and beyond my studies is an asset that I will continue to depend on.

I expresses deep sense of gratitude to **Dr. Prakash Gopalan** (Director, Thapar University), **Dr. O. P. Pandey** (Dean, Research and Sponsored Projects, Thapar University), for their support at all levels. I would like to express my sincere thanks to **Dr. S. K. Mohapatra**, (HOD, Mechanical Engineering, Thapar University and the members of Doctoral Committee), for their support, guidance and constructive feedback during the progress reviews.

This work would have not been completed without the support that I received from many individuals at VIIT, Pune and Thapar University, Patiala. Particularly thanks are due to **Hon. Shri Rajkumarji Agarwal** and **Shri Bharatji Agarwal,** Trustees of BRACT's, Pune, for their kind approvals. I am also thankful to **Prof. M. R. Khadilkar, Prof. S. M. Umrani, Dr. Mrs. B. S. Karkare, Dr. A. S. Abhyankar. Dr. Y. H. Dandawate, Dr. S. N. Londhe** for being instrumental in providing this opportunity. My special thanks to **Dr. R. R. Kulkarni, Prof. A. P. Kulkarni, Prof. A. R. Deshpande,** for their continuous support during experimentation and analysis. Special thanks to **Mr. Adsul S. S., Mr. Kharade D. J.** and many others who helped me during this work.

Last but not the least, I am thankful to my wife **Mrs. Jyoti Purandre** and my kids **Abhijeet** and **Ayush** for their support and considerate approach without which this work would have not been possible. I greatly appreciate their patience and understanding. I am also thankful to my family members specially **Mr. Deepak S. Purandare** for extending timely and valuable support and encouragement.

Purandare Pramod Shripad

ABSTARCT

The extensive use of heat exchangers in industries necessitates the high performance and compact sizes of the heat exchangers. With this necessity in industrial applications, various techniques are used to enhance the heat transfer. Some techniques are concerned with the modification in geometry or surface (passive); whereas, some others use an external power source (active). The selection of the proper heat transfer enhancement technique is important for efficient heat transfer.

In passive techniques, the coiled tubes are most widely used. The coils accommodate large heat transfer area in a small volume, and have high heat transfer coefficients. The commonly used configurations in coiled type heat exchangers are helical coil configuration and conical coil configuration. The studies related to heat transfer and pressure drop for these configurations are very important for their selection for a given application. In the literature many studies are available on helical coils, and a few are available on spiral coils. Each one of these configurations has certain advantages and limitations.

Conical coil is a coil that has a specified cone angle. These coils may offer the combination of advantages (high heat transfer coefficient, compact size, operations at high temperature, reduced induced stresses, elimination of expansion joints, high pressure capability, reduced fouling tendency, modular design) offered by helical and spiral coils. The conical coil with cone angle 0^O is known as helical coil whereas the one with cone angle 180^O is considered as spiral coil configuration.

The present work aims to carry out heat transfer and pressure drop analysis for conical coil heat exchangers. The analysis is carried out using fifteen coils of five different cone angles (0^O *(helical)*, 45^O, 90^O, 135^O *and (spiral)* 180^O) and three different tube sizes (8×10, 10×12 and 12×15). The coils were fabricated in-house and used in a specially designed heat exchanger test setup for the experimentation. This work is the first attempt to study the heat transfer in conical coil heat exchangers. The empirical correlations developed provide a basis to evaluate heat transfer coefficient for heat exchanger designers.

Heat transfer coefficient, based on the overall temperature difference, is calculated using the 'Wilson plot method'. The effect of flow rates (Q_h and Q_c), effect of flow ratio (Q_h/Q_c), effect of cone angle (θ), and effect of tube diameter on heat transfer coefficient are studied. Heat exchanger's effectiveness as a function of flow ratio is predicted, which can be used to predict outlet temperature of the shell side and tube side fluid. The correlations for *Nu* as a function of flow parameter (*Re/De*), fluid parameter (*Pr*) and coil parameter (δ) are proposed.

The friction factor is calculated by conventional Darcy-Weisbach equation. The effect of tube side flow (*Re*) on friction factor (f) for different cone angles (θ) and different tube diameters (d_i) is studied.

The results show that *Nu* increases with increase in tube side flow (Q_h) and flow ratio (Q_h/Q_c), whereas it reduces with increase in shell side flow (Q_c), cone angle (θ) and tube diameter (d). Also, the friction factor (f) increases with cone angle (θ) and decreases with increase in tube side flow (Q_h) and tube diameter (d).

PUBLICATIONS

International Journals

A) SCI Listed

1. Pramod S. Purandare, Mandar M. Lele, Raj Kumar Gupta, "Experimental investigation on heat transfer in conical coil heat exchanger with 90^{O} cone angle", *Heat and Mass Transfer*, Vol. 51, Issue-3, March 2015, pp. 373-379, Springer, DOI 10.1007/s00231-014-1418-x, **(SCI impact factor 0.946)**

2. Pramod S. Purandare, Mandar M. Lele, Raj Kumar Gupta, "Experimental investigation on heat transfer and pressure drop of conical coil heat exchanger with parameters tube diameter, fluid flow rates and cone angle", *Thermal Science*, *Vinca Inst. of Nucl. Sci. Serbia*, online first from Nov. 2014, DOI: 10.2298/ TSCI140802137P, **(SCI impact factor 1.22)**

3. Pramod S. Purandare, Mandar M. Lele, Raj Kumar Gupta, "Investigation on thermal analysis of conical coil heat exchanger", *International Journal of Heat and Mass Transfer,* Vol. 90, Nov. 2015, pp. 1188 - 1196 *Elsevier*, DOI: 10.1016/ j.ijheatmasstransfer.2015:07.044, **(SCI impact factor 2.383)**

B) Non- SCI

1. Pramod S. Purandare, Mandar M. Lele, Raj Kumar Gupta, "Effect of geometric and operating parameters on performance of helical coil heat exchanger", *International Reviews of Mechanical Engineering, Prize Worthy Prize*, vol. 7(1), Jan 2013, pp.105-109

2. Pramod S. Purandare, Mandar M. Lele, Raj Kumar Gupta, "Parametric analysis of helical coil heat exchanger", Int. Jour. of Engineering Science and Technology, vol. 1 (2), Oct 2012

TABLE OF CONTENTS

LIST OF FIGURES

LIST OF TABLES

NOMENCLATURE

A_c	Cross section area of pipe, m^2
C	Heat capacity of fluid, $kW.K^{-1}$
c_p	Specific heat, $kJ.kg^{-1}.K^{-1}$
d	Tube diameter, m
D	Coil diameter, m
D_h	Hydraulic diameter, m
f	friction factor
h	Heat transfer coefficient, $Wm^{-2}K^{-1}$
k	Thermal conductivity, $Wm^{-1}K^{-1}$
L	Tube length, m
LMTD	Log mean temperature difference
m	Mass of water, kg
Q	Volume flow rate, $m^3.s^{-1}$
q	Heat transfer rate, W
r	Tube radius, m
R	Radius of curvature, m
T	Temperature, K
U	Overall heat transfer coefficient, $W.m^{-2.}K^{-1}$
v	Average axial velocity of water, $m.s^{-1}$
ε	Effectiveness
Nu	Nusselt number based on h_i
Re	Reynolds number
Pr	Prandtl number
De	Dean number
Gz	Graetz number
Eu	Euler number
CFD	Computational fluid dynamics
FEM	Finite element method
FDM	Finite difference method

Subscripts

c	Cold fluid
cr	Critical
h	Hot fluid
i	Inside condition
m	Mean
o	Outside condition
s	Straight tube

Greek Letters

δ	Curvature ratio, *r/R*
ρ	Density, $kg.m^{-3}$
μ	Viscosity, $Ns.m^{-2}$
Θ	Cone angle, *rad*

Constants

C, n	Constants for tube side heat transfer coefficient *(eq. 4.8)*
a, b	Constant for effectiveness correlation *(eq. 5.1)*
a_1, a_2, a_3, a_4,	Constants for *Nu-Pr* correlations *(eq. 5.2)*
b_1, b_2, b_3	Constants for *Nu-Pr* correlations *(eq. 5.3)*
c_1, c_2, c_3	Constants for friction factor (*f*) correlations *(eq. 5.5)*
m_1, m_2, m_3, m_4	Constants for friction factor (*f*) correlations *(eq. 5.4)*

Chapter 1

Introduction

Heat exchangers are extensively used in the industries for a variety of industrial applications like, refrigeration and air-conditioning, steam power plants, nuclear reactors, chemical and food processing industries, and medical equipment [1-6]. Enhancement (augmentation or intensification) in heat transfer coefficient improves the performance of a heat exchanger and reduces surface area required for heat transfer. Various heat transfer enhancement techniques are reported in literature. In general these heat transfer enhancement techniques are of three types viz. active, passive and compound techniques [7-9].

1.1 Passive techniques

The techniques that do not need any input of external power directly are known as passive techniques. These techniques use the power from the system itself that increases the pressure drop in the system. The passive techniques generally use the concept of modification in geometry or flow surface by incorporating different types of inserts or additional devices. These increases heat transfer coefficients by changing the existing flow pattern. Some of these techniques are listed below:

1. *Tubes in coiled form***:** The secondary flow produced in the curved tube promotes heat transfer coefficient. These configurations have many applications in single phase and in boiling regions (phase change). These are relatively compact heat exchangers shell and tube heat exchangers.
2. *Treating the surfaces:* In this technique the surfaces are treated to have fine scale alteration by surface treatment or by applying different types of coatings. The surface treating or coating may be over the complete surface or in patches. These techniques are generally used for condensation and boiling.
3. *Rough surfaces:* The turbulence increase with surface modifications in the flow field in single phase flows. The surface area for heat transfer remains unaltered. Different methods are used to develop the rough surfaces from variety of sand grain to discrete protuberances.
4. *Use of extended surfaces:* Introduction of the extended surfaces provides the effective enhancement in heat transfer. The developments in the introduction of different type of extended surfaces lead to modified flow. This modified flow field with increased surface area for heat transfer due to fins enhances the heat transfer

coefficient. The development of non-conventional extended surfaces, such as integral inner and outer finned tubing improves the heat transfer coefficients.

5. *Use of the displaced enhancement devices:* The displaced enhancement devices are the different types of inserts that are used in confined situations of forced convection flow. These devices displace the fluid from heated or cooled surfaces from the core flow of the duct that helps to increase the heat transfer in the heat exchanger.
6. *Use of swirl-flow devices:* The flow in the form of swirl flow or recirculation flow like secondary flow is produced by theses type of devices in the axial flow field. The number of geometric alterations like twisted tube, corrugated tube etc. or different tube inserts to create rotating and/or secondary flow; vortex generators, inserts like twisted-tape, and screw-type axial-core inserts. These devices can find the application like single phase and phase change applications.
7. *Use of different surface-tension devices:* These devices generally refer to surface wicking or surface grooving which improves the surface tension in the fluid flow. These surface tension devices improve find their application particularly in boiling and condensation.
8. *Use of additives for liquids:* Different additives in the form of suspended solids, soluble particles which can be traced and gas bubbles in single phase fluid flow are used in this technique. Using these adhesives surface tension reduces which increase the heat transfer in boiling systems.
9. *Use of additives for gases:* These are the solid particles or droplets of liquid that are added in single-phase gas flows either in dilute form (gas in solid suspensions) or in dense form (fluidized bed systems).

1.2 Active techniques

The techniques that need direct input of external power for heat transfer enhancement are known as active techniques. In these techniques, use of external power is made to facilitate the flow modification as desired. These techniques enhance the heat transfer rate. Some of the techniques are listed below:

1. *Use of mechanical aids:* The different instruments like rotating surfaces or mechanical means are used to stir the fluid to improve the mixing. Scrapped

surface and Rotating surface tube type heat exchangers and type heat and mass exchangers are the examples of these techniques.

2. *Surface vibration:* The vibration of surface at low or high frequency changes the flow field which enhances the heat transfer. These techniques are generally used to improve heat transfer in single-phase flows.
3. *Fluid vibration:* In this type of method particle vibrations are used to change the flow field. This change in flow field enhances the heat transfer. In these type heat exchangers the vibrations are given to either fluid or surface of both.
4. *Use of electrostatic fields (dc or ac):* In this form of enhancement technique the electric field or magnetic fields or combination of these two from are used to change the flow field which is useful for the enhancement. The electric or magnetic fields are applied in heat exchange systems. It can produce forced convection or electromagnetic pumping and greater bulk mixing that enhances the heat transfer.
5. *Use of injection involves:* Injection involves injecting same type of fluid in the upstream of the heat transfer section or supplying gas to liquid through a porous surface of heat transfer. Similar to gas injection surface degassing of liquids produce enhancement.
6. *Use of suction:* Fluid is withdrawn from single-phase flow through a porous heated surface or vapors are removed through a porous heated surface in nucleate or film boiling applications.
7. *Use of Jet impingement:* In this method the directions of heating or cooling fluid flow in perpendicular or oblique to the heat transfer surface decides the amount of enhancement.

1.3 Compound techniques

When any two or more enhancement techniques are used simultaneously to achieve more heat transfer it is known as compound technique. With the compound technique; the enhancement is more than that produced by either of the technique when used individually. Similarly the compound techniques have limited applications because of the complexity involved.

Many researchers proved the importance of various heat transfer enhancement techniques for the different applications in the industries. Fair attention is paid by researchers towards the passive techniques because of self-enhancing aspect and less requirement of servicing in the applications.

A coiled or curved tube is a swirl producing geometry where the secondary fluid motion is generated by the continuous curvature of tube that changes the direction of fluid flow. This results in local deflection of fluid flow velocity. It has been reported that the helical coil tube heat exchangers gives higher heat transfer coefficient with compact structure. Many investigators reported the flow pattern in helical coiled tube that is complicated due to the formation of secondary flow induced by centrifugal force. Secondary flow is the result of difference between the local velocity of fluid particles at tube core and fluid particles close to the tube inner wall. The fluid particles close to the wall have the boundary layer with lower axial velocity and lower centrifugal action, whereas, higher axial velocity and centrifugal action is observed in fluid particles away from the tube wall. Since velocity is highest at the center, it is subjected to maximum centrifugal action which pushes the fluids towards the tube wall to set the secondaries in the tube.

Several studies by different researchers have indicated that in heat transfer applications helical coil tube heat exchangers are superior to straight tubes. The enhancement in the heat transfer rate is due to the secondary flow developed in the fluid flowing through the curved tube. These secondaries are due to the centrifugal force acting on the fluid particles when it flows through curvature. The flow phenomenon especially in laminar flow regime is more beneficial. Jeschke [10] observed the significant difference in the heat transfer coefficient in his study on coiled tubes and straight tubes heat transfer analysis. The factor base parameter on curvature ratio (δ) was proposed as:

$$Nu_c = Nu_s[1 + 3.5(r/R)] \qquad \text{------ } 1.1$$

In the sequential study by Seban and McLaughlin [11], he shows that this factor i.e. (1 + 3.5 (r / R)) was not accurate and noted that more enhancement could be attained in the heat transfer coefficient.

It is observed in the literature that [12], the coiled tube configuration has emerged as an important passive heat transfer enhancement technique. In applications, the coiled tube configurations are popular in heat transfer equipments because of following advantages:

1. *High heat transfer coefficient:* Due to secondary flow in the tube, tube side fluid mixed properly in the tube and second important reason is that the secondaries set in the tube reduces the laminar boundary layer developed inside the tube surface effects in high heat transfer coefficient.
2. *Compact size:* As heat transfer coefficient increases, size of the heat exchanger reduces and system becomes more compact.
3. *Operations at high temperature:* As coils are developed in a single seamless tube, these may be used at higher temperatures. These can handle thermal shocks very easily as well as handles extreme temperature difference.
4. *Reduced induced stresses:* As single seamless tube is used for the development of the coils and the coil itself easily accommodates thermal expansion, resulting into reduced induced stresses.
5. *Elimination of expansion joints:* Thermal expansion of the tube can be very easily accommodated by coils itself so the costlier expansion joints are considerably reduced.
6. *High pressure capability:* Coils are developed with single seamless tube; due to which high pressure can be very easily handled.
7. *Reduced fouling tendency:* As secondary flows are developed in coiled geometry the turbulence in the tube gets increased, which increases the cleaning tendency of the tube and reduces the fouling tendency.
8. *Modular design:* As each coil is to be developed separately in separate module. It provides the advantages of the modular design.

Helical coil configuration is very popular for various applications such as reactors and heat exchangers because in small volume this type of heat exchangers accommodates a large heat transfer area, with high heat transfer coefficients and time distributions with narrow residence. The extensive use of helical and spiral coiled heat exchangers in the industry requires the data about heat transfer, pressure drop and flow patterns for these exchangers.

1.4 Helical and spiral coil heat exchangers

In applications the most frequently used configuration is helical and spiral coiled tube is in shell and coiled tube heat exchanger (Fig. 1.1). These coiled tube configurations find wide use in applications because of the several advantages like high heat transfer coefficients, compact structure, reduced fouling tendency and modular design.

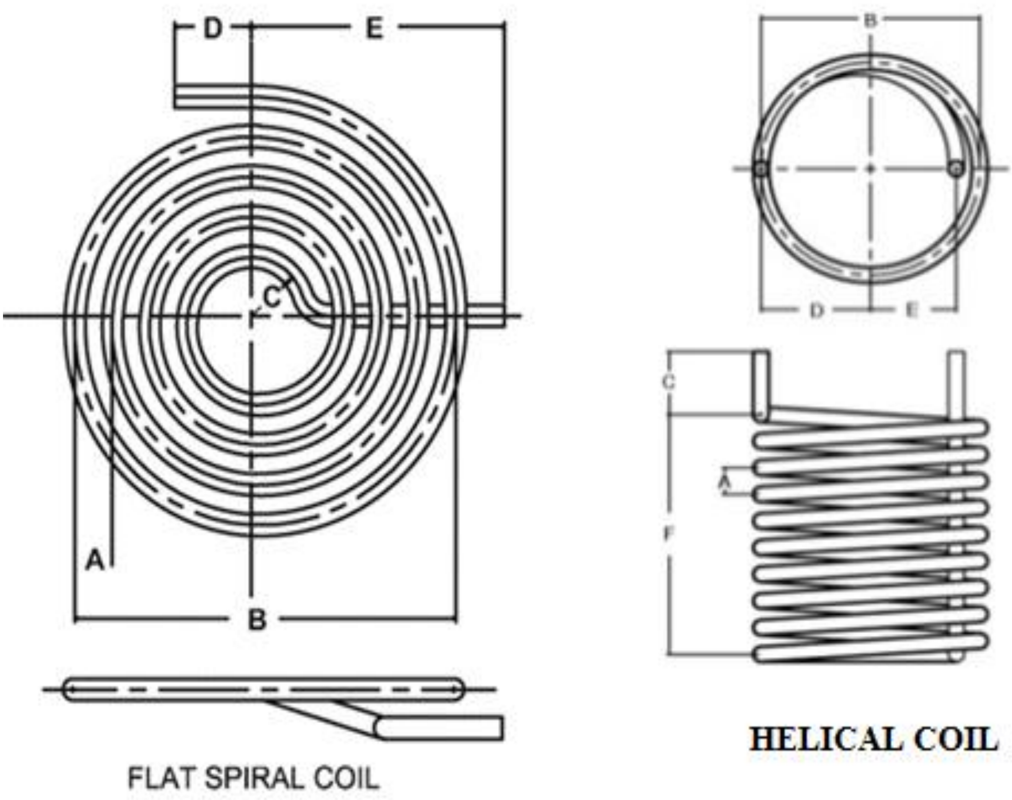

Fig. 1.1 Spiral and helical coiled tubes for heat exchanger [13]

The enhancement in heat transfer coefficient in the coiled tube is due to the secondaries developed in the tube. The secondary flow pattern is developed perpendicular to the main axis due to centrifugal forces acting on the flowing fluid (Figure 1.2). In this secondary flow pattern two vortices are developed. The fluid moves along the vortices from the inner wall of the tube across the center of the tube to the outer wall. After reaching the outer wall the fluid follows the wall and travel back to inner wall. The secondary flow moves the fluid across the temperature gradient causing an increase in the heat transfer rates. Thus, there is an additional heat transfer based on convective heat transfer mechanism, caused by the flow perpendicular to the axial flow, that supplements the conventional mechanism in straight tube heat exchangers (except that produced by buoyancy forces).

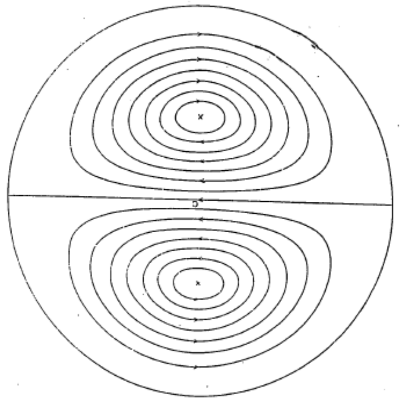

Fig. 1.2 Secondary flow developed in the curved tube [14]

The intensity of secondary flow developed in the curved tube is a function of the two parameters: coil diameter (*D*) and tube diameter (*d*) [15, 16]. This phenomenon is beneficial particularly in laminar flow range. For the small coils and tube diameters the intensities of secondaries developed are high. This allows better mixing of the fluid and heat transfer coefficient (h_i) gets improved for the same flow rate. As coil diameter goes on increasing the intensity of secondaries developed reduces, this reduces heat transfer coefficient (h_i).

In case of helical coil heat exchanger the coil diameter remains same and the intensity of secondaries developed does not change along the length of tube. The overall effect is constant h_i over the entire length of coiled tube of a given diameter. In spiral coiled configuration the diameter of the coil continuously changes from innermost to the outermost section which alters the local h_i from innermost to the outermost section. At the innermost section of spiral coil, h_i is considerably higher than at the outermost section.

Secondaries developed in the coil influences the pressure drop (ΔP) across the coil. As intensity of secondary flow increases the pressure drop increases. Due to higher intensity of secondary flow, the flow pattern in the tube changes, this reduces the laminar boundary layer development in the coiled tube and increases the pressure drop. Helical coil shows the lesser pressure drop than spiral coil configuration for the same mean coil diameter because of constant coil diameter of helical coil and variable in spiral coil.

In the comparison of helical and spiral coiled configuration it is observed that the performance of helical coils are more superior in terms of heat transfer and shell side pressure drop; whereas, compactness and the bypass factor are the advantages that the spiral coils offer.

1.4 Conical coil heat exchangers

The configuration specified in the present work, known as conical coiled configuration (CCC), is a combination of helical and spiral coiled configurations. The conical coil configuration is shown in Fig. 1.3.

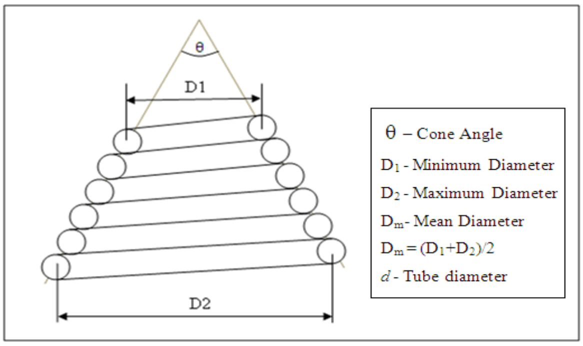

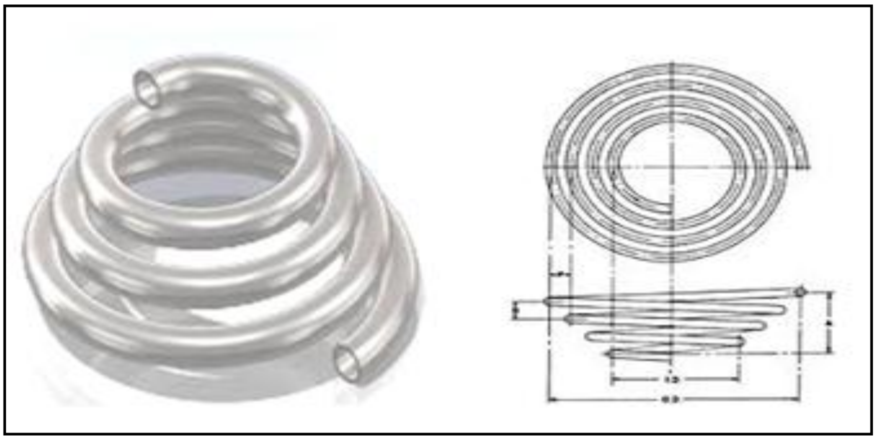

Fig. 1.3 Conical coil configuration for heat exchanger [13]

The two extreme angles of the conical coil configurations are 0^{O} (helical coil) and the 180^{O} (spiral coil). As cone angle changes from 0^{O} to 180^{O}, the performance of the conical coil heat exchanger also changes from helical coil to the spiral coil heat exchanger.

The conical coil configuration has higher heat transfer coefficient and less pressure drop as compared to the spiral coil whereas, it is more compact than the helical coil heat exchanger. In heat transfer applications, helical coil configuration shows maximum fluid bypass and less pressure drop whereas spiral coil shows minimum bypass and maximum pressure drop across the coil [12]. In conical coil fluid bypass is less than helical coil and pressure drop is less than spiral coil configuration. Due to these advantages, it may be considered as an alternative for the analysis of heat transfer application.

In the literature much efforts are devoted on the analysis of the helical coil heat exchangers, where as no data is available for the analysis of conical coil configuration. This is the first attempt to study the effect of cone angle on thermal performance for the application with flow rates in laminar section ($Re < Re_{critical}$).

The present work aims to carry out experimental analysis of conical coil heat exchangers, in terms of the heat transfer and pressure drop characteristics, with respect to geometric and operating parameters. The geometric parameters selected for the study are tube diameter (d_i), coil diameter (D), cone angle (θ). The operating parameters selected are mass flow rates of the shell side (m_c) and tube side (m_h) fluids and inlet temperatures of shell side and tube side fluids. Also, the functional relationships between Nu and flow parameter (Re), fluid parameter (Pr) and geometric parameter (δ), and f and flow parameter (Re) are proposed.

1.5 Organization of thesis

The thesis is organized in six chapters. The first chapter introduces heat transfer enhancement techniques the coiled tube heat exchanger and the advantages that these exchangers offer. This is followed by consecutive topics of literature review. In this chapter the contribution of different researchers on various aspects of the heat transfer in coil tube heat exchangers are discussed. The flow pattern in curved tubes, heat transfer characteristics of helical and spiral tube heat exchanger, pressure drop and friction factor across the helical coil heat exchanger, critical Re, influence of pitch in helical coil heat exchanger and applications of coiled tube heat exchangers are discussed. Chapter 3 gives various geometric and operating parameters selected for the present study. It also includes coil fabrication methodology, details of experimental setup and experimental procedure used for the present study. Chapter 4 gives the methodology adopted for the experimental data analysis. It includes the analysis for obtaining the heat transfer coefficient and friction factor for conical coil configuration. The uncertainty analysis of the experimental observations is also predicted. Results are discussed in Chapter 5. This chapter comprises of three different sections: (a) thermal analysis, (b) pressure drop analysis and (c) heat transfer enhancement as compared with straight tube heat exchangers. Chapter 6 comprises of the conclusions that are drawn from the present work for conical coil configuration. The recommendations for the future work are also included at the end.

Chapter 2

Literature Review

The effective design of heat exchangers requires considerations of simultaneous improvement of the heat transfer performance and reduction in the pressure drop. Enhancement in heat transfer coefficients has an important relation with improvement in heat transfer performance of heat exchangers. Modifications made to improve heat transfer coefficient generally costs in increased pressure drop in the heat exchanger [17]. Thus the important consideration in design of a heat exchanger is the selection of most appropriate configuration.

Heat exchangers are used extensively in variety of applications, like chemical processing, nuclear reactors, power plants, heat recovery systems, food industries and in refrigeration and air-conditioning systems. The enhancement in heat transfer coefficient has two important outcomes in the heat exchangers. Firstly it improves the performance and secondly it reduces the size of the heat exchanger. In applications, many techniques are used to enhance the heat transfer and are classified in two types as active and passive techniques. Coiled tube configuration in the heat exchangers is the one of the important passive heat transfer enhancement techniques [18, 19], due to high heat transfer coefficient and compact structure. Helical coiled configuration is very effective for some heat transfer equipments such as heat exchangers [20, 21] and reactors because in small space (volume) they accommodate a large heat transfer area. The curvature in tube induces secondary flow patterns [16] due to centrifugal force developed in the fluid when the fluid is flowing through the curved tube. The secondaries developed in the coiled tubes are as shown in Fig. 2.1.

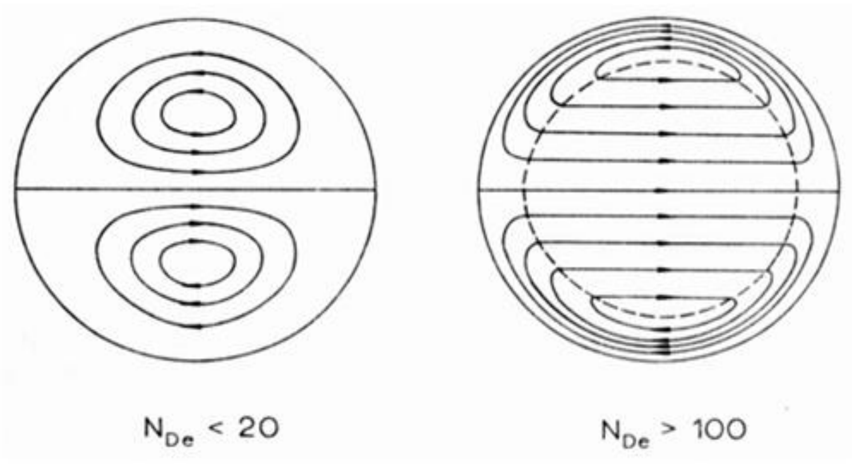

Fig. 2.1 Secondary flow for low and high Dean Number [16]

For the same flow rate, these secondaries allow mixing of the fluid that enhances the heat transfer coefficient, whereas pressure drop across the coiled tube increases due to these secondaries.

It was noted by Shah and Joshi [22], that the enhancement depends on the intensity of secondaries developed in the coiled tube. In case of smaller coil diameter and tube diameters (*D* and *d*) the intensity of secondary flow developed is high.

The Eustice [23] was the first to observe the fluid motion in curved pipes. Since then many researchers presented their studies on the fluid flow that develop in curved pipes, including helical coils [17- 19, 24, 25]. They provided the flow fields and temperature field analysis experimentally and numerically. They indicate that *De* strongly affects the secondary flow pattern. Further they studied the effect of changed flow patterns in heat transfer applications. Many researchers presented the results on the effect of flow parameter (*Re*) and flow parameter (*Pr*) on the flow patterns (*De*) and heat transfer (*Nu*).

The major effects observed in the helical coil configuration were due to the flow pattern in the curved tube; hence it is very essential to understand the effect of the flow pattern in curved tubes.

2.1 Flow pattern in curved tubes

Grindley and Gibson [26] firstly noted the effect of curvature on flow in coiled tubes. In the analysis, they observed the effect of curvature on fluid flow in a coiled tube. With this reference Williams et al. [27] carried out the work on curved tube and noted that the location of the maximum axial velocity was shifted towards the outer wall of curved tubes, which was due the centrifugal force acting on the flowing fluid through the curved tube.

Eustice [23a] compared the flow in curved tubes with straight tubes and noted the change (increase) in resistance to flow. They correlated this increase in the resistance with the curvature ratio (δ). However, in some of the trials where cooling of the tube was involved, they noticed appreciable deformation cross section of the tube. They used ink injection technique in experiments for visualization and experiments were carried out on curve tubes, U-tubes and elbows. He used sand to observe the fluid motion in curved pipes at turbulent flow conditions. The similar flow patterns were observed in turbulent flow.

Eustice [23a and 23b] and Dean et al. [24] made attempts to describe the flow mathematically in a coiled tube. They analysed the fluid flow (incompressible) in coiled pipe of circular cross section. They observed that at low velocities the flow rate reduces due to geometrical parameter, $[2(Re)^2 r/R)]$. This work was carried out for the smaller curvature ratio (δ). The important observation noted in the analysis was that the analytical calculations are only applied to streamline flows. Dean et al. [24] also observed the similar effect. He observed that the fluid particles were oscillating between the central and out part of the curved tube. These oscillations were caused due to centrifugal forces exerted on fluid due to curvature of the pipe, and results in energy loss. In another study, White [25] used water and mineral oil to study the flow behavior in curved pipes in laminar conditions. He concluded that the starting point of turbulence did not depend on flow parameter (*Re* or *De* [$De = Re(r/R)^{1/2}$]) alone. He also noted the more stable flow observed in curved pipes than that of flow in straight pipes and the resistance to flow in the curved pipe is a function of the *De* and the *Re*. He further concluded that the resistance to the flow was same for curved and straight tubes for *De* less than 11.6.

Koutsky and Adler [28] observed the flow field experimentally and numerically and suggested that the velocity profiles in both laminar and turbulent flow tends to flatter than in straight tubes. They also presented the effect of *Pr* and *Re* on the flow pattern and *Nu*. Mori and Nakayama [29, 30] presented the fully developed flow for large *De* in a curved tube with a uniform heat flux. They analyzed the temperature and flow field both experimentally and analytically. The observations were very similar to that of Dean el al. [24]. Similar observations were made by McConalogue and Srivastava [31] in study of secondary flow characteristics for developed laminar flow that the maximum velocity shifted towards outer wall. This results in increased velocity and migration of secondary vortices towards the outer wall.

The analysis of steady laminar flow was studied by Topakoglu [32] with an incompressible viscous fluid approximating the stream function in curved pipes. The two parameters *Re* and curvature ratio (δ) defines the flow rate in the pipe. Further the analysis was extended by Srinivasan et al. [33] and proposed the Re_{cr}. The flow transformation from laminar to turbulent may be characterized by Re_{cr} that depends on flow parameter (*Re*) as well as coil parameters (δ). They suggested the correlation for critical Reynolds number (Re_{cr}) in single-phase flow for coiled tube as in (Eq. 2.1):

$$Re_{cr} = 2100\left[1 + 12\left(d/_D\right)^{0.5}\right] \qquad -2.1$$

where, *d* and *D* were the inner tube diameter and the coil diameter.

Truesdell and Adler [34] performed the numerical studies of laminar flow with the help of FEM (square mesh element). They identified that for smaller *De* (for *De<2000*) the same numerical procedure could be applied. Further increase in the *De* diverges the values resulting from their solution method. The numerical analysis is carried out by considering both circular and elliptical cross sections in helical coils for the analytical models.

Joseph et al. [35] studied the rectangular cross section helical coiled tubes for *De* (0.8 < *De* < *307.8)*. In their numerical study they found similar observation as in circular tube as two secondary flow vortices for *De* < 100. The flow visualization experiments were also conducted for *De* greater than 100 and found that four vertices are developed in the flow field. They also found that the direction of secondary flow reversed for the oscillations were strong enough. Masliyah [36] also performed the similar study, highlighted that initial conditions of the flow field confirms the two or four vortices in secondary flow. He conducted both experimental and numerical studies to confirm his results. The laminar flow was further analysed by Dennis and Ng [37] through curved tubes with FDM for condition of two versus four vortices in the fluid flow through the curved tube.

Smith [38] analytically studied circular, triangular and rectangular cross section curved tube in laminar flow for large *De.* Anwer et al. [39] studied the effect of bend curvature on fully developed turbulent flow in a pipe. They presented the effect of U-bend on downstream flow for curvature ratio (*r/R*) of 0.077 and *Re* of 50000. The analytical solution for the fully developed laminar flow for high *De* was developed by Dennis and Riley [40]. They further noted that there was strong evidence of flow development with viscous boundary layer at high *De.*

Flow pattern in turbulent region was analysed for fully developed condition with the use of large eddy simulations by Boersma and Nieuwstadt [41]. They compared the results of their numerical study with the data reported in literature and noted that the results were acceptable from the large eddy simulations and their approach was feasible.

Park et al. [42] measured the velocity of flow in curved tubes with the help of a laser photo chromic velocimetry method. The analysis was carried out for *Re* of 250 and a curvature ratio of 1:6. From the measured velocities, shear stress at the wall, flow vorticity, and pressure field were determined.

Huttl and Friedrich [43, 44] studied the curvature and torsion forces for turbulent flow conditions in coiled pipes. They used direct numerical simulations to show that the turbulent fluctuations in curved pipes were less than as straight tubes. They also showed that the curvature effect is much higher than that of effect of torsion on the axial velocity.

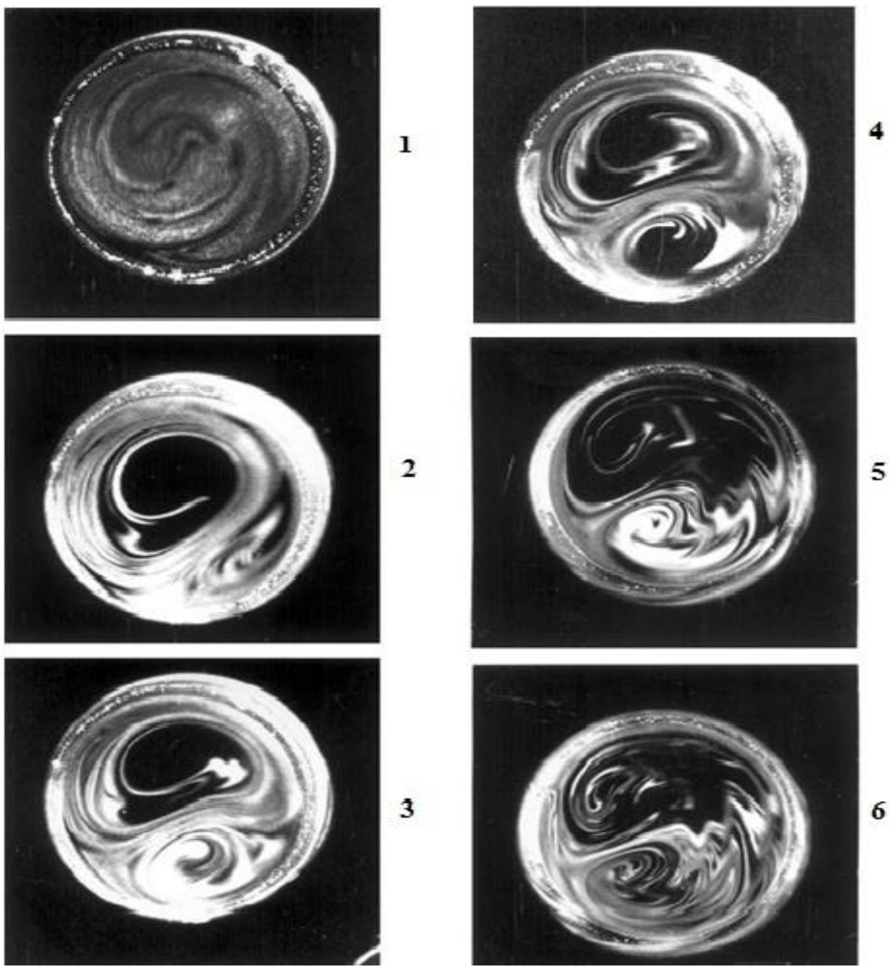

Fig. 2.2 Visualization of the secondary flow
(K. Yamamoto et al. [44])

K. Yamamoto et al. [45, 46] investigated the secondary flow structure with large torsion in a helical tube. They used the smoke visualization technique (Fig 2.2) to study the fluid particle trajectory and validated numerically. In the analysis they observed that, at a constant *De*, in secondary flow, two counter-rotating vortices structure was transformed to a one-recirculation structure in a cross-section with increase of the torsion of the pipe. The increase in torsion changes the direction of line separating the two vortices from horizontal to vertical.

Enough literature is available which gives the idea about the flow through curved tubes with different tube geometry, curved channels and varying curvature. Some of these works are referred in [47 - 53].

2.2 Thermal analysis of coiled tube heat exchanger

The numerous publications have been recorded in the literature to carry out the analysis of heat transfer of coil tube heat exchangers. Several researchers published their results on heat transfer and other aspects of heat exchangers. Some of the important aspects are as follows:

The main focus of the analysis was on inside tube heat transfer with following two conditions [54-57];

a. Constant Wall Temperature (CWT)
b. Constant Heat Flux (CHF)

For the analysis of outside heat transfer coefficient in coil tube heat exchangers few attempts were made, which were on the basis of the same above two conditions. The condition of constant wall temperature on the tube surface is closely approximated or achieved using phase change medium (as the condensation is a constant temperature process). The vapour condenses on the surface of the coil at a given temperature. The heat flux at that point decides the amount of vapour condensing at an area.

The constant heat flux type heat exchangers are developed by using heating coil in or around the tube wall. The constant electrical power is provided to heating element that generates uniform heat along its length to achieve the constant heat flux condition. Another method is to supply the electric potential to the ends of the tube which is made out of electric conducting materials to generate the heat.

In application many times third condition arises, that is neither a constant heat flux nor constant wall temperature. In case of fluid-to-fluid heat exchanger this condition is frequently arising. These types of problems are tackled by considering the properties of both fluids at mean bulk temperature. In this situation, the heat exchanger calculations are performed on the basis of LMTD. However, the main assumption is of constant convective heat-transfer throughout the heat exchanger. For the analysis carried out with temperature dependent fluid properties, this assumption is not valid. Many researchers have worked on the thermal characteristics of helical and spiral coiled heat exchangers as follows;

2.2.1 Helical coil heat exchangers

In literature very less information is available on liquid heat exchangers design [58, 59], for helical coil heat exchangers. The self cleaning tendency in the helical coil configuration due to secondary flow reduces the number of cleaning cycles required for these heat exchangers whereas the cleaning process is slightly difficult than that of conventional heat exchanger.

The estimation of heat transfer coefficient in designing such type of heat exchanger has two difficulties;

1. One side fluid (generally shell side fluid) should be steam so as to achieve the constant heat flux condition.

2. The another important second difficulty is to estimate the area of heat transfer surface.

These conditions affect the effectiveness of the heat exchanger.

The outside heat transfer coefficient calculation is another approximation for the calculation for the complex geometry. In this the analysis is on the basis of the flow over tubes. These problems were highlighted by Prabhanjan [60]. The ineffective methods to predict the flow around the coil increases these problems.

For the heat transfer applications, it is reported in the literature that as compared to straight tubes helically coiled tubes are superior. The fluid flowing in the curved helical coiled tube observes the centrifugal force which effects in the development of secondary flow. The secondary flow developed in the tube helps to enhance the heat transfer rate. This phenomenon is predominant in laminar flow regime. Prabhanjan et al. [21] performed the comparative study of the heat transfer between straight tube and helical coil tube in liquid to liquid configuration and showed that the helical coil heat exchangers shows higher heat transfer coefficient. Similar results were recorded by Coronel and Sandeep [61] in their work for turbulent conditions.

The heat transfer in the coiled tube considering constant heat flux condition for both laminar and turbulent flow was first studied by Seban and McLaughlin [11] with the coils of curvature ratios (δ) of 1/17 and 1/104. The range of *Re* and *Pr* for the study was selected as 12 to 5600 and from 2.9 to 5.7. The results showed that in case of helical coils outer periphery had higher *Nu* than that of the inner, and as compared to straight tube, both inner and outer *Nu* values were substantially high under the same conditions. They further claimed that thermal entry length may cause this effect. In the sequential work with the same experimental setup Seban and McLaughlin [11] worked for the *Re* for the turbulent flow ranged from 6000 to 65600. They also observed that for the curvature ratios of 1/104 and 1/17, the ratios of the heat transfer coefficients at inside to outside periphery were in the order of 2 and 4 for the coils respectively.

Rogers and Mayhew [62] analysed curved tubes for the heat transfer and pressure drop with assumption of uniform wall temperature. The relationship was proposed for the tube side *Nu* based on the film temperature.

$$Nu = 0.021\, Re^{0.85}\, Pr^{0.4}\, (r/R)^{0.1} \qquad 2.2$$

Berg and Bonilla [63] presented their work on the helical coil under constant wall temperature condition and presented the results of heat transfer in terms of Greatz number (*Gz*). Kubair and Kuloor [64] carried out the analysis of two different coil configurations (helical and spiral configurations) under uniform wall temperature created by steam bath on the outside of the coil. Thermal analysis for laminar flow with glycerol was presented with *Re* (80 to 6000), δ (1/10.3 to 1/27) and no of turns (7 to 12). They noted that the results for the interaction between heat transfer rates and the Graetz number of Berg and Bonilla [63] were opposite to those of Seban and McLaughlin [11]. They speculated that this difference might have been due to the fact that the two studies used different boundary conditions, one being constant wall temperature [63] and the other at constant heat flux [11].

Fully developed turbulent flow analysis in flow field and heat transfer analysis was carried out by Mori and Nakayama [29, 30]. By considering constant thermophysical properties, heat transfer characteristics were studied for the constant heat flux conditions. They observed the difference in *Nu* for straight and curved tubes, and the difference decreases slightly with increase in *Pr*. Experiments were carried out with air as a working fluid for two curvature ratios (1/18.7 and 1/40). They extended their earlier work [65] and showed that the *Nu* was same for both the conditions.

Ozisik and Topakoglu [66] analysed the laminar flow heat transfer by a method of series expansion. The analysis highlighted that flow parameter (*Re*), Fluid parameter (*Pr*) and geometry parameter (δ) influences the heat transfer in curved tubes. A steady flow and fully developed laminar forced convection was analysed by Akiyama and Cheng [67] analytically with uniformly heated curved pipes for $De \leq 200$. They observed the shifting of center of the secondaries towards the outer wall as *De* increases. However, further increase in the *De* changes the direction of the center of secondary and it begins to move back towards the inner wall. They extended their work by considering the uniform wall temperature condition. They showed that the same results for heat transfer are observed in both boundary conditions, but distinct, for laminar flows.

The research on velocity field and temperature fields with uniform heat flux condition and peripherally uniform wall temperature were performed by Kalb and Seader [68] in a range of properties ($1 < De < 1200$, $0.005 < Pr < 1600$, and $1/100 < \delta < 1/10$). They found that the average *Nu* has negligible effect of δ for any given *Pr*. However; the peripheral variation of the *Nu* was recorded with δ, though the effect was still not large. With increasing *De*, the local *Nu* on the outer wall continued to increase. Kalb and Seader [69] further carried out work with uniform wall temperature condition and by applying the same conditions. The analysis showed that the peripheral variation of the *Nu* has slightly affected by curvature. However, average *Nu* remains same. Kalb and Seader [69] observed that the temperature field affects significantly by thermal boundary condition.

The equation of fluid motion in the coiled tube configuration was analytically studied by Austin and Seader [70] for isothermal, incompressible, viscous Newtonian flow. Analysis was carried out with finite-difference approach. The ranges were ($1 < De < 1000$, $10 < Re < 4000$ and $1/100 < \delta < 1/5$). They showed the parabolic nature of the axial velocity profile at low *De*. They obtained the similar effect as that Kalab and Seader [68].

Laminar and convective heat transfer was studied by Janssen and Hoogendoorn [20] for both conditions as uniform heat flux and constant wall temperature. In the analysis of thermal entry region it was observed that the secondary flow has a significant effect on length of the thermal entry region which is analysed for temperature distribution profile. The different kind of boundary conditions was not affecting significantly in flow field. Zapryanov et al. [71] studied fully developed laminar flow numerically for a wide range of *De* ($10 < De < 7000$) and *Pr* ($0.005 < Pr < 2000$). The work was carried out with constant wall temperature condition showed that for same *De*, the *Pr* has significant effect on *Nu*. The isotherms and streamlines were also presented for different *De* and *Pr*.

The tube-in-tube helical heat exchanger was studied by Kumar et al. [72] for pressure drop and heat transfer analysis. They found that the overall heat transfer coefficient was the function of *De* and increases with the increase in inner coiled tube *De* for a constant flow rate in the annulus region. They numerically modeled a double helically coiled tube for various flow rates in the outer inner and inner tube.

The steady state, natural convection heat transfer was reported by Moawed [73] for uniformly heated helical coil tubes in vertical and horizontal orientation. Four helical coils were analysed with different curvature ratios, pitch to tube diameter and length to tube diameter with the range of *Ra* ($1500 < Ra < 110000$). The analysis showed that the overall *Nu* increases with increase in δ. Thermal analysis of laminar forced convection for optimal δ with uniform heat flux in a coiled tube were presented by Ko [74].

Jaykumar et al. [75] carried out experimental and numerical analysis of a helical coil heat exchanger with considering water to water heat transfer. The effects of actual fluid properties instead of constant values were established after validating it with the CFD analysis of a heat exchanger. Heat transfer characteristics of tube side flow in helical coil were compared for different boundary conditions. The temperature dependant properties were considered for the conjugate heat transfer in heat exchanger analysis. A correlation was proposed on basis of experimental results and validated by CFD to calculate the inner heat transfer coefficient.

Numerical investigations were carried out to study the forced laminar fluid flow by Conte and Peng [76] in rectangular helical coiled pipes with circular cross-section. The laminar fluid flow was studied to find the flow and its influence on heat transfer. The results showed that flow pattern influences the temperature distributions.

A CFD analysis was proposed by Ferng et al. [77] to study the helically coiled-tube heat exchanger. They carried out the analysis at different *De* and pitch sizes. Based on the analysis they captured shell side variation in flow acceleration and flow separation, the turbulent wake, the secondary flow in the tube and the flow development.

The numerical study at the entry region was presented by Dravid et al. [17] in laminar flow heat transfer, for $De > 100$. They assumed the fully developed flow field at coil entrance. They showed that at the tube inlet for the short distances the secondary flow does not have any effect on the heat transfer rate. They also investigated that the heat transfer coefficient increases along the tube. They suggested that along the whole length asymptotic *Nu* should be used along the whole length of the coil.

The entry flow was studied by Singh [78] for both conditions. The flow in the near-entry region was affected by the conditions of the flow development; however in downstream the effect is not significant in the flow. A correlation of steady laminar flow of the entry region length was presented by Austin and Seader [70] as a function of the flow parameter (*De)* and geometry parameter (δ). The entry region length was noted to be anywhere between 90° and 225° and It was smaller for the coil smallest *De* and the largest curvature ratio.

Finite-difference method was used by Patankar et al. [80] and solved flow of fluid in a helically coiled tube. The temperature and velocity were analysed for thermodynamic and hydrodynamic of fluid flow, for large curvatures the developing entry flow. They confirmed the results from open literature. They also confirmed that the secondary flow creates the oscillations in the wall temperature in the developing entry flow as stated by Dravid et al. [16] and Seban and McLaughlin [11]. The work was extended for curved tubes in turbulent flow region. A turbulence model (two equations), one was for the kinetic energy of the turbulence and another was for its dissipation rate was used for the analysis. The predictions were compared to experimental work with reasonable agreement.

In their study on developing flow, Kalb and Seader [81] analysed helical coil heat exchanger with uniform wall temperature to measure *Nu*. Developing turbulent heat transfer was numerically studied using a control-volume finite element method by Li et al. [82]. The effects of pitch, δ and *Re* on the thermal fields and the *Nu* were analysed. They also showed that pitch, δ and *Re* has stronger effect on *Nu* in helical coil heat exchanger. Li et al. [83] in their sequential study studied the similar effect for heat transfer and laminar flow. They numerically studied the uniform wall temperature convective heat transfer at entrance region turbulent heat transfer a curved pipe. They observe the third vortex as the buoyancy forces became apparent which affected the local *Nu*. The *Nu* in the entrance region gets drastically increased due to the buoyancy forces but negligible effect was observed in overall *Nu* as short entrance region. Both the *Nu* and the friction factor (*f*) oscillated in the entrance region. They found that as δ decreases, the increase in both the *Nu* and the friction factor (*f*). Lin et al. [84] performed the study on helical coil tubes numerically. They found at the walls the reduced velocity gradient was observed due to increased inlet turbulence in the pipe though on the maximum axial velocity, it had negligible effect. The increase in inlet turbulence intensity develops the thermal boundary layer quicker. The developing heat transfer in a helical coil was studied by Rindt et al. [85] with a linear wall temperature. The conditions used for the analysis of the coil were different from usual ones. They found that the *Nu* varies along the axial position.

The single phase flow and two-phase bubbly flow in the helical coils at entrance length (hydrodynamic) was studied by Saffari et al. [86] using numerical techniques. The analysis was carried out for the characteristics of fluid flow varying helical coil parameters in the development region length. The numerical and experimental analysis for the local parameters indicates that for the single and two-phase flows, with increase in *Re,* the hydrodynamic developing length (*L*/*D*) increases. It also indicates that the increase of tube diameter and decrease in coil diameter increases the development entrance length.

Xin and Ebadian [87, 88] studied the *Pr* effect on the heat transfer in helical coil tubes on both the average and local *Nu*. The different curvature ratio and torsions were considered with fluids of different properties. The analysis showed that for higher *Pr* and *De* the peripheral *Nu* for laminar flow shows larger variation. The turbulent heat transfer was studied in horizontal configuration in helical coil by Bai et al. [3]

experimentally. They concluded that, the effect of secondary flow on heat transfer reduces with increase in *Re* and at higher *Re* it approaches to that of a straight tube. This was due to smaller boundary layer at higher *Re*. The local heat transfer coefficient was 3 to 4 times higher, on the outer wall than that of the inner wall.

A fully developed laminar water flow with temperature dependant viscosity in a curved duct was analyzed by Andrade et al. [89] under heating and cooling conditions. The numerical analysis with variable viscosity and constant property assumptions shows that, the *Nu* and friction factor (*f*) showed significant dependence on the viscosity variations in the coil tube cross-section. The analysis was carried out in the range of $2<De<20$. *Nu* correlation based on the *Re*, *Pr* and the number of bends in the pipe was developed by Lemenand and Peerhossaini [90]. For the same *Re* and *Pr*, the analysis showed that with increase in number of bends, *Nu* slightly decreases. Arvind et al. [91] studied the helical coil heat transfer experimentally with the coolant. Three different solutions water, soap and carboxy methyl cellulose solutions were used as bath liquids in a cylindrical vessel of known dimensions without any mixing of the bath liquid. Experimentation was carried out under conditions of natural convection. The overall heat transfer coefficients for soap and carboxy methyl cellulose solutions were found to be below that of water. Prabhanjan et al. [61] carried out the analysis of helical coil in water bath. A method was proposed to predict the outlet temperatures from the helical coil. In this analysis neither constant wall temperature, nor constant wall heat flux, was assumed. The natural convection heat transfer on the outside of the coils was considered. Thermal and pressure drop (Δp) of with and without crimped fins on helical-coil heat exchangers was analyzed by Paisarn Naphon [92]. The data recorded from the experimental measurement of the average in-tube convective heat transfer coefficient has been presented. The thirteen turns concentric helically coiled tubes heat exchanger, with and without helically crimped fins was considered for the analysis. He concluded that, the outlet cold water temperature was influenced by tube side hot water mass flow rate and average heat transfer rate increases with increase in hot and cold water mass flow rates. They also found that the friction factor reduces with increase in hot water temperature and effectiveness was influenced by inlet hot and cold water mass flow rates and inlet hot water temperature.

Heat transfer characteristics was analysed by Salimpour [93] on the temperature dependent properties of fluid in shell and coiled tube heat exchangers. From the analysis it was observed that, heat transfer coefficient decreases with increase in inlet oil temperature. It also observed that for the large pitches the coil-side heat transfer coefficient was less than those of the ones with smaller pitches. It is also observed that at low temperatures the effect of pitch is more distinct.

Kharat et al. [94] presented the work related to heat transfer coefficient for flow between two concentric helical coils. They introduced one extra parameter known as Gap ratio, which was $Gap\ ratio = (Do\text{-}Di)/d.$ Sufficient data was considered, which covers a wide range of the *Re* (20000 to 150000). The developed equation was valid, for specified ratio (Coil gap / Tube diameter) ranging from (0.55 to 2.25).

Ghorbani et al. [95] presented his investigation of the mixed convection heat transfer in a coil-in-shell heat exchanger for various *Re* and *Ra,* various δ and dimensionless coil pitch experimentally. The analysis also deals with the effect of different geometric parameters and operating parameters on heat transfer and effectiveness (modified) of helical coiled tube heat exchangers. They found that an axial temperature profile was affected by flow ratio. They analysed the heat transfer in helical coil heat exchanger for various *Re*, curvature ratio (δ) and different dimensionless coil pitch. The result showed that the shell diameter was the best characteristic length for the helical coil analysis. Thermal performance of a helical heat exchanger was investigated by Jung-Yang Sen et al. [96]. The helical coil heat exchanger was considered for the analysis with rectangular cross section and cover plates with inside mixed flow and the flow was unmixed on outside the tube. The analysis was carried out to study the behavior of friction factor and heat transfer coefficient. The analysis of water- water heat exchanger was carried out with numerical model by Fernandez-Seara et al. [97] with outer surface in natural convection. The analysis was validated with experimental data with two helical coil heat exchangers tested under same operating conditions and the analysis show that the *Nu* increases with increase in tube diameter.

The effects of buoyancy forces with constant heat flux on fully developed laminar flow were studied analytically by Yao and Berger [98]. Furthermore Lee et al. [99] also studied the same effect in the flow field and Thermal field. The system for fully developed laminar flow was numerically analysed with constant heat flux along the axis and constant wall temperature condition along periphery. They found that average *Nu* was affected by buoyancy. They also found that the rotation of the secondary flow patterns depends on the buoyancy forces. Padmanabhan [100] studied the entry flow into curved pipes for constant heat flux and for constant wall temperature condition axially. The secondary motion was affected by buoyancy. Futagami and Aoyama [101] studied the buoyancy forces for fully developed laminar flow. They developed an expression to predict the average *Nu* where heat transfer coefficient was the function of the secondary flow and buoyancy forces. The range of the experimentation was selected such that the centrifugal and buoyancy forces affect the secondary flow with uniform heat flux boundary conditions.

Goering et al. [102] studied the curvature effects and buoyancy in developed laminar flow, on the heat transfer rates. The Navier-Stokes equations and the energy equation solved by constant volume approach, considering buoyancy into account. Regime maps were deduced. Accordingly three separate regions were designated as free convection, forced convection and mixed convection. For developing flow, turbulent heat transfer in curved tube was investigated by Li et al. [83] using a control volume FEM with water near the critical point. The secondary flow was strongly affected by buoyancy forces, as near critical points, which were stronger than centrifugal forces. Near the critical pressure the heat transfer and friction factor increases significantly.

An investigation was carried out by Shokouhmand et al. [103] to study heat transfer coefficients of the helically coiled tube heat exchangers. In their analysis they showed that the shell-side h_o of the coils with larger pitches was more than the ones with smaller pitches. The overall *h* of counter-flow configuration is upto 40% more than those of parallel-flow configuration. The analysis was carried out with Wilson plot method for calculating h_i and h_o. Inagaki et al. [104] presented his work for helical coil tubes for *Re* in the range of 6000 to 22000, on the outside heat transfer coefficient and found relationship for their particular setup.

In the Natural convection heat transfer on outer surface of the heat exchanger A. Zachár [105] showed that, the outside heat transfer rate depends on the tube side flow rate and temperature differences between two working fluids. Park et al. [106] presented helical ground heat exchanger analysis with various helical pitches and performed the indoor thermal response tests in dry sand. The tests were based on axi-symmetric finite element analysis adding finite-length line source solution for spiral coil heat exchanger by considering return pipe vertical at the center of helical heat exchanger. The analysis performed of by Neshat et al. [107] was carried out to understand unsteady natural convection from helical coils outer surface by experimental and numerical investigations. Four helical coils with two different curvature ratios were used. The cold water was supplied through coiled tubes and the hot water in the shell was in an unsteady natural convection process. A CFD code was developed to simulate natural convection heat transfer. Equations of tube and shell were solved simultaneously. Statistical analyses were done on data points of temperature and natural convection *Nu*. It was revealed that shell-side fluid temperature and the *Nu* of the outer surface of coils were functions of tube side flow rate, specific heat of fluids and geometrical parameters including length, diameter of the tube, volume of the shell, and time.

The effect of orientation of helical coil was analysed under natural convection heat transfer by Moon et al. [108]. The analysis reveals that the heat transfer rate was influenced by plumes in the inclined helical coils with higher numbers of turns. In case of very small pitches, the preheating effect, in case of moderate pitches, the velocity and chimney effects and in case of larger pitches, the plume effect was dominant. The important observation was about angle of inclination; it affects the physical arrangement of the helical coil and influences the heat transfer.

The investigation on double-pipe heat exchanger developed in helical coil form was studied by Rennie [54, 55] and presented to study the residence time and temperature. The process uniformity required by food processing was also studied in his applications. The analysis was carried out in both heating and cooling at laminar flow range, with both configuration viz. counter flow and parallel flow configurations in the inner tube. The increased flow rates in both the inner tube and in the annulus make the distribution of residence time uniform. However, it was found that uniformity gets affected due to the flow rate change in the annulus. The uniformity in heating the inner tube increases with increased flow rates. They also found that in case of uniform processes the cooling process was more uniform than the heating process.

In further study in a double-pipe helical heat exchanger Renni et al. [56, 57] also conducted the experiments for both parallel flow and counter flow to study the effect of thermal properties on the heat transfer characteristics. The result showed the linear relationship in *De* for inner surface to *U*. However, *U* is strongly influenced by fluid flow conditions in the annulus. The annulus *Nu* was correlated with a *De*.

In the investigation on heat transfer characteristic Vimal Kumar et al. [109] presented the investigation in tube-in-tube helical heat exchanger with hydrodynamics characteristic. To increase the turbulence the outer surface of inner tube was fitted with semicircular plates. The analysis was carried out by Wilson plot method to calculate the overall heat transfer coefficients. For the validation the results were simulated with CFD. The comparison was carried out between the inner and outer values of *Nu* and *f*

The investigation on concentric helical coils heat exchangers were experimentally investigated by Gomaa et al. [110] for its thermodynamic and hydrodynamic characteristics. Various parameters were considered for study as coil curvature ratio, number of turns, flow configuration, and addition of surface. Extensive experimentation was carried out to study the hydrodynamic and thermal characteristics. The annulus side range was of *Re* (5,000–19,000) and that of the inner side *Re* (11,000–27,000). The results showed that the annulus *Nu* was affected by annulus curvature ratio, δ and number of turns in such way the Nu has direct relation with annulus curvature ratio, δ and inverse relation with number of turns. Similar relation was obtained with friction factor, and noted that it increases with curvature ratio, δ and decreases with number of turns.

In the analysis of tube in tube helical coil heat exchanger Mandal and Nigam [111] studied the transfer and fluid flow under turbulent condition. For both side in the heat exchanger water was used as working fluid. The tube side operating condition of inside tube was as *Re* in the range of 14,000 to 86,000. The data was validated by CFD analysis

An investigation on vertical helical coiled tubes in water was performed by Pawar S.S et al. [112]. Three coils with δ as 0.0757, 0.064, 0.055; *Pr* from 3.81 to 4.8 and *Re* from 3,166 to 9,658 were considered in this work. They correlated *Nu* with dimensionless number 'M' proposed which was a function of *Re* and δ. Several other correlations based on experimental data were developed. For various applications suitable generalized correlations were proposed.

Multi tubes in a tube helical coil heat exchangers were proposed as a compact heat exchanger by Nada et al. [113]. The analysis was carried out to study the effects of various parameters on heat exchanger. The different parameters in the form of geometry parameters as number of inner tubes, annulus hydraulic diameter etc., were considered with fluid flow parameters as *Re* and input heat flux. Coils with different numbers of inner tubes are fabricated with 1, 3, 4 and 5 tubes in a single bigger tube, were considered for application. In this analysis the data reveals that coils with 3 inner tubes were higher heat transfer coefficient with compactness parameter (hA_h) than the others. The analysis also indicated that the increase in both *Re* and number of inner tubes increases pressure drop. The analysis presented the correlations from experimental data for *Nu* as a function of *Re, Pr,* number of inner coils tubes and coil hydraulic diameter.

Enough literature is available that highlight the heat transfer phenomenon in the helical coil heat exchanger. The studies were performed on both numerically and experimentally for three different conditions that are constant heat flux, constant wall temperature and the mixed flow conditions.

2.2.2 Spiral coil heat exchanger

In the analysis of spiral coiled tube heat exchanger Naphon et al. [114, 115] investigated the effect of curvature on heat transfer and flow development in the spiral coil tubes. He analysed this effect by using different coils with different curvature ratios (δ) of (0.02 to 0.05) under constant wall temperature condition with the cold water supplied at the innermost and flowing out at the outermost turn. The CFD analysis was carried out to simulate results. The results obtained by both the analysis show the reasonable good agreement. From the analysis they understood that, the heat transfer and pressure drop enhancement was influenced by secondaries developed in the tube. They understood that the *Nu* for the spiral coiled tube was about 1.5 times higher than that of straight tube. In their continual study Naphon et al. [116, 117] analyzed the average heat transfer coefficient of chilled water in the spiral tubes heat exchanger consisting of six layers coiled tubes with five turns. They further discussed thermal analysis under dry and wet surface conditions. They also understood that the inlet conditions of both fluids have considerable effect on the heat transfer coefficients. The correlations were proposed for the tube-side and shell-side heat transfer coefficients.

The effect of heat conduction on its effectiveness in spiral and radial direction of the solid partition on spiral tube heat exchanger was analysed by Duc-Khuyen et al. [118]. The Archimedes spiral heat exchanger was developed for analysis. In this analysis they revealed that at maximum effectiveness, the *NTU* value was influenced by number of turns. The maximum effectiveness value was obtained at large number of transfer units (*NTU*). The heat conduction in the spiral-direction reduces the effectiveness. This effect was observed due to the decrease in partition's thermal conductivity. The increase in effectiveness was recorded with radial-direction heat conduction. The effect of solid heat conduction on the effectiveness was less for $0.01 < Bi < 0.1$.

In the similar analysis Ho et al. [119] studied a spiral-coil heat exchanger. The analysis was made to predict the thermal performance of the spiral-coil heat exchanger for the cooling and dehumidifying application. The analysis was carried out on laboratory model of the spiral-coil unit to validate the predictions of the theoretical analysis. The investigation of multilayer spiral tube heat exchanger was done by Lu et al. [120] for the shell-side flow and heat transfer performances. The analysis was carried out for three layers of heat exchanger under heat flux specified boundary conditions to validate a numerical method. Wilson plot method was used for analysis..

An attempt was made by Pongsoi et al. [121] to fin-and-tube heat exchangers and analyzed the results of an experimentation of the air-side performance of spiral coil heat exchanger. The fined tube spiral heat exchanger was tested as economizer system for the waste heat recovery. They carried out the work numerically as well as experimentally. They analysed the effect of different parameters as fin configurations, tube arrangements and operating conditions on shell side of the spiral fin-and-tube heat exchangers. The performance correlations were developed for circular fin-and-tube heat exchangers.

The analysis of the literature shows that in the heat transfer characteristics the extensive work has been carried out in the helical and spiral coil heat exchangers and many researchers are working on the various aspects of the coiled tube heat exchanger. Few other references are as in [122-130]. Some of the important correlations of the different researchers are given in Table 2.1 for *Nu* in different conditions for the applications.

Table. 2.1: Available correlations of *Nu*

Author	**Correlation**	**Condition**
Seban and McLaughlin [11]	$Nu = 0.644 Pr^{1/3} \left[\frac{f}{8} Re^2 \frac{2r}{x}\right]^{1/3}$	*δ=1/17 and 1/104* *12<Re<5600;* *100<Pr<657*
	$Nu\,Pr^{-0.4} = \frac{f}{8} Re$	*δ=1/17 and 1/104;* *6000<Re< 65600;* *2.9<Pr< 5.7*
Rogers and Mayhew [62]	$Nu = 0.023 Re^{0.85} Pr^{0.4} \left(r/_R\right)^{0.1}$	*Steam condensation*
Mori and Nakayama, [27]	$Nu = Nu_s(0.1976)\ De^{0.5}$	*De>2000*
Mori and Nakayama, [28]	$Nu = 0.023\ Re^{0.85}\ Pr^{0.4}\ (d/D)^{0.1}$	*Re(d/D)>6*
Kubair and Kuloor [63]	$Nu = \left[1.98 + 1.8\left(r/_R\right)\right] Gz^{0.7}$	*10<Gz<1000,* *80<Re<6000, and* *20<Pr<100*
Dravid et al. [14]	$Nu = \left[0.76 + 0.64\sqrt{De}\right] Pr^{0.175}$	*50<De<2000;5<Pr<175*
	$Nu = 0.913 De^{0.476} Pr^{0.2}$	*80<De<1200; 0.7<Pr<5*
Kalb and Seader [69]	$Nu = 3.31\ De^{0.113}\ Pr^{0.0108}$	*20<De<1200* *0.005<Pr<0.05*
	$Nu = 0.913 De^{0.476} Pr^{0.2}$	*80<De<1200;0.7<Pr<5*
Acharya et al. [16,17]	$Nu = 0.69\left(r/_R\right)^{0.13} Re^{0.5} Pr^{0.43}$	*Pr<1*
	$Nu = 0.67\left(r/_R\right)^{0.13} Re^{0.5} Pr^{0.21}$	*Pr>1*
Inagaki et al. [109]	$Nu = 0.78\ Re^{0.51} Pr^{0.3}$	*6000<Re<22000*
Guo et al. [140]	$Nu = 0.328\ Re^{0.58} Pr^{0.4}$	*6000<Re<180000*
Naphon et al. [95]	$Nu_{avg}=27.358\ De^{0.283}\ Pr^{-0.949}$	*De>=30, Pr>=5*
Arvind et al. [91]	$Nu_{coil}= Nu_{st}[1+(3.5(di/d_h))]$	
Naphon et al.[122]	*For dry-surface conditions:* $Nu= 4.0\ De^{0.464}\ Pr^{-0.755}$	$200 \le De \ge 3000$, *Pr>7* $Re_o<4000$

(Spiral Coil)	$j = 0.178\ Re_o^{-0.239}$	
	$Nu=19.0\ De^{0.464}\ Pr^{-0.755}$ $j = 0.029\ Re_o^{-0.202}$ Wet-surface conditions	$200 \leq De \geq 3000$, $Pr>7$ where $Re_o<4000$
Renni et al. [56,57]	$De = \frac{\rho V}{\mu}\left(\frac{D_o^2-D_i^2}{D_o+D_i}\right)\left(\frac{D_o-D_i}{R}\right)^{0.5}$	Hydraulic Diameter
	$Nu = 2.08\ De^{0.20}Pr^{0.28}$	for $18<(De*2Pr)^{1/2}<100$
	$Nu = 0.39\ De^{0.58}Pr^{0.46}$	for $100<(De*2Pr)^{1/2}<500$
	$Nu = 2.70\ De^{0.30}Pr^{0.29}$	$500<(De*2Pr)^{1/}<2315$
	$Nu = 5.27De^{0.20}Pr^{0.19}$	$500<(De*2Pr)^{1/2}<1610$
Shokouhmand et al.[108]	$Nu_o = 0.50\ Re^{0.55}.Pr^{0.33}.(\eta/\eta_w)^{0.14}$	
Shokouhmand et al. [74]	$Re_{opt}=2100\ \beta 1^{-0.45}(\beta 2/10^{-10})^{-0.53}\ \delta^{-0.19}$-For air	$\delta= 0.01$ to 0.3, $\beta_1=1$ to 20 and 0.1 to 2 for water $\beta_2/10^{-10}=0.01$ to 0.2
	$Re_{opt}=1790\ \beta 1^{-0.05}(\beta 2/10^{-10})^{-0.53}\ \delta^{-0.02}$ - For water	
Jaykumar et al. [75]	$Nu= 0.025\ De^{0.9122}\ Pr^{0.4}$	$2000<De<12000$
Coronel and Sandeep [61]	$Nu=0.0302\ Re^{0.85}\ Pr^{0.4}\ (d/D)^{0.099}$	$5000<Re<30000$; $2<Pr<3.5$; $0.078<d/D<0.004$
Salimpour [96]	$Nu_i=0.554\ De^{0.496}\ \gamma^{-0.388}\ Pr^{0.151}\ \varnothing^{0.125}$	$35<De<410$, $0.058<\gamma<0.095$, $160<Pr<325$, $0.113<\delta<0.157$ and $0.34<\Phi<0.60$.
Salimpour [96]	$Nu_i= 0.152\ Re_i^{0.431}\ Pr^{1.06}\ \gamma^{-0.277}$ $Nu_o= 19.64\ Re_o^{0.513}\ Pr^{0.129}\ \gamma^{-0.0938}$	$500<De<5000$ $0.113<\delta<0.157$
Kharat et al. [97]	Gap ratio = (Do-Di) / d, $Nu= 0.0265Re_i^{0.88}Pr^{0.3}\ \gamma^{-0.097}$	$20000<Re<150000$
Pizza et al. [79]	$Nu=0.00619\ Re^{0.92}\ Pr^{0.4}\ (1+3.455\delta)$	$(0.7<Pr<5)$
J. S. Jayakumar et al. [78]	$Nu=0.116\ Re^{0.71}Pr^{0.4}\delta^{0.11}$	$3000<De<22{,}000$; $3.0<Pr<5.0$ $14000<Re<70000$, $0.05<\delta<0.2$
Srbislav B. Genić et al. [131]	$Nu_o = 0.50\ Re^{0.55}.Pr^{\frac{1}{3}}.(\eta\eta_w)^{0.14}$	$1000<Re<9000$, $2.6<Pr<6$, $9.1<d_h<18.3$
Xing Lu et al. [126]	$Nu_o = 0.179\ Re_o^{0.862}$,	$500<Re_o<3500$.

Xing Lu et al. [126] (Spiral coil)	$Nu_o = 0.179 \cdot Re_o^{0.862}$	for $500 \leq Re_o \leq 3500$

2.3 Pressure drop and friction factors (*f*)

The pressure drop in the heat exchanger directly relates to the pumping power required for the heat exchanger. This is the important consideration for the selection of the effective heat exchanger for the application. Friction factor is the representation of pressure drop in the analysis.

The first analysis of the friction factor (*f*) was presented by Ito [131] He carried the experiments on the smooth pipes in turbulent flow conditions. For the analysis he selected the curved pipes in such a way that the tube diameter to curvature diameter ratio is about 1/16.4 to 1/648. The analysis was carried out with the distribution law with the range of *De* of 0.034 to 300 and for above. The very important observation he noted was that, the friction factor in the curved tube is equivalent to straight tube for values of $De < 0.034$.

The motion of flow for large *De* was analyzed by Barua [13] in a stationary curved pipe. The non-turbulent core was the main assumption where the fluid moved towards the outer periphery. In the same analysis he also noted the water moved back to the inner periphery of the tube via a thin boundary layer. He also correlated the friction factors (*f*) between curved tube and a straight tube in terms of *De*. The friction factors for straight tubes and highly curved tubes were reported by Nunge and Lin [132] with different curvature ratios. The analysis showed that the increase in curvature reduces the friction factor (*f*) at high *De.* The results obtained were contradicted with the results of Austin and Seader [70]. In the sequential study Sarin [133] analysed the elliptical cress section tube and showed that the lowest and highest shear stress was on the inside and outside wall respectively for an elliptical cross section.

Akagawa et al. [134] measured the pressure drop across the helically coiled tubes with different curvature ratios (δ) of a two-phase (gas-liquid) flow and developed a correlation. They found 1.1 to 1.5 times higher friction factors (*f*) than the straight pipe. Kasturi and Stepanek [135] correlated the pressure drop and void fraction in two-phase flow of a gas-liquid mixture through helical coils. For the different fluid combinations, a helical coil with of ID 12.5 mm and a coil radius of 332.5 mm was considered for the analysis. The Lockhart-Martinelli and Dukler's correlations were used to correlate the pressure drop and Hughmark's correlation was correlated with void fraction. Rangacharyulu and Davies [136] presented the pressure drop for two-phase flow of air-liquid in his experimental study. With the help of modified Lockhart-Martinelli parameter, they developed a correlation for the two-phase flow.

Tarbell and Samuels, [137] developed the friction factor (*f*) correlation which was based on the *Re* and the δ, rather than just the *De*. A technical note on a friction diagram was published by Grundmann, [138] for helical coils with smooth pipes. The char for the friction factor (*f*) was published by Hart et al. [139] for helical coil tubes for the range of ($Re < 200000$), and ($\delta < 0.2$). The experimentation was also performed by them on to determine pressure for gas-liquid flows that included liquid holdup.

The pressure drop oscillations were characterized by Guo et al., [140,141] in a closed loop steam generator system for two-phase flow of steam-water. They analysed the helical coils with the effect of inclination in single-phase and two-phase flow on friction factor (*f*). The friction factor (*f*) variation is considerably less in single phase. The effect was significant for the two-phase flow and depending on the inclination angle the friction factor increases up to 70%. For the miniature helical channels Downing and Kojasoy [142] studied the pressure drop characteristic for two-phase flow.

The calculations of friction factors for helical coils were discussed Jayanti and Hewitt [143]. They suggested that the higher order terms should be considered in calculations of Van Dyke [144] to evaluate the better friction factor. Ali [145] presented the extensive review and summarized the equations of friction factor in his study. He made an attempt to understand the dimensionless group for steady flow for better characterizing of Newtonian fluids in helical coil. He obtained the pressure drop experimentally with respect to flow rate for helical coils. He developed the pressure drop correlations in terms of *Eu*, *Re* and a geometrical group, $G = (d^{0.85}D^{0.15}/L_c)$. He found that the friction factor (*f*) was the function of *Re* and δ, and not by a dimensionless number *De* that is the dimensionless number in combination of *Re* and some δ and proposed the following four regimes.

1. Low laminar flow regime: upto Re_{critl},
2. Laminar flow regime: in between Re_{critl1} and Re_{critl2}
3. Mixed flow regime: in between Re_{critl2} and Re_{critl3}
4. Critical Reynolds number: above Re_{critl3}

In the analysis of frictional loss Pimenta et al. [146] have studied on frictional losses in Newtonian and non Newtonian fluid and found that the calculation of the friction factors for Newtonian fluids had no significant change between the values calculated with the physical properties at the mean film temperature of the fluid (T_f) and at the mean bulk temperature of the fluid (T_m).

Enough literature is available which gives the idea about the friction factor and pressure drop analysis in the helical and spiral coil heat exchangers. The analysis highlights that the friction factor in the coiled type heat exchanger is a function of flow parameter (*Re* or *De*) and the coil parameter as curvature ratio.

2.4 Critical *Re*

Critical Re is the important parameter to define the type of the flow in the coil heat exchanger. In this regards many researchers have presented their findings in literature.

Ito [131] performed the experimental work in smooth curved pipe for the range of δ of 1/15 to 1/860. In his investigations, he proposed an empirical correlation to calculate critical *Re* for the range of δ (1/15 to 1/860).

$$Re_{cr} = 20000 \left(\frac{r}{R}\right)^{0.32} \tag{2.3}$$

He also highlighted that, for (δ < 1/860), the Re_{cr} was found equal to that of a straight tube. In the study on carioles forces Soeberg [147] showed that these forces predominantly influence the stability of the laminar flow, for *De* > 100, this effect in delaying the transition from laminar flow to transitional flow at higher *Re*, and weakly dependent on the curvature ratio.

For transitional flow though helical coils Webster and Humphrey [148, 149] used the laser-Doppler velocimetry. The measurements were made for a coil with a δ (1/18.2) and showed that the turbulent fluctuations were suppressed due to coil curvature that would normally be present in the steep velocity gradients at the walls. The increasing

Re, suppresses the tendency of turbulent fluctuations. He also observed the unsteady flow in non turbulent range. In the experiments of flow visualization Sreenivasan and Strykowski [33], Taylor [150] observed that in the transitional region, the flow is unstable and showed traveling wave instability. These traveling waves were well shown by numerical calculations. Hon et al. [151] in his study of the downstream flow of a helical coil showed that in helical coil the traveling wave originated and in straight tube was affected by the flow.

Yamamoto et al. [45] analysed the transition flow for large curvature and large torsion for helical coils. They showed that flow and torsion has different effects on curvature. They also showed that critical *De* decreased with increase in torsion parameter and reaching a minimum, and then began again increases.

2.5 Influence of pitch

The next important parameter in the coil configuration is the coil pitch. Austin and Soliman [152] with the help of uniform wall heat flux condition showed that pitch has a significant effect on both *f* and *Nu*, at low *Re,* and effect weakened with increase in *Re*. They suggested that free convection was affected by these pitch effects, and decrease as the forced convection becomes more dominant at higher *Re*.

Perturbation method was used in analysis of helical coil by Xie [153] to study the fully developed laminar flow with cylindrical coordinate system. The analysis shows that no effect on the flow rate was recorded by curvature within the second order of the perturbation parameter. This second order affects on vortices exerted on torsion.

The secondary flow field was affected by pitch and torsion which was investigated by Liu and Masliyah [154] for fully developed laminar flow. They found that, *De*, curvature ratio, and torsion affects the critical value for the transition of two vortices to a single vortex. They also studied the pressure drop and *f* for developed laminar flow. Their results were further validated by experimental results [155]. Laminar Newtonian flow and heat transfer development was studied by Liu and Masliyah [154] numerically using parabolic equations in the axial direction. The pitch of the helix was also considered in their study. The analysis was performed with a ($20<De<5000$) and ($0.1<Pr<500$). Oscillation in the *Nu* was observed for small *De* and *Pr*.

The effect of the pitch on the *Nu* was studied by Yang et al. [156] in the laminar flow of helicoidal pipes. The analysis shows that the temperature gradient in pipe increases with increased torsion and on the opposite side it decreases.

Numerical study on the laminar flow in a duct was studied by Wang and Andrews [157] with rectangular cross section for an incompressible fluid. The analysis was carried out to study the relationship between different coil parameters viz., pitch ratio, pressure gradient, and curvature ratio with the velocity distribution and the fluid resistance for fully developed flow. They observed that the pitch ratio affects the secondary flow and friction factor. The pitch ratio affects the change in two-vortex flow into a single vortex flow. The curvature ratio affects the friction factor for rectangular helical duct flow.

Jaykumar et al. [158] performed the work on helical coil by varying the coil pitch from 0 to 60 mm. They observed same *Nu* at top and bottom of the coil at zero pitch. As the coil pitch increases the difference between the local *Nu* at the top and bottom also increases. This indicates that three forces are comes into effect which are centrifugal force, torsional force and rotational force. The increase in pitch increases the magnitude of difference at any given corresponding cross-section. It was observed that the Nu_{avg} increases marginally with increase in pitch and almost insensitive to its further changes at higher pitches.

2.6 Applications of coiled tube heat exchanger

Coiled tube heat exchangers are extensively used in industries due to their inherent advantages over the straight tube heat exchangers. There are fair numbers of publications available in the literature which gives applications of coiled tube heat exchangers. Some of the applications are listed as in Table 2.3.

Table. 2.3 Applications of coiled tube heat exchanger

Sr. No.	**Researchers**	**Application**
1	Mihail and Straja [159]	**Polymerization reactor** Application of polymerization reactor with helical coil was analysed for different characteristics

2	Sedahmed et al. [160]	**Electrochemical reactors**, In this the helical coil is used for both as a electrode as well as heat exchanger for the heat transfer application
3.	Prasad et al. [161]	**Waste heat recovery device** – The waste heat recovery unit was developed and analysed for its thermodynamic analysis.
4	Allen and Ajele [162]	**Shell and coil heat exchanger** – The shell and coil heat exchanger was developed with helical coil configuration and analysed for hydrodynamic and thermodynamic analysis.
5	Taherian and Allen [163, 164]	**Solar domestic hot water systems.** – The vertical helical coils in natural convection are used to develop the solar domestic water heating system.
6	Klunge et al. [165]	**Microfiltration of silica suspensions** – The microfiltration of silica suspensions with helical coils analysed and compared with straight tube filtration system.
7.	Fleming et al. [166]	**Hydrogen separation system –** This system was developed with helical tube packed with Palladium deposited with outer shell hot and cold nitrogen gas is supplied for analysis.
8	Sahoo et al. [167,168]	**Milk sterilizer-** They designed milk sterilizer with ultra-high temperature helical tube and used for it for bacterial kill using the sterilizer.
9	Gao et al. [141]	**Separators in the petroleum industry** – Curved tube petroleum separator was developed and tested for given operating conditions.
10	Yi et al. [169]	**Evaporator** – The evaporator section of the heat pipe section was developed by helical coil evaporator.

11	Hameed and Muhammed [170]	**Falling liquid films in reactors -** To study the mass transfer, the helical coils reactor was developed for gases into falling liquid films.
12	Fernández-Seara et al. [171]	**Ammonia-water vapour absorption system –** An ammonia-water vapour rectification process by use of a helical coil in for absorption systems was studied
13	Yu et al. [172]	**Refrigeration system -** The helical coil with different orientation viz. vertical, horizontal, and inclined and effect of these orientations on thermal performance.
14	Xiaomen and Lee [173]	**Domestic water-cooled air-conditioner** – The water-cooled helical coil heat exchanger was tested for air-conditioner application.
15	Mosaad et al. [174]	**Refrigeration** – The study was carried out for investigation on R-134 refrigerant with coiled tube for refrigeration.
16	Zhao et al. [175]	**Synthesis gas (syngas) in membrane** – Membrane helical-coiled heat exchanger and membrane serpentine-coiled heat exchanger with synthesis gas were analysed for thermal and fluid flow characteristics under different operating pressures, inlet velocities and pitches.
17	Yang et al. [176]	**Pressurized coal gasifier** – Cooling section of pressurized coal gasifier with the helical coils and spiral coil membrane was investigated under high pressure convection.
18	Kumbhare et al. [177]	**Heat recovery system** – Experimental investigation on analysis of heat recovery system by helical coiled tube with square and circular pattern is reported for the variation in tube side Reynolds number for the

		laminar flow.
19	Bazargan Hassanzadeh et al. [178]	**Steam generator -** A symmetric helically coiled tube steam generator that operates by methane has been simulated analytically and numerically

2.7 Conclusions from the literature

The following conclusions are drawn from the literature:

1. The secondary flow developed in the curved tube due to centrifugal force exerted on fluid particles in the flow field of coil tube configuration enhances the *Nu* by about 1.5 times higher than that of the straight tube heat exchanger. However due to these secondaries the pressure drop across the coil also shows appreciable increase as compared to straight tube.

2. In the helical coil heat exchanger shell-side heat transfer coefficient in counter-flow configuration is slightly higher than that of parallel-flow configuration. The overall heat transfer coefficient of counter-flow configuration was higher upto 40% more than that of parallel-flow configuration.

3. The increase in inlet temperature of shell side fluid decreases the heat transfer coefficient. The tube side heat transfer coefficients of the coiled tubes with larger pitches are less than those of the ones with smaller pitches; and the effect of pitch on *Nu* was more discernible at high temperatures.

4. Flow ratio (Q_h/ Q_c) is found to be effective in the axial temperature profiles of heat exchanger. The quadratic form of temperature profile was observed for helical coil heat exchanger from bottom to top for the flow rates greater than unity.

5. Inlet hot and cold fluid mass flow rates have significant effect on the heat exchanger effectiveness.

7. The heat transfer in coil tube configuration is governed by three independent parameters, viz. flow parameter (*Re/De*), fluid parameter (*Pr*) and configuration parameter (curvature ratio (δ)) of the coil.

8. The coil pitch is found to have significance only in the developing section of heat exchanger. The torsional forces induced by the pitch causes variation in the *Nu*. However, the average *Nu* is not affected by the coil pitch.

9. The helical coil configuration (vertical) shows higher heat transfer enhancement than in spiral coil configuration (horizontal) for the same flow rate and geometric parameters.

10. In case of helical and spiral coil heat exchanger, the increase in both *Nu* and *f* is observed with decrease in curvature ratio. This shows that the secondaries developed in the coil configuration is the function of both tube diameter and the coil diameter.

11. The literature also highlights that the outer side heat transfer rate was dependent on the inner flow rate of coil tube heat exchanger tube.

12. The supply of cold water through coiled tubes and the hot water in the shell leads in an unsteady natural convection process.

13. Shell-side fluid temperature and the *Nu* are functions of in-tube fluid mass flow rate, specific heat of fluids and geometrical parameters including length, inner diameter of the tube and the volume of the shell.

14. Wilson plot method can be used for determining the heat transfer coefficient (tube side and shell side) in the coiled tube heat exchanger.

15. The development of entrance length depends on tube diameter and coil diameter. It increases with the increase of tube diameter and decreases with increase in coil diameter.

16. The average *Nu* increases with increase in buoyancy effects, as well as modifying of the local *Nu* distribution and the buoyancy forces results in the orientation of the secondary flow patterns.

17. The coil pitch is significant only in the entrance section of heat exchanger. However, the average *Nu* is not affected by the coil pitch.

18. Pumping power is evaluated by pressure drop characteristics required to provide the necessary flow rates in the heat exchanger. The secondary flow developed in

the curved tube perpendicular to axial flow increases the pressure drop across the coil.

19. The pressure drop is characterized by friction factor (f). The friction factor (f) decreases with increasing tube side flow rate. The friction factor (f) is a function of tube side fluid flow (Re) and curvature ratio (δ) for coil tube configuration.

2.8 Motivation for the present work

Sufficient data is available in the literature to prove that the helical coil configuration enhances the heat transfer. Therefore, this configuration is popular in the industrial applications. Considerable data is also available on spiral coil heat exchanger, which proves that the heat transfer coefficient is the function of curvature ratio *(δ)*. The pressure drop *(Δp)* in the spiral tube configuration is also considerably higher due to the secondary flow developed in the tube are continuously changed.

The conical coil configuration shows advantages of both helical coil (high heat transfer coefficient less pressure drop) and spiral coil (compact design, less bypass factor) apart from other advantages of coil configurations are observed.

To the best of our knowledge, for combined configuration of helical and spiral coil heat exchanger that is conical coil configuration no data is reported in the literature on heat transfer and pressure drop analysis.

Development of heat transfer and pressure drop data correlations for this configuration would make it a candidate for the heat exchanger design alternative.

2.9 Objectives of the work

The following objectives were set for this work:

1. To carry out the parametric analysis on the performance of the CCC heat exchanger:

   Geometric parameters: a. Tube diameter *(d)*.

   b. Average coil diameter *(D_m)*.

   c. Cone angle *($\varnothing$)*.

Operating Parameters: a. Mass flow rates *(hot and cold fluid).*

b. Temperature Gradient *(hot and cold fluid).*

2. To study the effect of above geometric and operational parameters on heat transfer coefficient and pressure drop.

3. To establish correlations to determine the design parameters of conical coil heat exchangers.

The heat transfer analysis for the conical coil heat exchanger is carried out by a methodology given in figure 2.3.

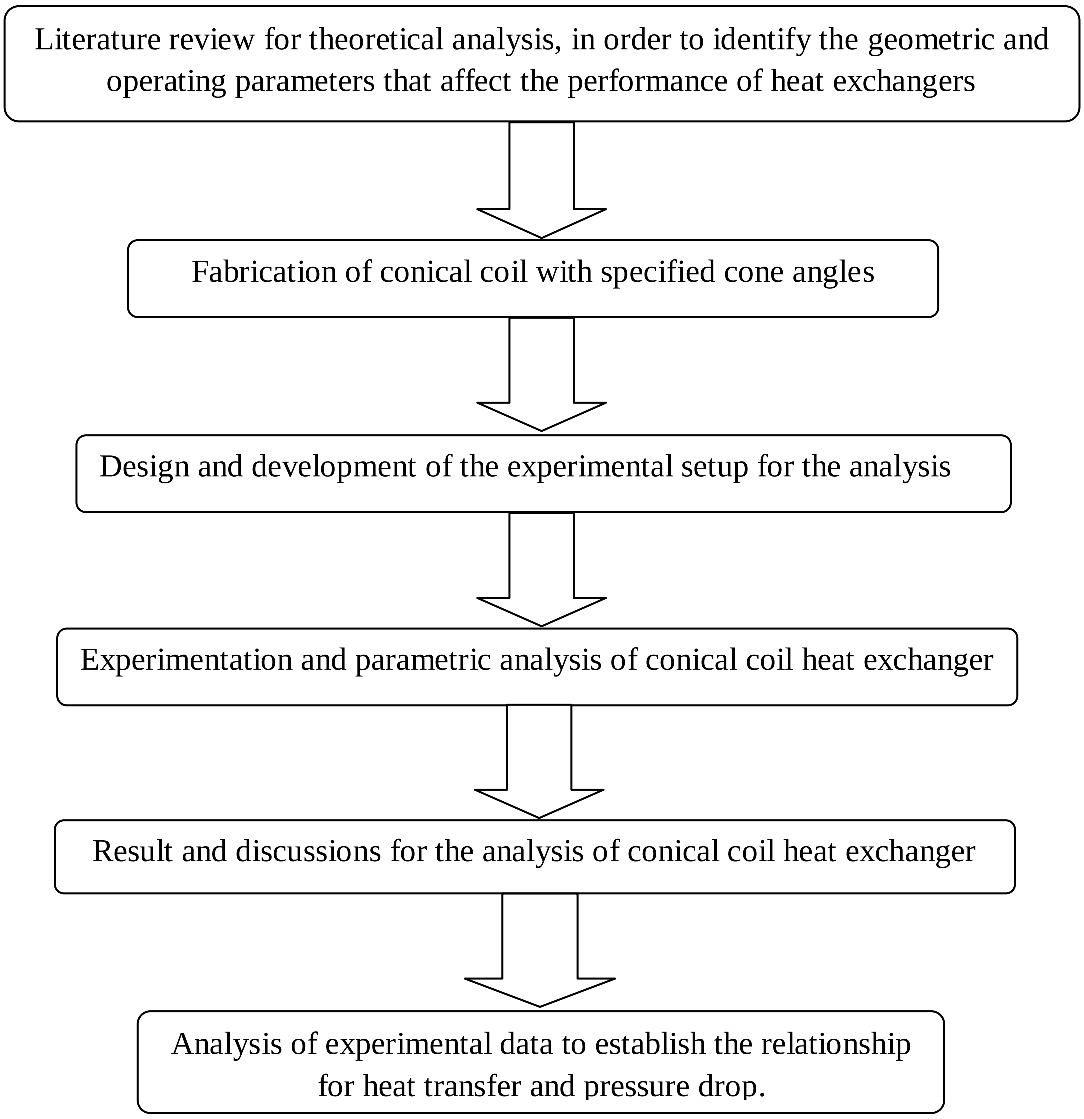

Fig. 2.3 Methodology for thermal and flow analysis in conical coil heat exchangers

Chapter 3

Experimental setup and Procedure

3.1 Selection of geometric and operating Parameters

For the selection of geometric parameters (coil diameter, tube diameter, cone angle) and the operating parameters (flow rates of tube side and coil side fluids, and inlet temperatures of shell side and tube side fluids) an extensive review of the similar studies in literature is done and presented in Table 3.1.

Table 3.1 Literature reviewed for selection of geometric and operating parameters

Reference	**Coil type**	**Data for experimentation**
Naphon [95] (Helical Coil)	Helical	Tube diameter: 7.75 × 9.5 mm Coil Diameter:127mm to 197mm Cold water flow rate: 0.1 to 0.22 kg/s Hot water flow rate : 0.02 to 1.12 kg/sec Inlet temperatures : Cold fluid– 15 to 25 ^{O}C Hot fluid – 35 to 45 ^{O}C
Jamshidi et al.[125] (Helical Coil)	Helical	Tube diameter 9 x 12.7 mm Coil diameters - 0.0813 to 0.116 m. Coil pitches of 0.013 to 0.018m. Shell side 0.0167 to 0.0667 kg/s Tube side 0.0167 to 0.0667 kg/s Inlet temperatures: Cold fluid – 25 ^{O}C Hot fluid– 50 ^{O}C
Shokouhmand et al. [103]	Helical	Tube diameter: 9 x 12, 12 x 16 mm Coil diameter : 120 mm Coil pitch of : 20.9, 21.4 and 26.7 mm Length of coil 225, 230 and 280 mm Hot fluid flow rate: 0.016 to 0.113 kg/sec Cold fluid flow rate : 0.019 to 0.136 kg/sec Inlet temperature: Cold fluid- 10.9- 19.2 ^{O}C Hot fluid- 33.4-53.2 ^{O}C

Genic et al. [130]	Helical	Tubes Sizes : 8x10 and 10x12 mm Coil diameters : 70 to 236 mm Coil pitch : 26.24 to 60 mm Length of tubes 5.97 to 9.5 m *Re* range : 1000 to 9000 *Pr* range : 2.6 to 6.0 Hydraulic diameter : 9.1 to 18.3 No. of coils : 2 to 16
Jaykumar et al. [158]	Helical	Tube size : 10×12 Coil diameter : 300 mm Pitch of Coil: 30 mm. Flow velocity in the pipe : 1.0 to 3.0 m/s *De* range: 3500 to 11,000 Inlet temperature Hot fluid : 85^{O}C Cold fluid: 27 ^{O}C
Ghorbani et al. [179]	Helical	Tube diameter: 8 × 10 and 11 × 13 Coil diameter: 125.71 Coil pitch: 16.47, 23.57 Tube side flow rate: 0. 0.09 - 0.113 kg/s Shell-side flow range: 024, 0.05 kg/s Inlet temperature: Hot water: 80^{O} Cold water: 24^{O}
Salimpour [181]	Helical	Tubes diameter : 9 × 12, 12 ×16 mm Coil diameter: 120 mm. Tube side flow rate : 0.013 to 0.122 kg/s Shell side flow rate : 0.058 to 0.062 kg/s Inlet temperature: Hot fluid:45 to 70 ^{O}C Cold fluid : 11.9 to 16.2
Naphon and Suwagrai [115]	Spiral	Tubes diameter 8 × 10 mm Length of tube: 5200, 4800 and 4000 Curvature ratio (δ) of 0.02 to 0.05 Hot water flow rate: 0.05 to 0.12 kg/s Cold water flow rate: 0.05 and 0.12 m/s

		Inlet temperature: Hot -45 to 60 ^{O}C Cold: 20 to 25 ^{O}C
Lu et al. [126]	Spiral	Tube size : 10 $\times$12 mm Coil diameter of 175, 201 and 227 mm pitch of 21, 19.16 and 19 mm *Re* in range of 500 to 3500
Gomaa et al. [180]	Spiral	Tube diameter 8 $\times$ 9.6 mm Lengths of tube 4500, 4200 and 4000 mm Tube side chilled water (5 ^{O}C) Mass flow rate of 0.05 to 0.14 kg/s Outside : air of velocity 1.4 to 9.60 m/s

In the analysis of coiled heat exchangers, many researchers used the tubes of 8X10 and 10X12 mm. Hence to study the effect of tube diameter (d_i) on the performance of the conical coil three different tube sizes are selected as 8x10, 10x12 and 12x15. The coil diameter is selected as 200 mm from the above literature review considering the possibility of coil fabrication without changing the shape of the tube and avoiding the formation of pinch in the coil.

For the analysis, five different cone angles are selected 0^{O}, 45^{O}, 90^{O}, 135^{O}, 180^{O} to study the effect of variation in heat transfer and fluid flow characteristics as a function of cone angle. The cone angles are selected on the basis pilot experimentation for the different cone angles.

In many studies, the heat transfer and fluid flow analysis is carried out for *Re* below 3500 or above 3500. To accommodate the upper range and lower range in the present study, the *Re* range from 500 to 5500 is selected. Flow rates are decided on the values reported in literature, with tube side velocity as 0.02 to 0.5 m/s in the laminar zone ($Re < Re_{critical}$). The critical value of *Re* ($Re_{critical}$) in *is* the value at which laminar flow changes into turbulent. In the literature, it was observed that many researchers have considered the *De* values upto 1200. This parameter was also taken into consideration at the time of finalization of the tube sizes and the flow rates. The parameters selected for the present work are given in Table 3.2.

Table 3.2: Geometric and operating parameters selected for analysis

Sr. No.	Parameter	Specification(s)
1	Coil Mean Diameter (*mm*)	200
2	Coil Pitch (*mm*)	O.D. of the tube
3	Cone angle	0^O (helical), 45^O, 90^O, 135^O, and180^O (spiral)
4	Tube size: I.D.× O.D. (*mm*)	8X10, 10X12, 12X15
5	Inlet temperature of tube side fluid (^OC)	70 (water)
6	Inlet temperature of shell side fluid (^OC)	24 (water)
7	Hot water flow rate (*lph*)	10 to 100 (*Re:*500 to 5000; *De:* 120 to 1200)
8	Cold water flow rate (*lph*)	30 to 90

3.2. Fabrication of conical coils

The analysis of the conical coil heat exchanger is carried out using the coils of same length with different tube sizes and cone angles. Copper tubes of different sizes, 8×10, 10×12 and 12×15 (mm), and cone angles, 0^O, 40^O, 90^O, 135^O and 180^O were fabricated. The length of all the coils was same (3m). Each coil was prepared using a wooden former having the required dimensions for and a specific cone angle. Five different wooden formers (Fig. 3.1) were prepared for this purpose. Coils were tightly wound over theses formers.

During the formation of the coil, the possibility of tube pinch and deformation in the uniform shape was reduced by filling the tubes with fine sand before winding on the wooden formers. To reduce the spring back action of the coils during winding, the tubes were preheated to about 80-100 ^OC and then wound over the formers. This process also helped in maintaining the required dimension by reducing the deformations. After completing the winding process, the coils were flushed using compressed air to completely remove the sand. A total of 15 coils were prepared with the geometric parameters as shown in Table 3.2.

Fig. 3.1 Conical coil formers for coil fabrication

Table 3.3 Geometric parameters of the coils formed

Sr. No.	Tube dim. (IDXOD) in mm	Cone Angle	Coil Diameter in mm	Pitch in mm
1	8X10 (Tube length=3m)	Helical (0^O)	200	8
		45^O	200	8
		90^O	200	8
		135^O	200	8
		Spiral (180^O)	200	8
2	10X12 (Tube length=3m)	Helical (0^O)	200	10
		45^O	200	10
		90^O	200	10
		135^O	200	10
		Spiral (180^O)	200	10
3	12X15 (Tube length=3m)	Helical (0^O)	200	12
		45^O	200	12
		90^O	200	12
		135^O	200	12
		Spiral (180^O)	200	12

The coils were fabricated with end connections in the form of bends with the same size of the tubes and the extensions that are required for connecting the other accessorial parts required for the test setup (Fig. 3.2). The dimensions of the extensions were selected in such a way that the surface area remains same for all coils. After fabrication of the coils with extensions coils were tested for leakage.

Fig. 3.2 Conical coils fabricated for analysis

3.3 Assembly of heat exchanger

For the experimental analysis, the conical coils were housed in a mild steel cylindrical shell (diameter: 300 mm, length: 160 mm). The shell dimensions were selected such that the all sizes of the fabricated coils could be accommodated in the shell. Two connections were provided on the curved surface of the shell for inlet and outlet flows. In the top cover of the shell, the provision for the two connections (inlet and outlet) of the coil extensions was made. All the four ends of the extensions (shell side & tube side) were brazed with threaded adaptors (½' 'T'). One end of the T was connected to heat exchanger and other opposite end was connected to supply/discharge line. At the third end, a thermocouple probe is inserted with proper mountings to avoid leakage of water. With this arrangement the temperatures of inlet and outlet cold and hot water were measured. The shell and the extensions were insulated by Polyurethane foam layer of 6 mm thick to avoid the heat loss due to convection from outer surface.

3.4 Experimental setup

The experimental setup comprised of the following main components:

a. Conical coil heat exchanger
b. Hot water supply system
c. Constant temperature cold water source

The schematic of the experimental setup is shown in figure 3.3 and the actual setup developed for the analysis is given in figure 3.4 The components selected for the experimental setup are properly arranged on the specially developed frame considering operational safety and suitability of recording the observations.

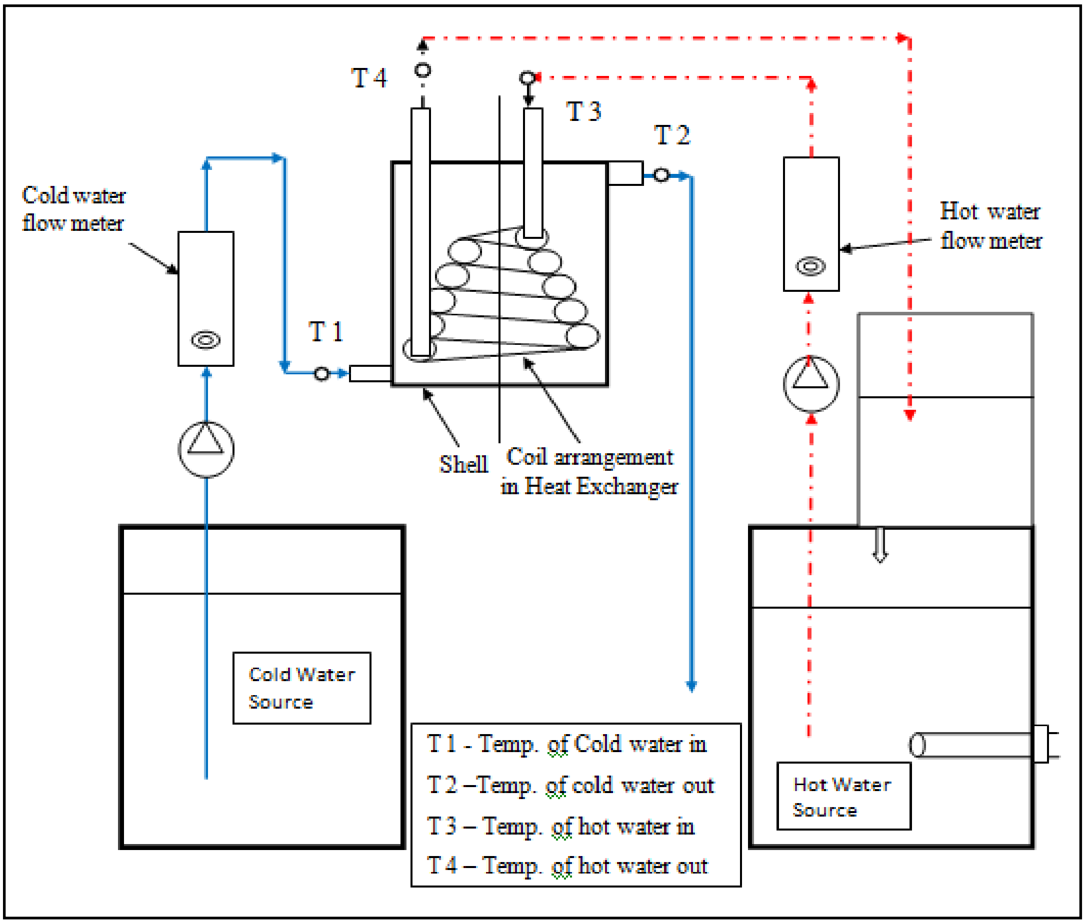

Fig 3.3 Schematic of experimental setup

For the experimental runs on a particular size coil, the coil was fitted in the shell. Cold water was supplied from a storage tank of capacity 500 liters, which ensured the constant temperature of the cold water at the inlet. The hot water was supplied from the hot water source which was maintained at constant temperature. The hot water source was developed with thermostatic feedback controlled system. The variation of ±1.5% over the set maximum temperature of $70^{O}C$ for the hot water source is allowed by this control.

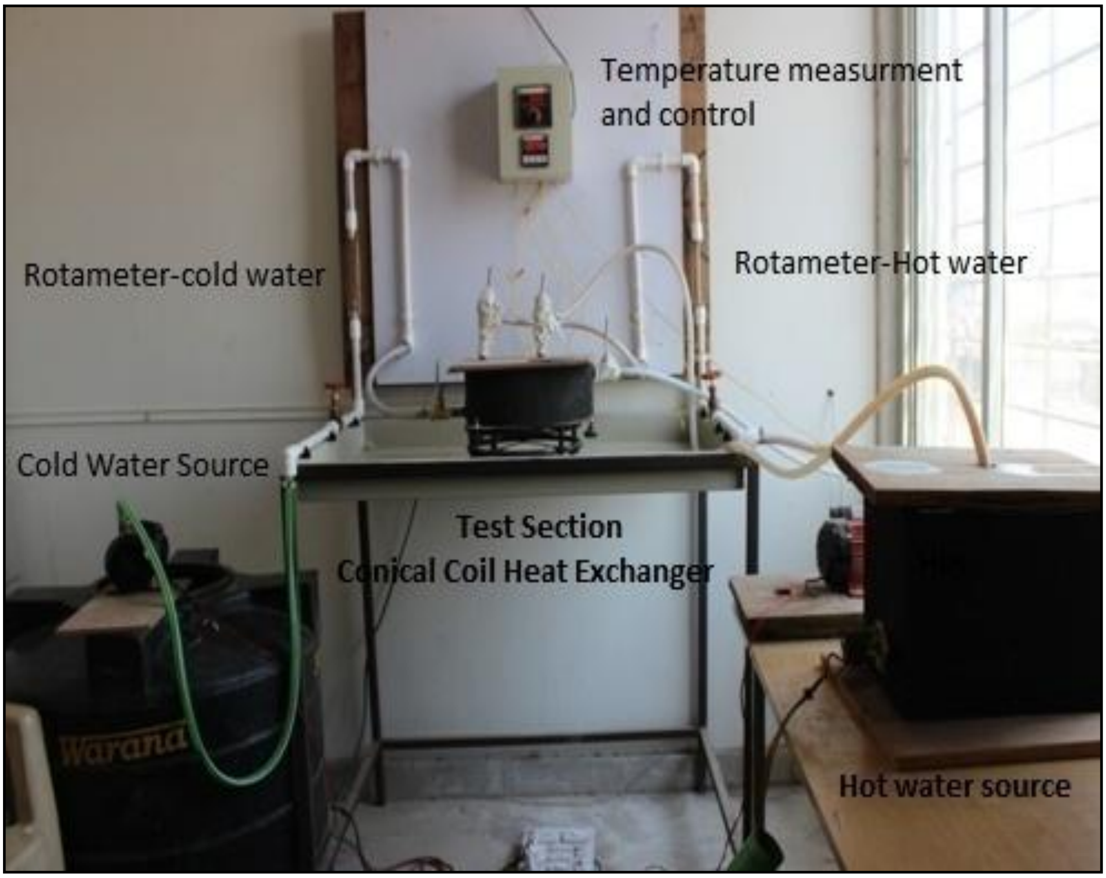

Fig. 3.4 Actual Experimental setup

The flow of water (hot and cold) to the heat exchanger was maintained by pumps. The flows were controlled by flow control valves installed on both hot and cold water supply lines. The flows were measured with the help of rotameters (error of measurement upto 1.5% for maximum flow condition). The temperatures were recorded with the eight channel temperature scanners with five different temperature sensors (*k-type thermocouple, Make – Kristake Instruments and transducers, with* *accuracy of 0.1*). First four channels are used for recording the temperatures of the inlets and outlets of heat exchanger, and the fifth was for hot water bath temperature controller. The inlet temperature of the hot and cold water were always monitored and maintained for entire test runs.

Pressure drop analysis was carried out with the help of piezometer tube, with the accuracy of 0.5 mm of water column. For the pressure measurements, the temperature probes are replaced by pizometer tube connection which directly gives the pressure drop across the coil placed in the heat exchanger.

3.5 Experimental Procedure

The experimental procedure was set for conducting the experiments. Before starting the experiments, sufficient amount of water was stored in the hot and cold water tanks to avoid the dry out condition. The flow of cold water on shell side was started by switching on the pump provided on the cold water flow path. The temperature of hot water was brought to 70^{O} and then the supply of hot water was started to the tube side in the heat exchanger. The flow of cold and hot water were adjusted to desired values by adjusting the valves mounted in the lines. The steady state was confirmed by no change in the temperature readings with respect to time.

For the pressure drop measurements the thermocouples were replaced by pizometer tube connections. By adjusting the flow with the help of the valve, pressure drop reading were recorded for different tube side flow rates.

Chapter 4

Methodology for Data Analysis

4.1 Calculation of overall heat transfer coefficient

The overall heat transfer coefficient was calculated from the temperature and flow rate data recorded using the following equation [179],

$$U_O = \frac{q_{avg}}{A_o * LMTD} \quad \text{----- 4.1}$$

q_{avg} was calculated from the average values of q_h and q_c, given by the following equations:

$$q_h = m_h. Cp_h. (T_3 - T_4) \quad \text{------ 4.2}$$

$$q_c = mc. Cp_c. (T_2 - T_1) \quad \text{------ 4.3}$$

LMTD is calculated as,

$$LMTD = {\Delta T1 - \Delta T2} \Big/ {\ln(\frac{\Delta T1}{\Delta T2})} \quad \text{-------4.4}$$

Where,

$$\Delta T_1 = T_3 - T_2 \quad \text{------ 4.5}$$

$$\Delta T_2 = T_4 - T_1 \quad \text{------ 4.6}$$

4.2 Calculation of tube side heat transfer coefficient

One of the most widely used methods for calculations of heat transfer coefficient is the Wilson plot method. This method was developed for condensation heat transfer. However, Wilson plot method was used for the heat exchanger (water/water configuration) by Shokouhmand et al. [79] and Salimpour [180] in their works.

In this method, the heat transfer coefficient is calculated based on the overall temperature difference and the rate of heat transfer. This method is selected to avoid the disturbances caused by flow patterns and thus heat transfer during the experimental runs. Wilson plots were plotted by calculating the overall heat transfer coefficients for a number of trials where shell side fluid flow was kept constant and the tube side flow was varied. The overall heat transfer coefficient was correlated with the inside and outside heat transfer coefficients, in the form of a straight line, as shown in the following equation:

$$\frac{1}{U_0} = \frac{A_o}{A_i h_i} + \frac{A_o \ln\left({D_i}/{d_o}\right)}{2\pi k L} + \frac{1}{h_o}$$

------ *4.7*

In this equation, the unknown variables are the heat transfer coefficients. The outside heat transfer coefficient was considered to be constant by keeping the mass flow rate in the shell side constant. The inside heat transfer coefficient was assumed to vary in the following manner [180]:

$$h_i = C\, v_i^n$$ ------ *4.8*

Substituting the value of h_i in above equation, the equation may be written in the following form,

$$Y = m\, X + C$$ ------ *4.9*

Where

$Y = 1/U_o$

$m = A_o/ (C.A_i)$

$X = 1/v^n$

$$C = \frac{A_o \ln\left(\frac{D_i}{D_o}\right)}{2\pi k L} + \frac{1}{h_o}$$

------ *4.10*

The values for the constant, *C*, and the exponent *n*, were determined through curve fitting. The inside and outside heat transfer coefficients (h_i and h_o) were then calculated. This procedure was repeated for each value of shell side flow. After calculating the value of h_i, Nusselt number was calculated using the following equation,

$$Nu = \frac{h_i * d}{k}$$ ------ *4.11*

4.3 Calculation of effectiveness

Heat exchanger's effectiveness was calculated by using the ratio of actual heat transfer to maximum possible heat transfer as,

$$\varepsilon = \frac{C_h (t_1 - t_2)}{C_{min}\, (t_1 - t_3)} = \frac{C_c (t_3 - t_4)}{C_{min}\, (t_1 - t_3)}$$ ------ *4.12*

where,

C_h and C_c are the heat capacities of hot and cold fluids. C_{min} is the minimum of these two heat capacities.

$$C_h = m_h\, C_{pw}$$

$$C_c = m_c\, C_{pw} \qquad \text{------ } 4.13$$

4.4 Friction factor calculations

Friction factor is calculated by using the pressure drop across the coil as,

$$f = \frac{1}{2}\frac{\Delta P}{L}\frac{d_i}{\rho U^2} \qquad \text{------ } 4.14$$

4.5 Regression Analysis

4.5.1 Correlation of *effectiveness* (ε) Vs *flow ratio* (Z)

The functional relationship between the effectiveness and flow ratio was discussed by Ghorbani et al. [181], for the helical coil heat exchangers, in the following form:

$$\varepsilon = a.\,(Q_h/Q_c)^{\,b} \qquad \text{------ } 4.15$$

where, a and b are the constants.

These constants are calculated by curve fitting method separately for each cone angle. The relation of equation 4.15 is useful for the calculation of the exit temperatures of hot and cold fluids.

4.5.2 Correlation for *Nu*

The thermal analysis from the literature as well as experimental analysis shows that *Nu* is the function of flow parameter (*Re/De*), fluid parameter (*Pr*) and coil geometry parameter (δ) [75]. It is given in the power law form as,

$$Nu = a_1 Re^{a_2} Pr^{a_3} \delta^{a_4} \qquad \text{------ } 4.16$$

$$Nu = b_1 De^{b_2} Pr^{b_3} \qquad \text{------ } 4.17$$

where, a_1, a_2, a_3, a_4, *and* b_1, b_2, b_3, are the constants. These constants are evaluated by regression analysis for each cone angle separately.

4.5.3 Correlation for friction factor (*f*)

Friction factor (*f*) is mainly a function of two parameters viz. flow parameter (Re) and coil parameter (δ) [185]. The following functional form is generally used to relate *f* with Re and δ,

$$f = c_1 Re^{c_2} \delta^{c_3} \quad \text{------- } 4.18$$

Where c_1, c_2 and c_3 the constants, and are evaluated by regression for each cone angle.

4.6 Uncertainty analysis

Experimental analysis is the need in science and technology. Instrumentation inaccuracies, measurement techniques, limitations in the experimental facilities, environmental variability carry the error in the experimental results. To quantify the degree of accuracy, the concept of uncertainty is used in the experimental result and considered as the best estimate of the experimental error.

In practice, single-sample experiments are preferable in practical situations. In single-sample experiments, the uncertainty is measured from the input variables. To estimate the uncertainty the methodology associated with the propagation of the uncertainties in the input parameters are analyzed with the data reduction equations. Therefore, this provides a useful tool in understanding the behavior of the uncertainty in each input variable through the data reduction equations.

Calibration of flow and temperature measuring devices are necessary in order to minimize error occurred during measurements. The standard equations used for calculations of heat transfer, pressure drop, mixed convection heat transfer, thermo hydraulic performance and uncertainty in Reynolds number, Dean Number, friction factor and Nusselt number, are presented.

The errors in the experimentation are based on the least counts of the instruments used and the sensitivities of the measuring instruments used for the investigation. The sensitivity data of the instruments used in the present study is shown in Table 4.1.

Table 4.1 Sensitivity of instruments used for experimentation

Sr. No.	Quantity	Exact value (Q)	Error in measurement (Δ Q)	Uncertainty in measurement (Δ Q/Q)
1	Diameter of tube, d_i	10×10^{-3} *m*	0.0002 m	0.2
2	Mead diameter of coil, *D*	200×10^{-3} *m*	0.0002 m	0.01
3	Max flow rate of Hot water	100 *lph*	2.5 *lph*	0.025
4	Max flow rate of cold water	150 *lph*	2.5 *lph*	0.0166
5	Temperature , t_{hi}, average	70 ^{O}C	1^{O}C	0.014
6	Temperature, t_{ci} , average	20 ^{O}C	1^{O}C	0.05
7	Temperature , t_{ho}, average	50 ^{O}C	1^{O}C	0.02
8	Temperature, t_{co} , average	45 ^{O}C	1^{O}C	0.022
9	Total height of pressure drop column	0.5 m	0.001 m	0.0005

The uncertainty propagation in the data variables is calculated by following method as below,

1. Area

$$A = \frac{\pi}{4} \times {d_i}^2 \qquad \text{----- } 4.19$$

$$U_A = \frac{\Delta A}{A} = \left[\left(2\frac{\Delta d_i}{d_i}\right)^2\right]^{0.5} \qquad \text{----- } 4.20$$

2. Curvature Ratio

$$\delta = \frac{d_i}{D_i} \qquad \text{----- } 4.21$$

$$U_\delta = \frac{\Delta \delta_i}{\delta_i} = \left[\left(\frac{\Delta d_i}{d_i}\right)^2 + \left(\frac{\Delta D}{D}\right)^2\right]^{0.5} \qquad \text{----- } 4.22$$

3. Volume flow rate of cold fluid

$$U_{Q_C} = \frac{\Delta Q_c}{Q_c} = \left[\left(\frac{\Delta V}{V}\right)_C\right] \qquad \text{------ } 4.23$$

4. Volume flow rate of hot fluid

$$U_{Q_h} \frac{\Delta Q_h}{Q_h} = \left[\left(\frac{\Delta V}{V}\right)_h\right] \quad \text{------ } 4.24$$

5. Pressure drop

$$\Delta P \; \alpha \; h \quad \text{------ } 4.25$$

$$U_{\Delta P} \; \frac{\Delta(\Delta P)}{\Delta P} = \frac{\Delta h}{h} \quad \text{------ } 4.26$$

6. Heat Transfer coefficient

$$U_{h_i} = \frac{\Delta h_i}{h_i} = \left[\left(\frac{\Delta Q}{Q}\right)^2 + \left(\frac{\Delta d_i}{d_i}\right)^2 + \left(\frac{\Delta L}{L}\right)^2 + \left(\frac{\Delta(\Delta T)}{\Delta T}\right)^2\right]^{0.5} \quad \text{------ } 4.27$$

7. Reynolds Number

$$Re = {4\dot{m}}/{\pi d_i \mu} \quad \text{------ } 4.28$$

$$U_{Re} = \frac{\Delta Re}{Re} = \left[\left(\frac{\Delta \dot{m}}{\dot{m}}\right)^2 + \left(\frac{\Delta d_i}{d_i}\right)^2\right]^{0.5} \quad \text{------ } 4.29$$

8. Dean Number

$$U_{De} = \frac{\Delta De}{De} = [(U_{Re})^2 + \; (U_\delta)^2]^{0.5} \quad \text{------ } 4.30$$

9. Nusselt Number

$$U_{Nu} = \frac{\Delta Nu}{Nu} = \left[\left(\frac{\Delta h_i}{h_i}\right)^2 + \left(\frac{\Delta d_i}{d_i}\right)^2\right]^{0.5} \quad \text{------ } 4.31$$

10. Friction factors

$$f = \frac{1}{2}\left(\frac{\Delta P}{L}\right)\left(\frac{\rho d_i{}^3}{Re^2 \mu^2}\right) \quad \text{------} 4.32$$

$$U_f = \left(\frac{\Delta f}{f}\right) = \left[\left\{\frac{\Delta(\Delta P)}{\Delta P}\right\}^2 + \left\{\frac{\Delta L}{L}\right\}^2 + \left\{\frac{3\Delta d_i}{d_i}\right\}^2 + \left\{\frac{2\Delta Re}{Re}\right\}^2\right]^{0.5} \quad \text{------ } 4.33$$

The uncertainty in the experimentation is calculated by using the values of uncertainties contributed by each element as given in Table 4.2.

Table 4.2: Uncertainty of different parameters

Sr. No.	Quantity	Uncertainty	% Uncertainty
1	Area (*A*)	$4X10^{-3}$	0.04
2	Curvature ratio (δ)	0.0020	0.20
3	Volume flow rate cold fluid	0.0166	1.66
4	Volume flow rate hot fluid	0.0250	2.50
5	Pressure drop (Δp)	0.0020	0.20
6	Heat Transfer coefficient	0.0610	6.10
7	Reynolds Number (*Re*)	0.0250	2.50
8	Dean Number (*De*)	0.0254	2.54
9	Nusselt Number (*Nu*)	0.0610	6.10
10	Friction factor (*f*)	0.0532	5.32

Chapter 5

Results and Discussion

In heat transfer analysis, Nu is a measure of the thermal performance. The thermal performance of the conical coil heat exchanger is investigated by studying the effect of different parameters on Nu. The parameters selected for the analysis are: tube side and shell side flows (Q_h, Q_c), cone angle (θ) and flow ratio (Q_h/Q_c). The effectiveness of conical coil heat exchanger as a function of Re and tube diameter (d_i) is also analysed.

Pressure drop across the heat exchanger determines the power required for pumping. In the heat exchanger analysis, friction factor (f) is the measure of the pressure drop. The pressure drop analysis is carried out by investigating the effect of Re and tube diameter (d_i) on friction factor (f).

A total of 15 conical coils, of three different tube diameters (ID×OD: 8×10, 10×12, 12×15) and five cone angles (0^O, 45^O, 90^O, 135^O, 180^O), are used for the analysis. The constant parameters are length of tube ($L=3m$) and mean diameter of coil ($D=200\ mm$). Based on the analysis, the following correlations are proposed:

- Effectiveness as a function of flow ratio.
- Nu as a function of flow parameter (Re/ De), fluid parameter (Pr) and geometric parameter (δ).
- Friction factor (f) as a function of Re and δ.

Some of the results are presented as a function of tube flow rate (Q_h) instead of Re, because, the lower and upper limits of Re change with the change in tube diameter for the same value of flow rate.

5.1 Effect of Q_h on Nu

Figure 5.1 shows the variation of Nu with Q_h for different cone angles, keeping the other parameters (D_m, d_i, d_o, Q_c) same.

This figure shows that Nu increases with increase in tube side flow rate (Q_h) for all the coils. This may be due to an increase in the velocity of tube side fluid. The increased velocity causes an increase in the intensity of secondaries developed in the tubes [14, 181]. The secondaries move the fluid particles across the tube; thus, reducing the laminar boundary layer thickness along the flow, thereby improving fluid mixing.

It is also observed that, for a given Q_h, *Nu* is highest for the helical coil *(0^O)* and lowest for the spiral coil for in case of conical coils, for all cone angles and flow rates. However, a decrease in *Nu* is observed with an increase in cone angle.

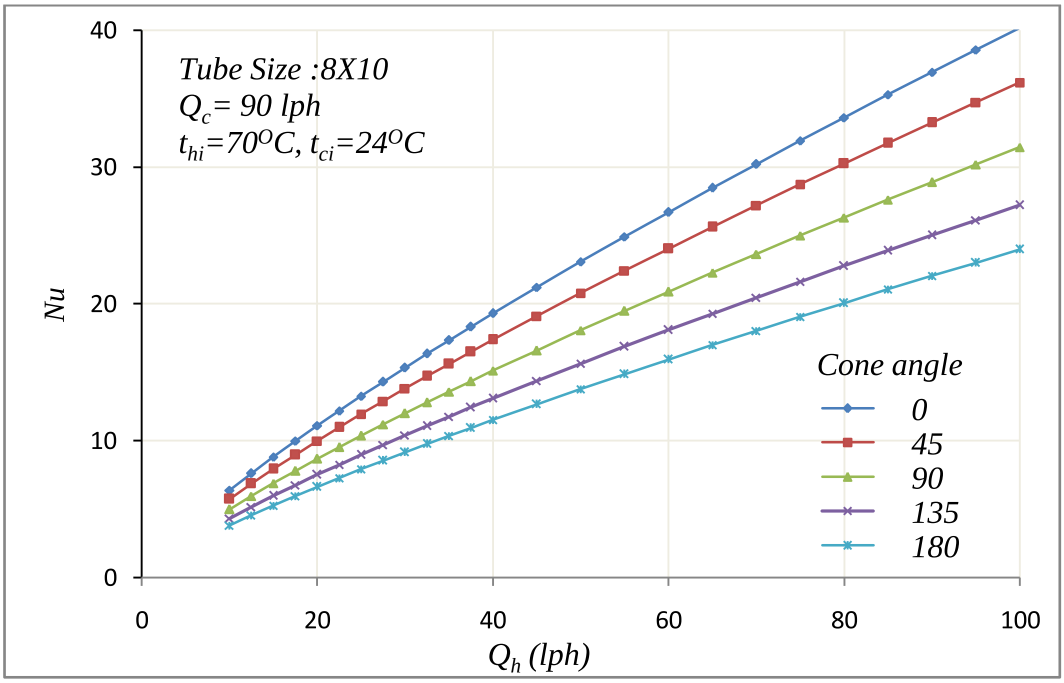

Fig. 5.1 Variation of *Nu* with Q_h for different cone angles (tube size- 8×10)

This may be due to the change in intensity of the secondary flow which is a function of coil diameter (*D*). For a helical coil, the coil diameter (*D*) is uniform throughout the length of the coil, and uniform secondaries are obtained throughout the length of the coil. This keeps the uniform heat transfer per unit surface area [59]. In case of a conical coil, the intensity of secondaries is more in upper part of the coil; whereas, the intensity of secondaries is less in the lower part. However, the tube surface area in the lower part of the coil is more as compared to the upper part area. As the cone angle increases, the variation in this area (below and above the mean diameter, D_m) increases, which results in the lesser heat transfer in the high intensity zone and more area in low intensity zone. This result in the reduction of overall intensity of secondaries developed in a coil, thus, *Nu* decreases with an increase in cone angle. The *Nu* drops to a value of about 48% from helical to spiral coil at Q_h = 100 *lph.*

Similar results were obtained for the coils of different tube diameters as shown in Figures 5.2 (a & b). Maximum value of 50 for *Nu* was obtained in 8×10 diameter tube at Q_h equal to 100 *lph* and Q_c equal to 30 *lph* (Figure A1).

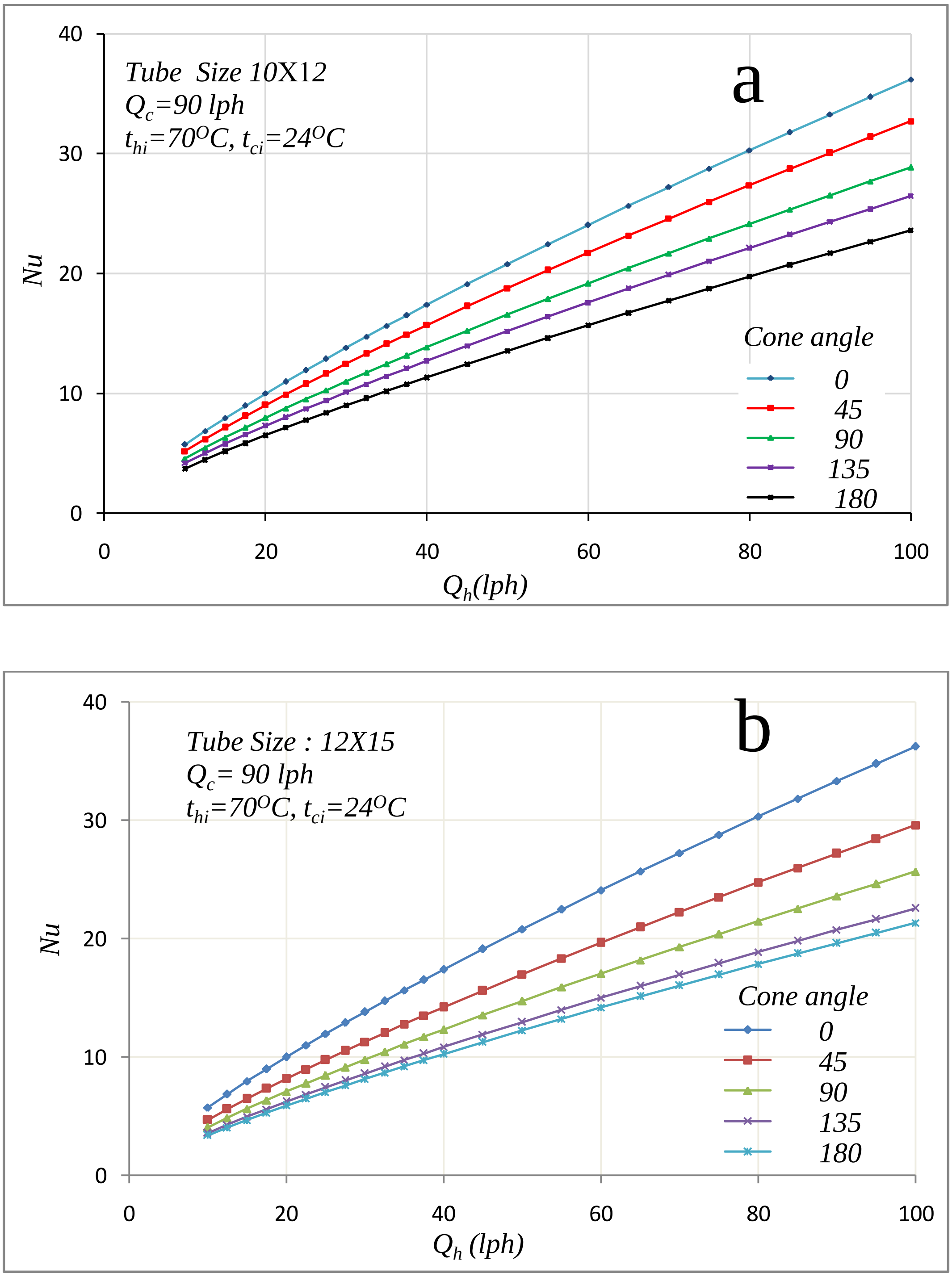

Fig. 5.2 Variation of *Nu* with Q_h for different cone angles [tube size: (a) 10×12 (b) 12×15]

Figure 5.3 shows the variation of *Nu* with tube side fluid flow (Q_h) for coils of different tube diameters (d_i) keeping other parameters (D, Q_c, *and* θ) same. The figure shows that the tube diameter (d_i) has significant effect on the performance of the coiled tube heat exchanger. As tube diameter (d_i) increases, *Nu* decreases for the same tube side flow rate, which may be due to the reduction in intensity of secondaries in larger diameter tubes. Kalb and Seader [69] have also reported that the intensity of the secondaries is a function of tube diameter.

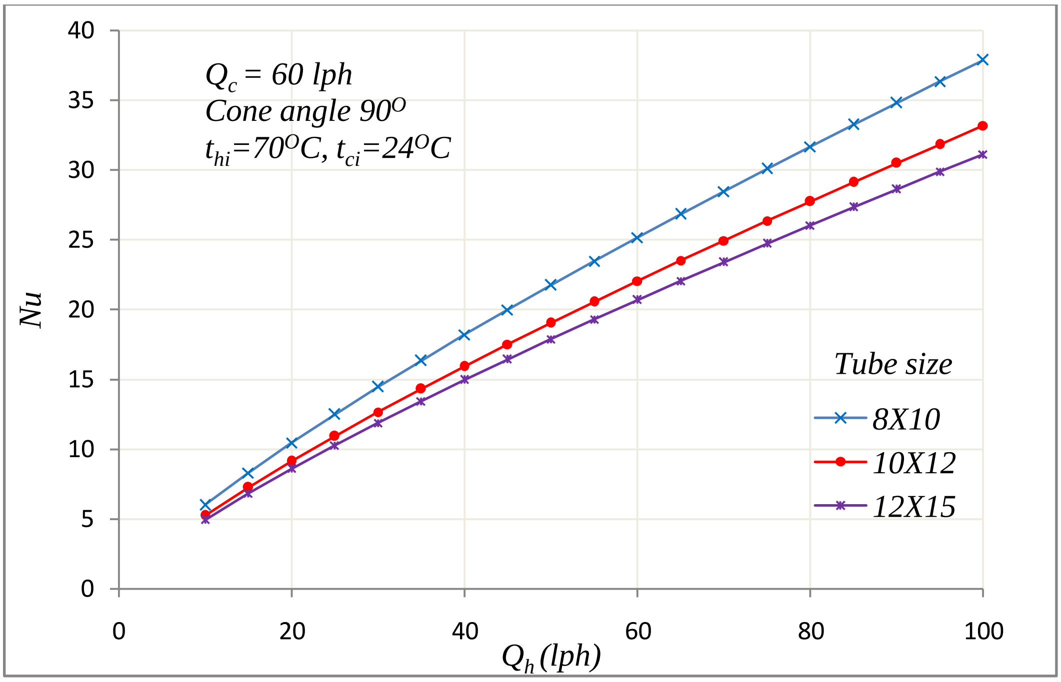

Fig. 5.3 Variation of *Nu* with Q_h for coils of different tube sizes (cone angle- 90^O)

Also, as tube diameter (d_i) increased from 8 mm to 10 mm, the average drop in *Nu* was 18%; whereas, when the coil diameter was changed from 10 mm to 12 mm the average drop in *Nu* was 10%. This shows that in the small diameter tubes, the intensity of secondaries gets remarkably enhanced which increases the *Nu*.

Similar results were obtained for the coils of different cone angles [Fig 5.4 (a & b)]. These figures show that when the tube size was changed from 8×10 to 10×12, the % reduction in *Nu* was about 17%, and when the tube size was changed from 10×12 to 12×15 the % reduction in *Nu* value is 9.5%.

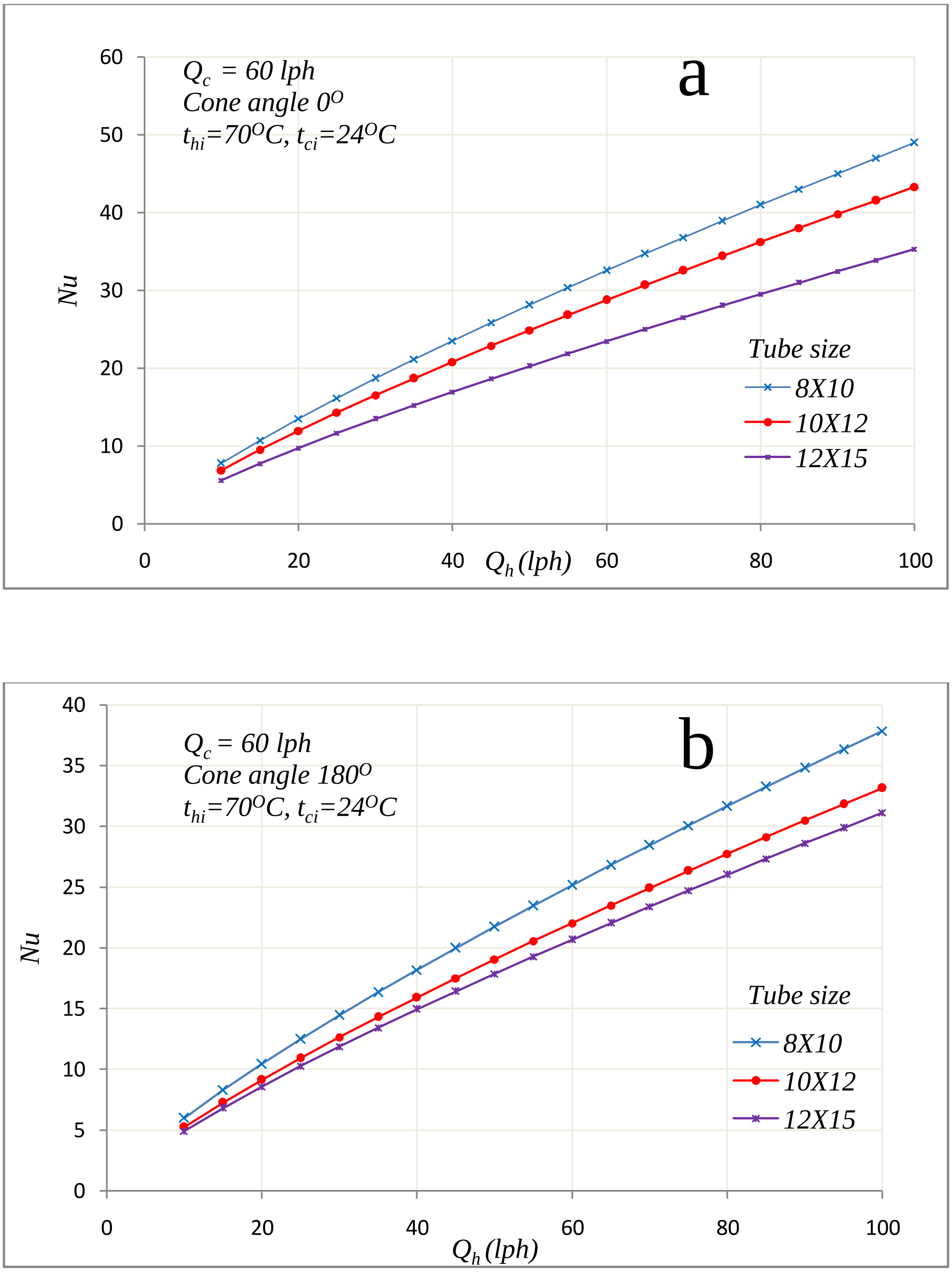

Fig. 5.4 Variation of *Nu* with Q_h for coils of different tube sizes [(a) cone angle 0^O and (b) cone angle 180^O]

5.2 Effect of Q_c on *Nu*

Figure 5.5 shows the variation of *Nu* with shell side flow rate (Q_c) for constant tube side flow rate (*Re*).

The figure shows that for a given tube side flow rate (*Re*), *Nu* decreases with increase in shell side flow rate (Q_c). This may be due to water stagnation between the coiled tubes, which acts as semi-dead zone for the fluid flow over the tubes.

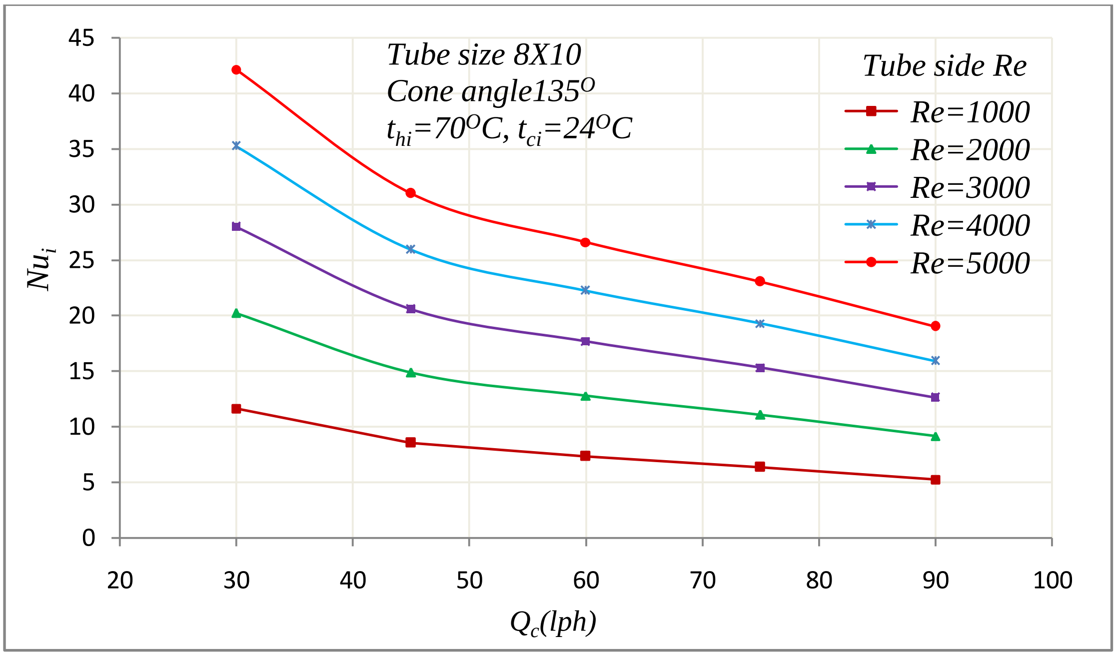

Fig. 5.5 Variation of *Nu* with Q_c for different tube side *Re* (tube size-8×10)

Also, the Figure (5.5) shows that at low flow rates, the tendency of fluid lock in between the tubes is less and fluid is flowing over entire periphery of the coiled tube, and a high value of *Nu* is observed. As shell side velocity (Q_c) increases, the tendency of fluid lock in between the turns of the coil increases due to flow of the fluid particles over the tube surface, this phenomena lowers the value of *Nu* at higher flow rates. The figure also shows that at high values of *Re* the effect of fluid stagnation on *Nu* is more. Also, the tendency of fluid stagnation between the turns of the coil increases with increase in cone angle.

Figures 5.6 (a & b) with the same flow rates and cone angles and different tube diameters show the similar trends. The value of *Nu* changes from 44 at 30 *lph* for 8×10 size tube to 5 at 90 *lph* for 12×15 size tube.

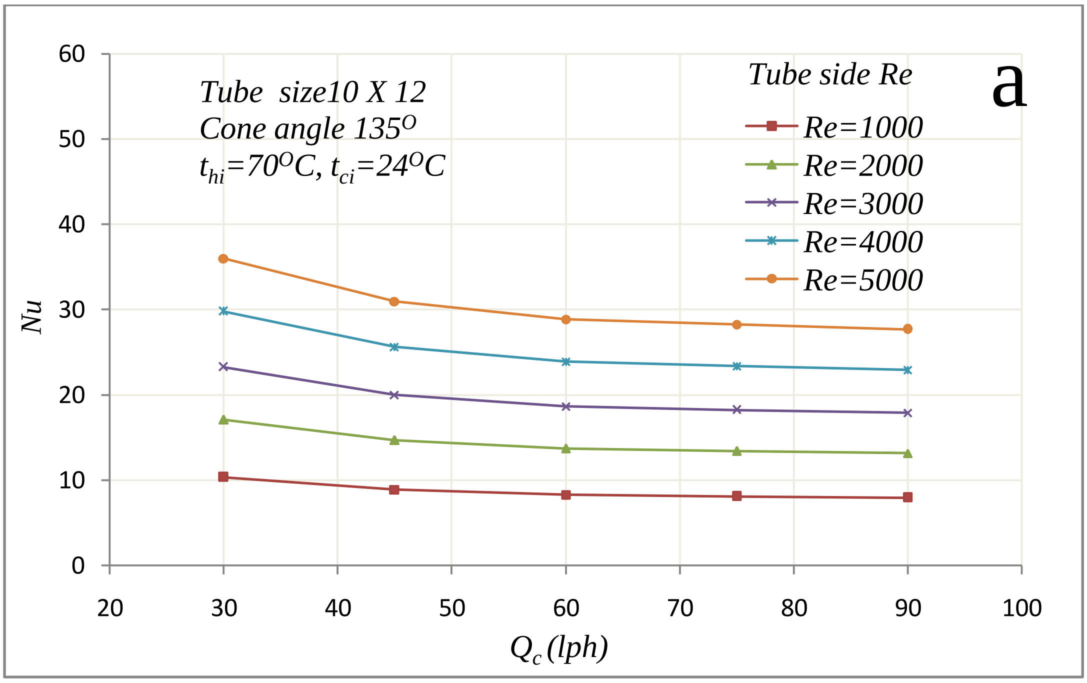

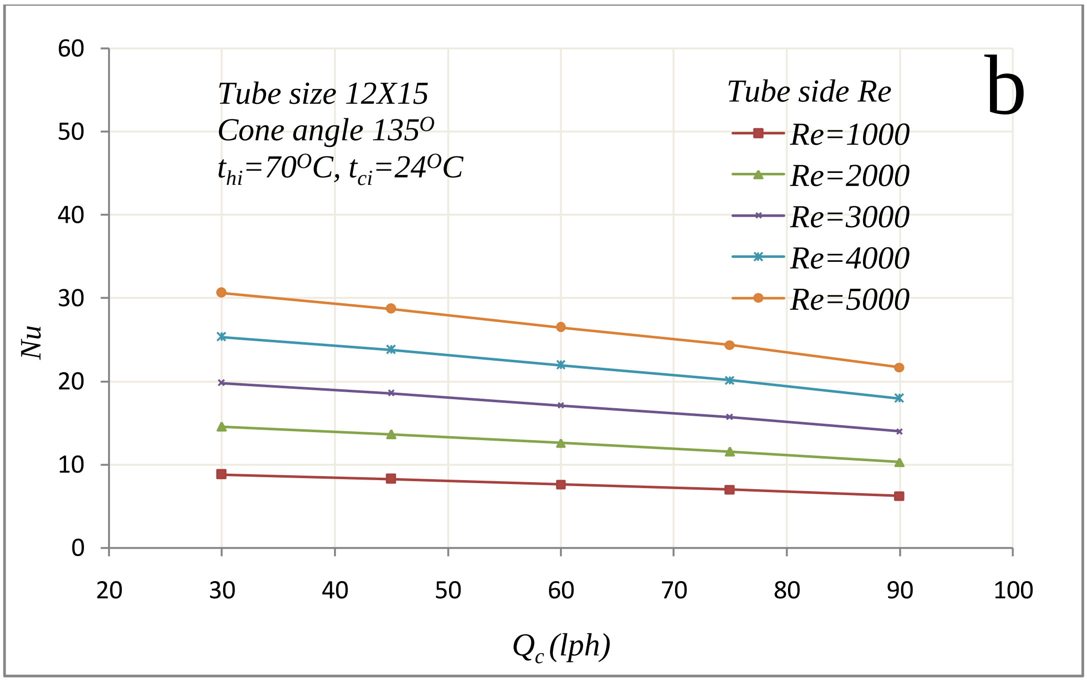

Fig. 5.6 Variation of *Nu* with Q_c for different tube side Re [(a) tube size-10×12 (b) tube size 12×15]

Figure 5.7 show the variation of *Nu* with Q_c for coils of different tube diameters (d_i) with same Q_h. As the tube diameter increases, *Nu* reduces for the same shell side flow rate (Q_c). This may be due to the compact structure of coil for large tube diameters. The compactness of the structure increases the fluid lock and results in the less heat transfer across the tube length. However, this effect may reduce if the pitch of the coil is increased as is observed in [101] for helical coils.

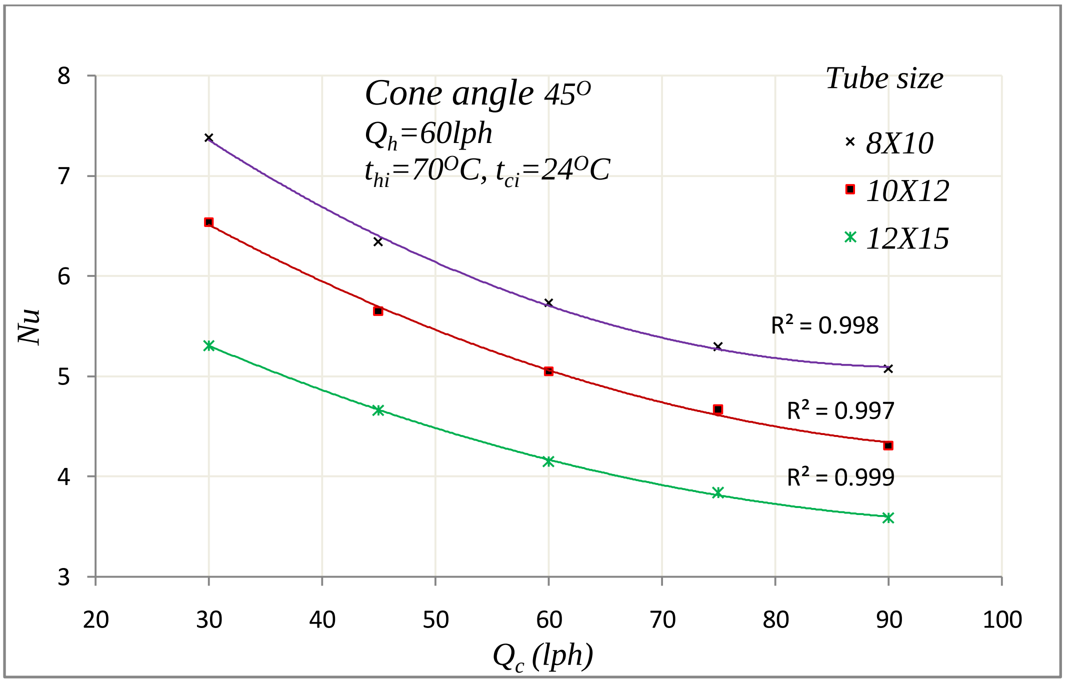

Fig.5.7 Variation of *Nu* with Q_c for coils of different tube diameters (d_i)

The figure shows that with increase in tube diameter, the % variation in *Nu* as a function of shell side flow reduces. At low flow rates, the % variation in *Nu* is high; this indicates that at low flow rates the effect of fluid lock is less. Hence, in the tested coils, for the shell side flow rate values of upto 45 *lph*, the conical coil heat exchangers are more efficient.

Similar results are recorded for helical and spiral coils (Figure 5.8 a & b). These figures show that the percentage variation in *Nu* with Q_c, for 8×10 size tube is higher as compared to the other sizes. As the tube diameter increases, the variation in *Nu* with Q_c reduces (for 10×12 tube: variation is 16 to 5%; for 12 × 15 tube: variation is 13 to 2%).

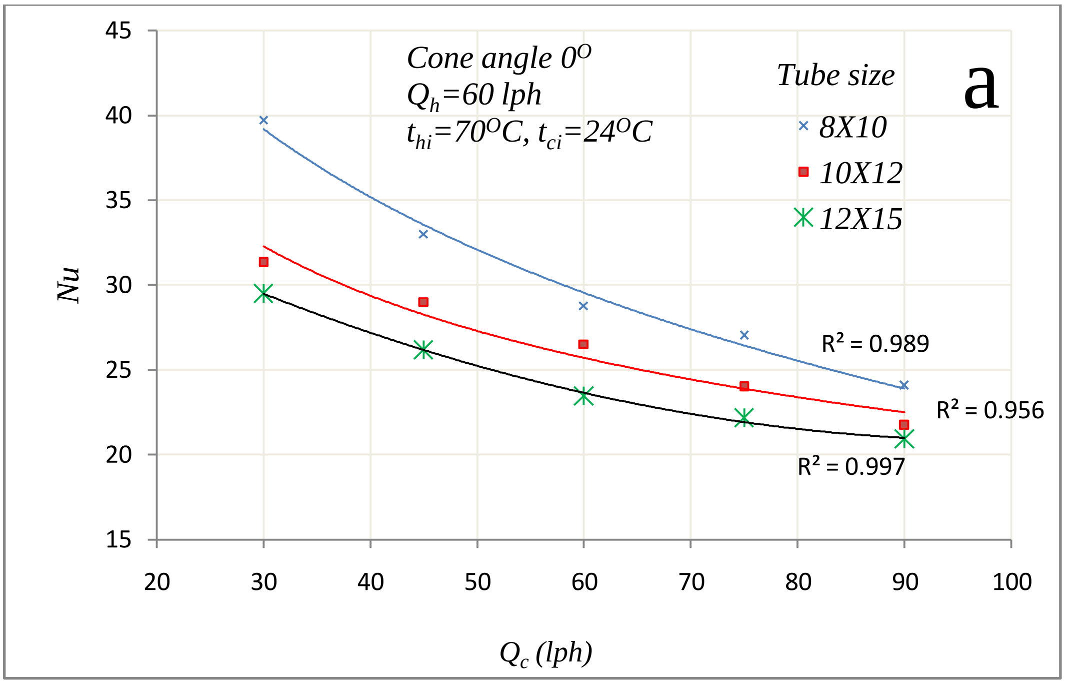

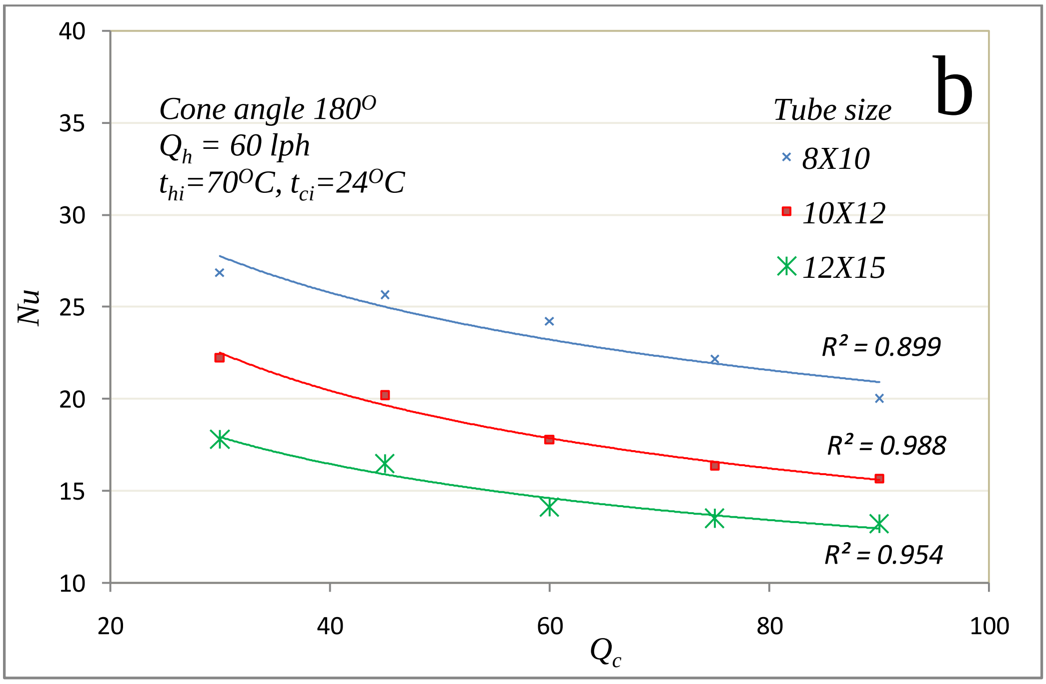

Fig. 5.8 Variation of *Nu* with Q_c with coils of different tube diameter [(a) cone angle 0^o (b) cone angle 180^o]

5.3 Effect of *flow ratio (Q_h/Q_c)* on *Nu*

The Figure 5.9 shows the effect of flow ratio on *Nu*. Figure shows that, *Nu* is the function of flow ratio, in such a way that it is directly proportional to tube side fluid flow (Q_h) and inversely proportional to shell side fluid flow (Q_c). From the figure it is also observed that the effect of tube side flow is more significant than that of shell side flow. The *Nu* is maximum for helical coil and it reduces with increase in cone angle for constant flow ratios. The calculations show that the % variation in *Nu*, for spiral to helical coils, with respect to the flow ratio is maximum upto 48% at low values of flow ratio.

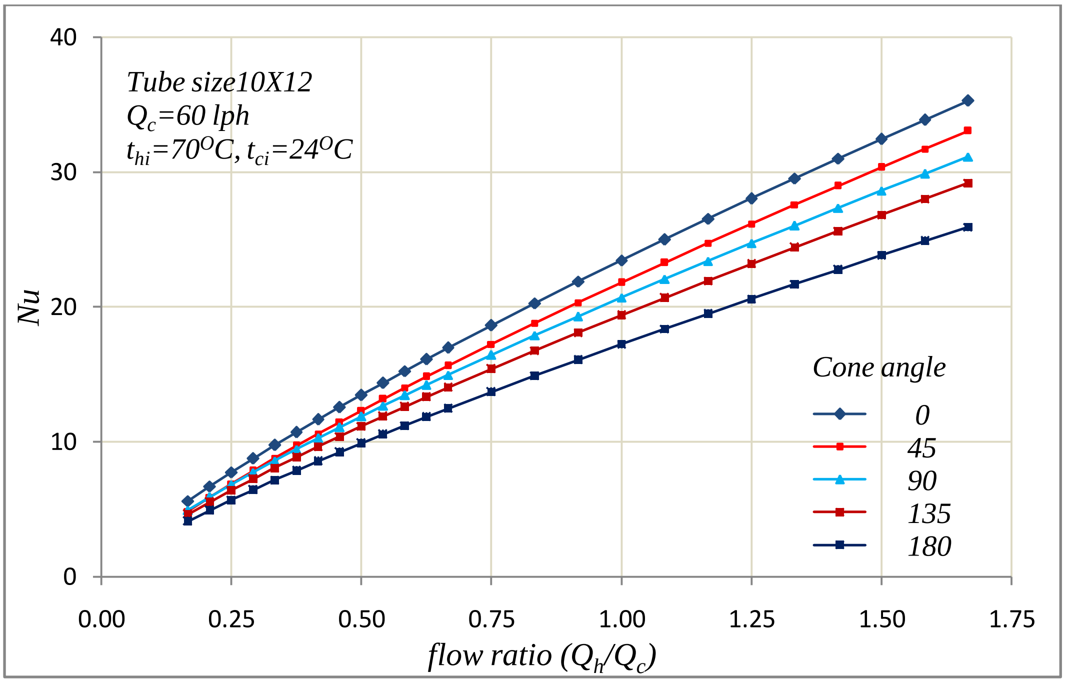

Fig. 5.9 Variation of *Nu* with *flow ratio, (Q_h/ Q_c)*

5.4 Effect of cone angle (θ) on *Nu*

Figure 5.10 shows that *Nu* decreases as cone angle increases from 0^O to 180^O, for same value of *Re*. It is also observed that *Nu* is the maximum for 0^O coil (helical coil). Also, the variation in *Nu* with respect to *Re* is more for helical coil and least for spiral coil. This shows that in helical coil heat exchangers the effects of secondary flow would translate into more heat transfer as compared to the other conical coils.

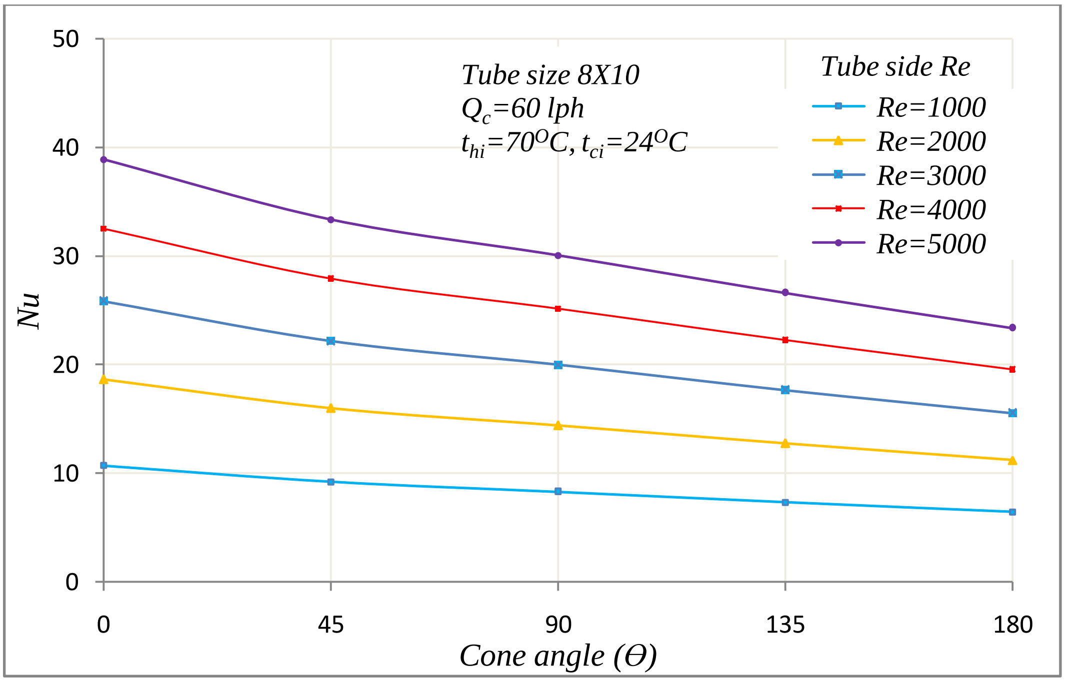

Fig. 5.10 Variation of *Nu with cone angle (θ)*

For helical coils, a maximum of 42% increase in *Nu* resulted when *Re* was increased from 1000 to 5000. Similar observations were recorded for the coils of different tube diameters and as shown in figures (5.11 a & b).

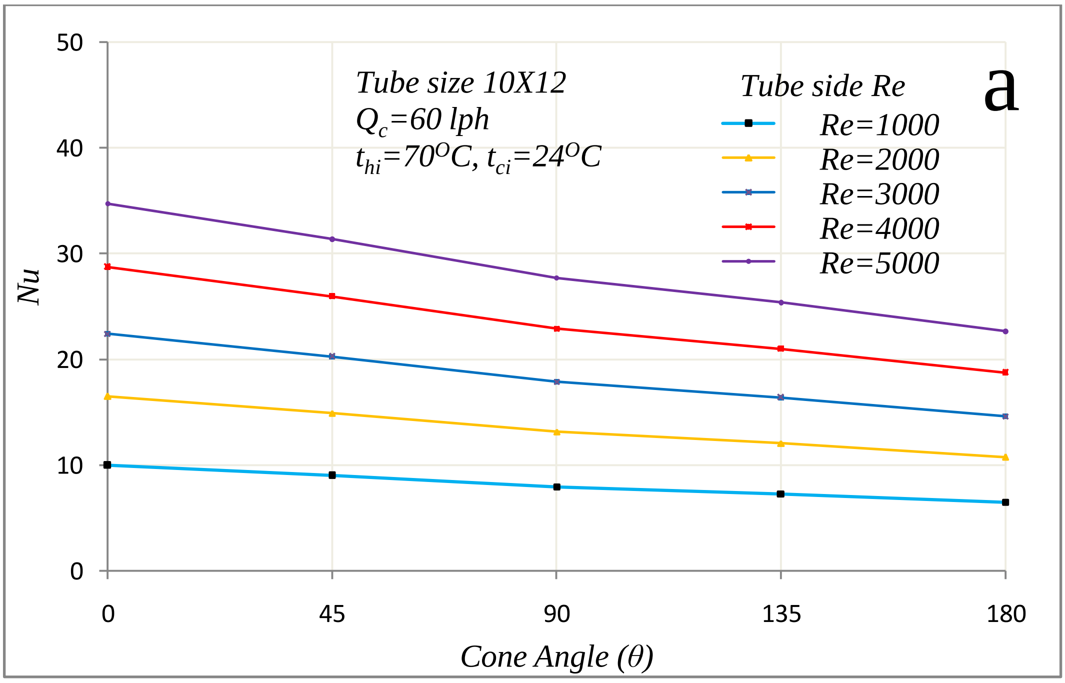

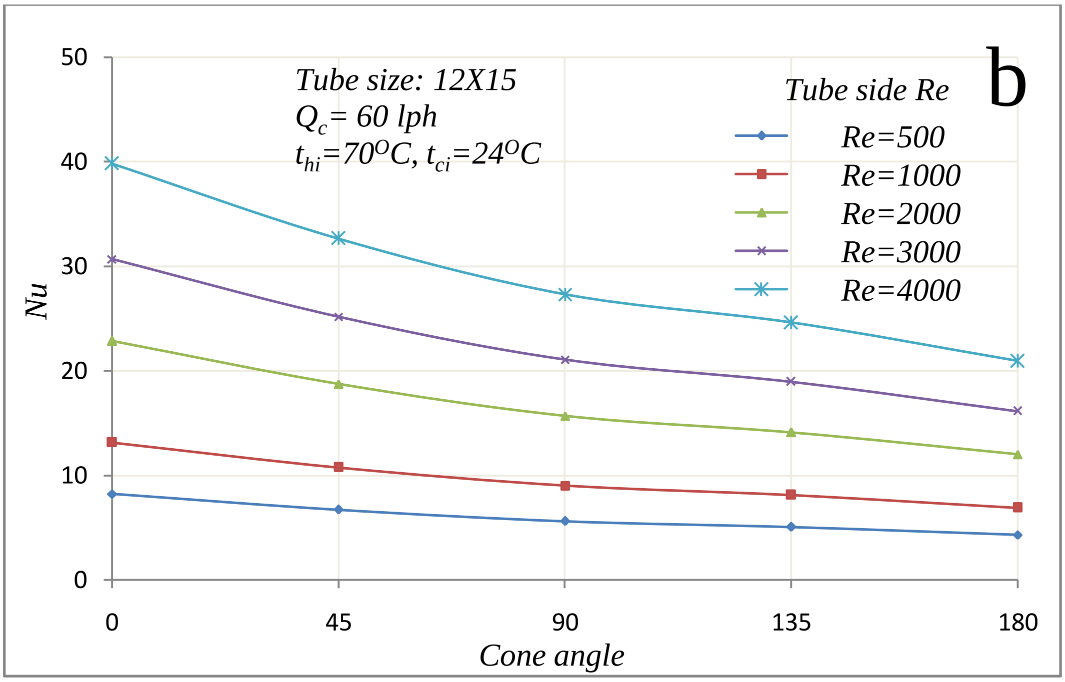

Fig 5.11 Variation of *Nu* with Cone angle (θ) for different tube side Re [(a) tube size-10×12 (b) tube size-12×15]

5.5 Heat exchanger effectiveness as a function of *Re*

The heat exchanger effectiveness is used to predict the outlet temperatures of tube-side and shell-side fluids. The effectiveness (ε) of heat exchangers of different cone angles (θ) as a function of *Re* is shown in Figure 5.12. This figure shows that the effectiveness decreases with increase in *Re* for all cone angles. The similar results were obtained by Ghorbani et al. [180] for helical coils.

In the analysis, the considerable variation is observed in the heat exchanger effectiveness with change in *Re*. At high values of Re, cone angle has no effect on heat exchangers effectiveness; however, marginal effect of cone angle on the effectiveness is observed at low values of *Re*.

The heat exchanger's effectiveness can be correlated with the *flow ratio*, (Q_h/Q_c), in a simple power equation similar to that used by Ghorbani et al. [179], as:

$$\varepsilon = a\,(Q_h/Q_c)^{b} \qquad 5.1$$

The values of the constants *a* and *b* are evaluated by regression analysis for different cone angle coils and are presented in Table 5.1.

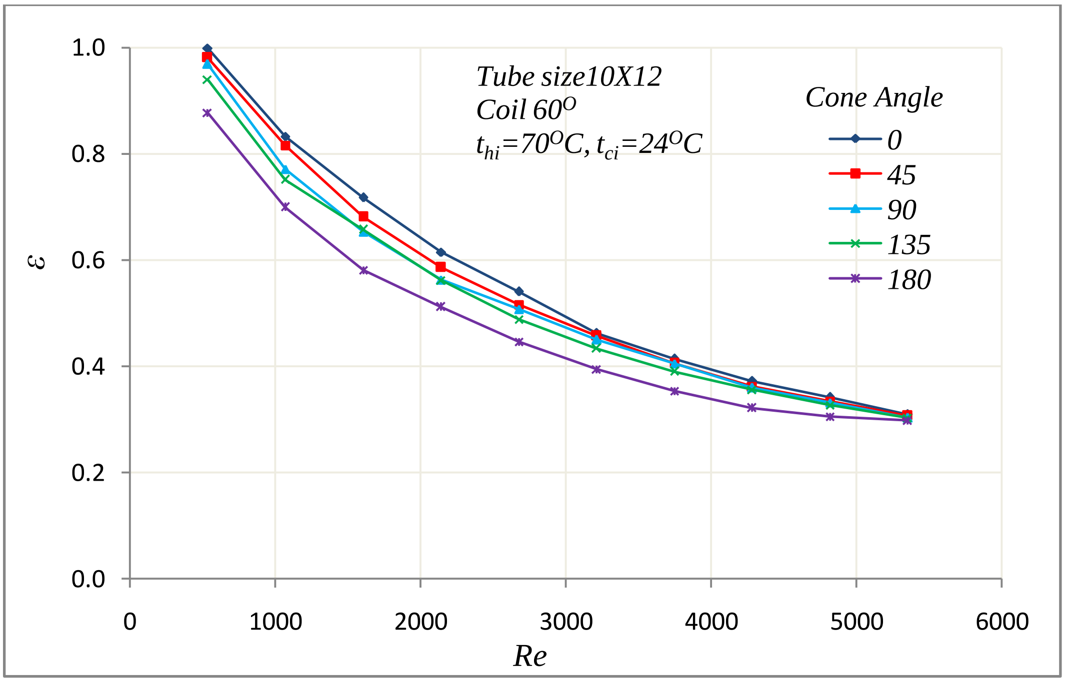

Fig. 5.12 Effect of *Re* on effectiveness of heat exchanger

Table 5.1: Constants for Eq. 5.1

Constants	0^O	45^O	90^O	135^O	180^O
a	0.5177	0.5047	0.4894	0.4624	0.4466
b	0.4114	0.4038	0.3833	0.3805	0.3804
R^2	0.9299	0.9042	0.9015	0.9217	0.9272
RMS error	0.06278	0.05954	0.05564	0.06393	0.04726

Number of data points for each cone angle 375

Ghorbani et al. [179] reported the values of *a* and *b* as 0.4745 and 0.4627 in their study for helical coil heat exchanger. These values of *a* and *b* when used in our experimental data under-predicted effectiveness by 8%, which may be due to the higher range of flow used by Ghorbani et al. [179] for their work. The parity plots these data are given in Figure 5.13 (a - e)

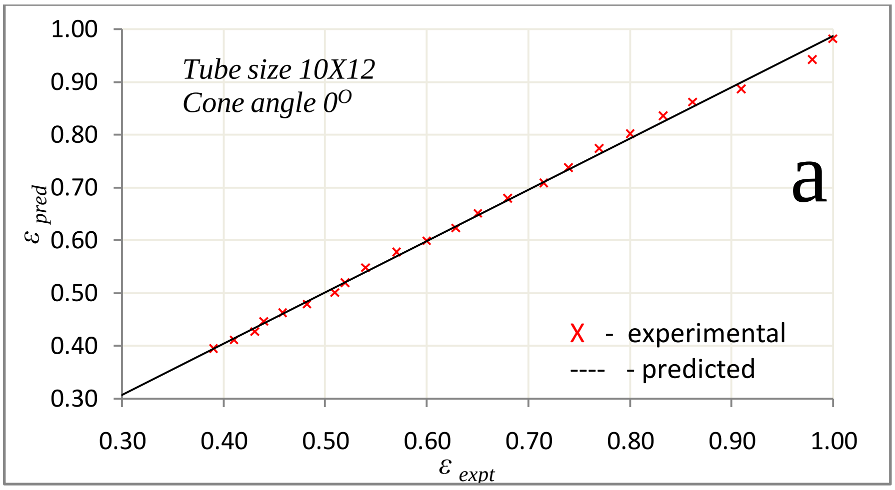

Fig. 5.13(a) Parity plot for effectiveness *(ε)* correlation

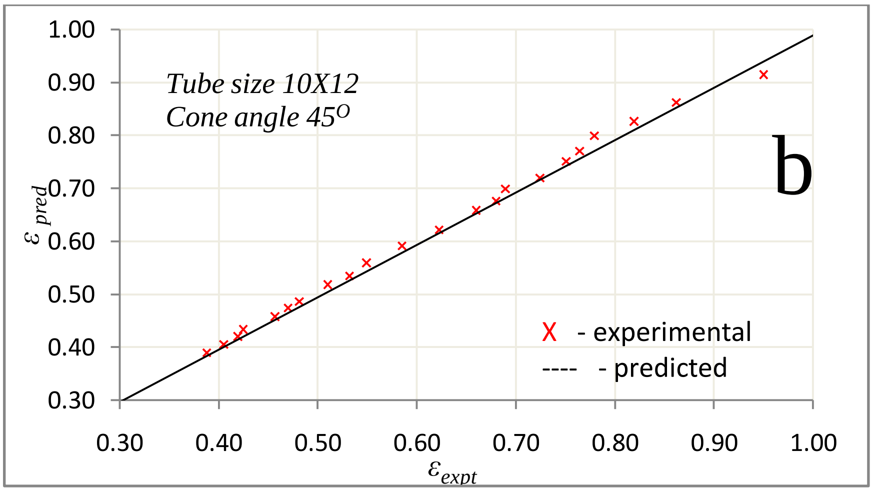

Fig. 5.13(b) Parity plot effectiveness *(ε)* correlation

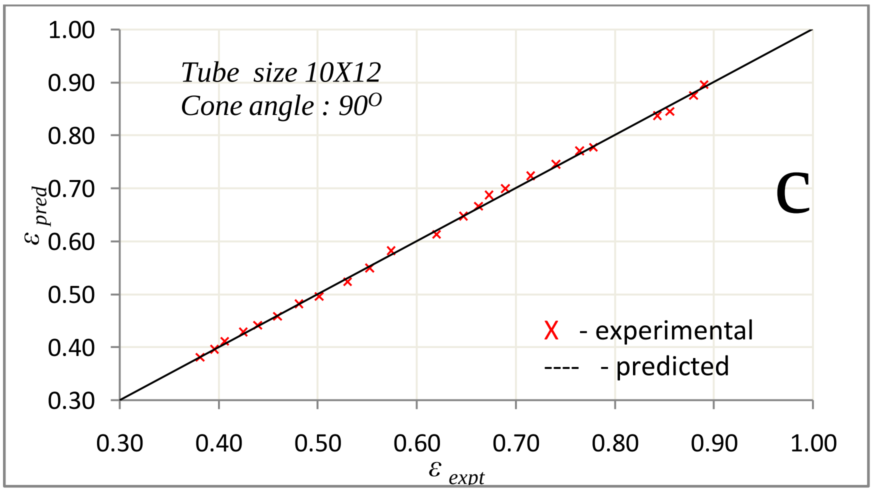

Fig. 5.13(c) Parity plot for effectiveness *(ε)* correlation

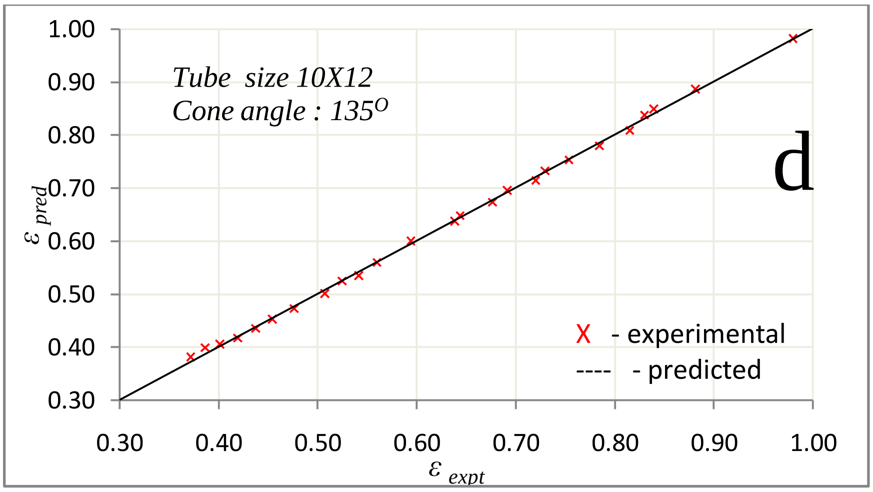

Fig. 5.13(d) Parity plot for effectiveness *(ε)* correlation

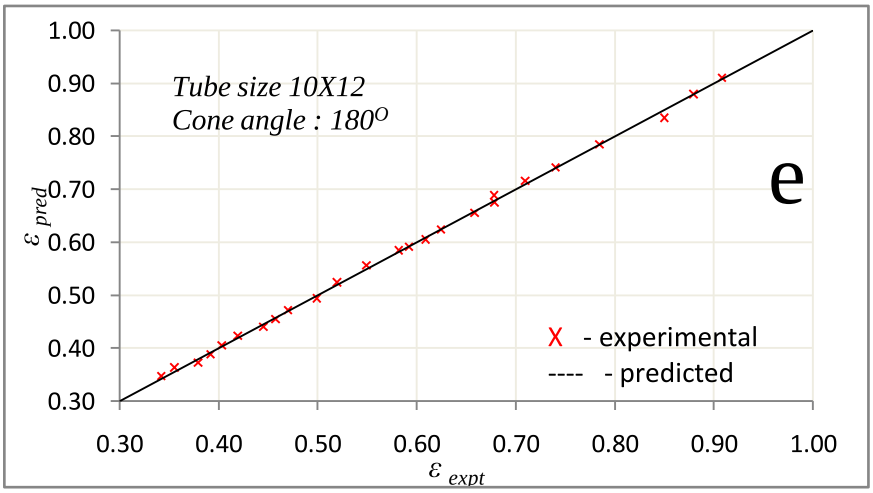

Fig. 5.13(e) Parity plot for effectiveness *(ε)* correlation

5.6 *Nu* – *Pr* correlations

Jaykumar et al. [75] in their work suggested that any correlation developed for evaluating the *Nu* contains three major parameters as, flow parameters, namely, flow parameter, fluid parameter, and coil parameter. There are many correlations reported in the literature in the form of *Nu* as a function of these parameters for helical coils. The experimental data shows that *Nu* is the function of flow rates (Q_h), properties of the fluid (*Pr*), and the coil geometry (δ). For relating *Nu* with these parameter following correlation is proposed for the conical coils:

$$Nu = a_1 Re^{a_2} Pr^{a_3} \delta^{a_4} \qquad \text{------ 5.2}$$

Also, some studies in the literature proposed *Nu* as a function of *De* and *Pr*. The correlation for *Nu* as a function of *De* and *Pr* is also proposed as:

$$Nu = b_1 De^{b_2} Pr^{b_3} \qquad \text{------ 5.3}$$

The experimental data for 15 different coils of different cone angles is used for evaluating the constants of the above correlations. The values of a_1, a_2, a_3, a_4, b_1, b_2 and b_3 for different cone angles are calculated by 375 data points and given in Table 5.3 for equation 5.2 and Table 5.4 for equation 5.3. The parity plots for this data are given in Figures 5.14 (a-e).

Table 5.2. Values of constants for *Nu* correlation (Eq. 5.2)

Constants	0^O	45^O	90^O	135^O	180^O
a_1	0.57	0.56	0.54	0.52	0.50
a_2	0.80	0.80	0.80	0.80	0.80
a_3	0.63	0.60	0.59	0.56	0.53
a_4	1.16	1.16	1.18	1.18	1.18
R^2	0.92	0.90	0.94	0.94	0.98
RMS error	1.2968	1.6590	1.7003	1.6744	1.1070

Number of data points for each cone angle: 375

Table 5.3. Values of constants for *Nu* correlation (Eq. 5.3)

Constants	0^O	45^O	90^O	135^O	180^O
b_1	0.16	0.150	0.141	0.136	0.124
b_2	0.8	0.8	0.8	0.8	0.8
b_3	-0.129	-0.139	-0.184	-0.190	-0.259
R^2	0.92	0.90	0.94	0.94	0.98
RMS error	1.6830	1.7934	1.7002	1.1746	0.8412

Number of data points for each cone angle: 375

The parity plots for the same (Eq. 5.2 & Eq. 5.3) are in Figure 5.14 (a-e). The comparison of the *Nu* value predicted using the correlations proposed in the present work with those predicted by the correlations available in literature for the helical coils is presented in the Figure 5.15.

The figure shows a good general agreement with other equations available in literature, for helical coil. However, the *Nu* values predicted in present work are closely matching with the work of Korne et al. [183] for the entire range of tube side flow. There is no correlation available in the literature for the comparison of conical coils of other cone angles.

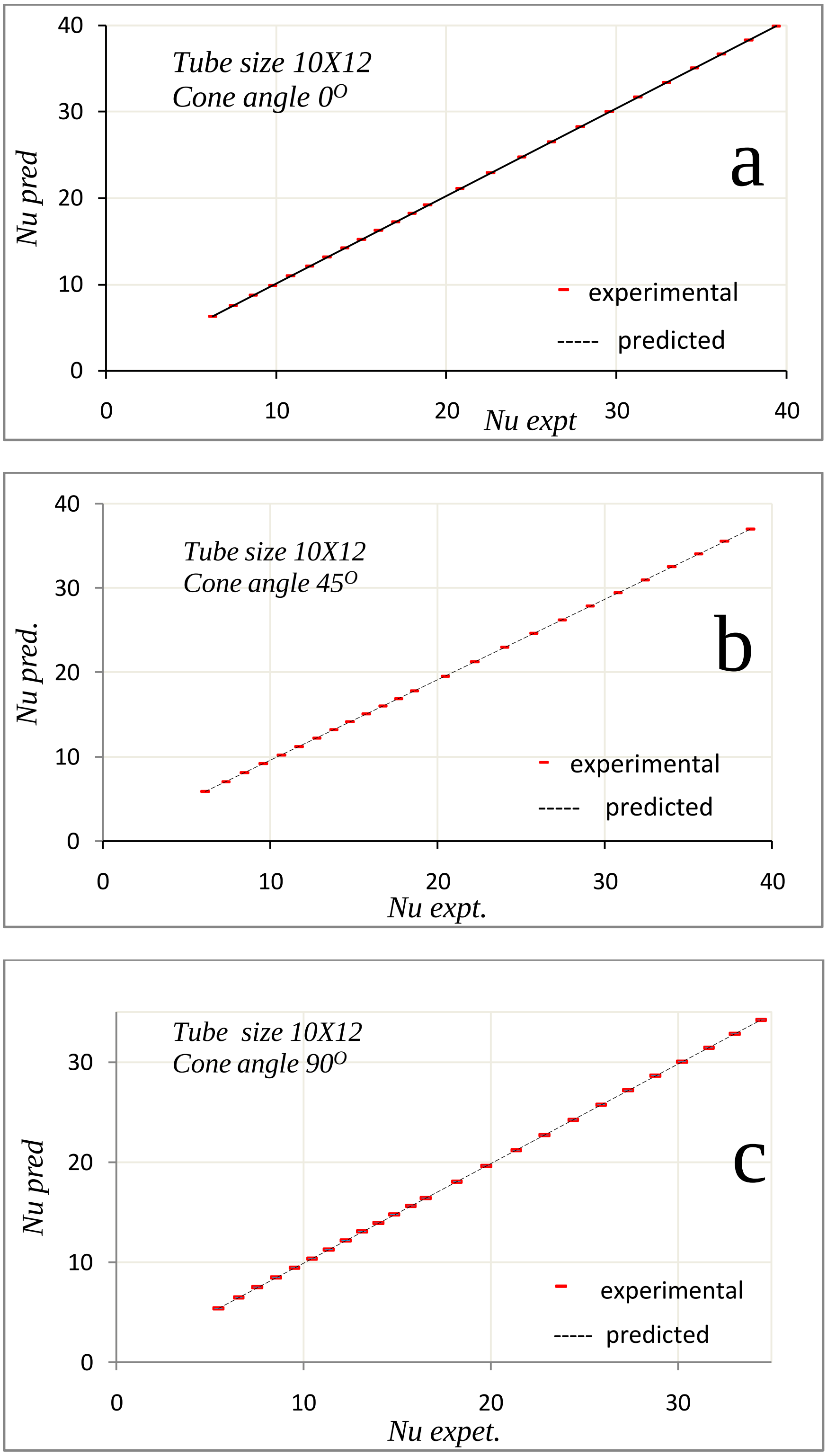

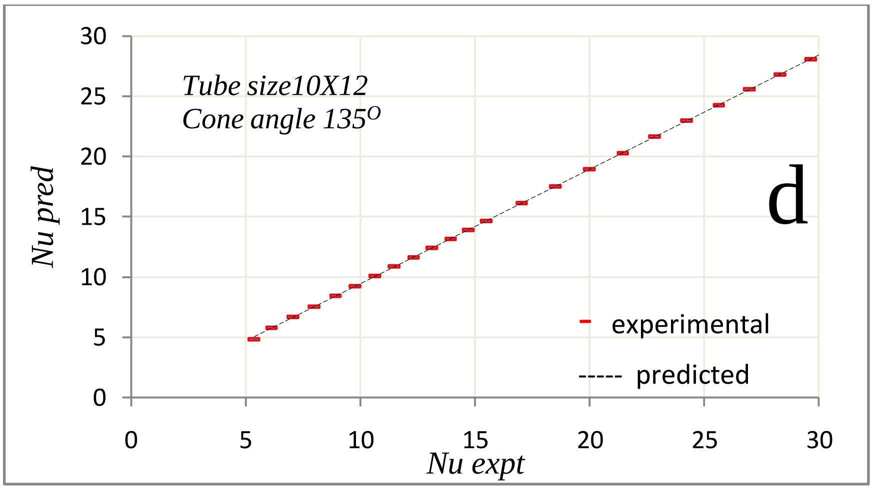

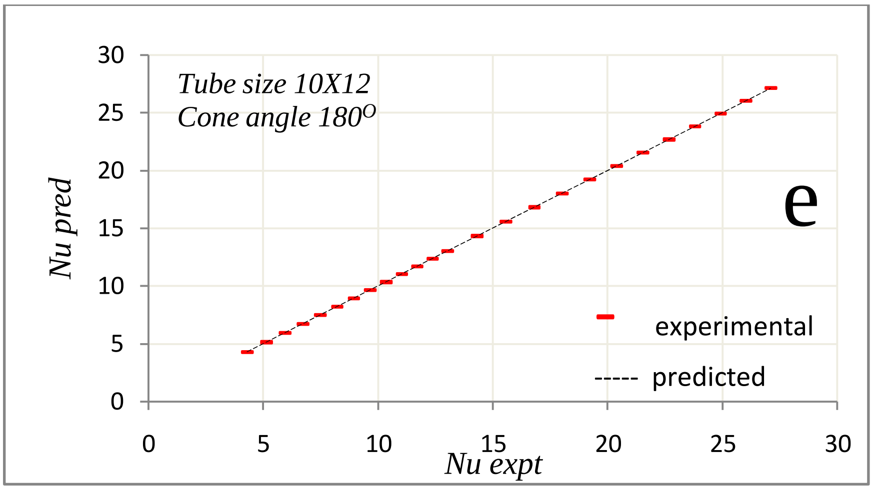

Fig. 5.14 Parity plot for *Nu* correlation [(a) for Cone angle *0°*, (b) for Cone angle 45°, (c) for Cone angle 90°, (d) for Cone angle 135°, (d) for Cone angle *180°]*

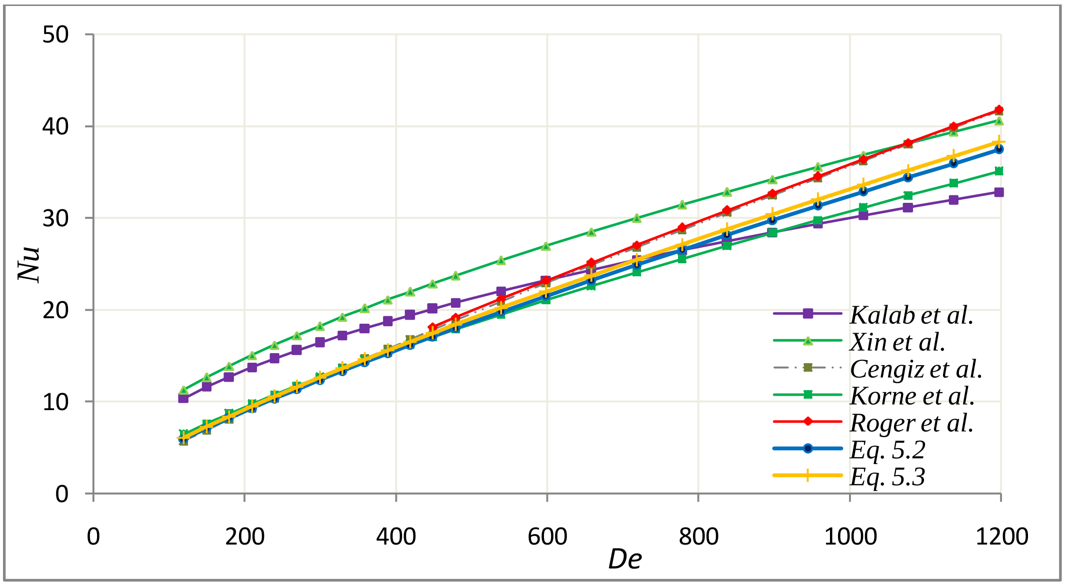

Fig. 5.15 Comparison of *Nu* as a function of *De* for various correlations

The compound correlation is proposed with the parameters *De*, *Pr* and cone angle (θ/θ_{180}) as;

$$Nu = m_1 \times De^{m_2} \times Pr^{m_3} \times \left(1 + \left({}^{\theta}/_{\theta_{180}}\right)\right)^{m_4} \qquad 5.4$$

where $m_1 = 0.148$, $m_2 = 0.814$, $m_3 = -0.114$, $m_4 = -0.671$ with $R^2 = 0.89$ and *RMS error* ranging from 4.15 to 2.34 with number of readings 1875.

5.7 Pressure drop analysis

Pressure drop analysis is important in the heat exchanger to calculate the pumping power required. Friction factor (*f*) is considered as the measure of the pressure drop.

The experimentally observed values of pressure drop are used to calculate the friction factor using Darcy's equation.

The variation of friction factor (*f*) with tube side flow rate (*Re*) is plotted for the coils of different cone angles (0^O, 42^O, 90^O, 135^O, 180^O). Further, correlations for friction factor (*f*) as a function of *Re* and δ are proposed.

Figure 5.16 shows the variation of friction factor (*f*) with tube side *Re* for the condition of constant coil diameter (*D)* and shell side flow rate (Q_c).

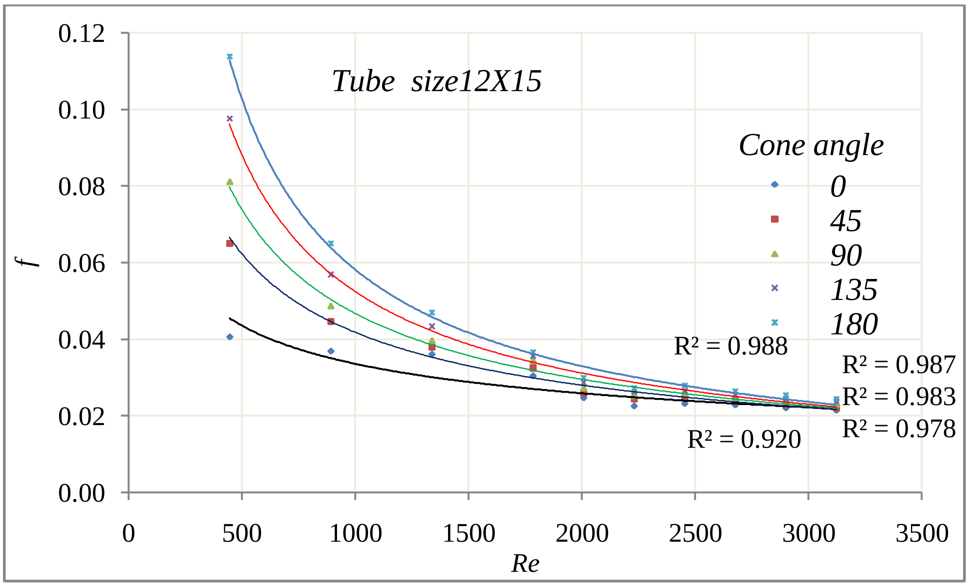

Fig. 5.16 Variation of friction factor (f) with Re for different cone angles (tube size-12×15)

Figure shows that friction factor (*f*) decreases with increase in *Re*. It is also observed that for the same value of *Re* (tube side flow) the helical coil has least value of *f*. The friction factor (*f*) increases with increase in cone angle. It is also observed that, the variation in friction factor with *Re* is large at lower *Re* and it reduces as *Re* increases.

Also, it is observed that the effect of cone angle (θ) on friction factor (*f*) is more at low values of *Re*. This may be due to the decrease in intensity of secondaries with increase in cone angle. Almost same value of *f* is observed for the coils of all angles at high values of *Re* (Re>3000). Similar observations were made for tubes of sizes10×12 and 8×10 (Figures 5.17a and 5.17b).

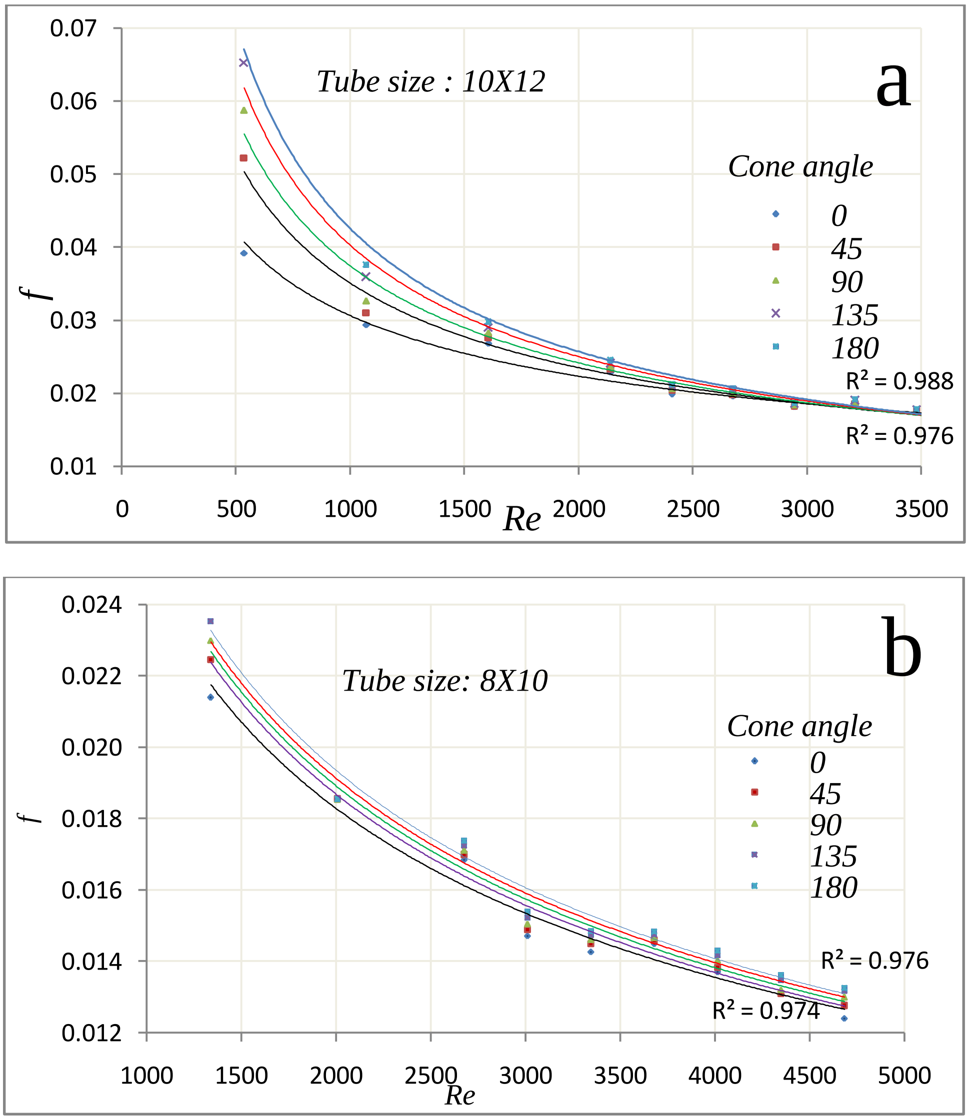

Fig. 5.17 Variation of friction factor (*f*) with *Re* for different cone angles [(a) tube size-10×12 (b) tube size-8×10]

Figures 5.18 (*a*, *b*, & *c*) show the variation of friction factor (*f*) with *Re* for different tube sizes for a given cone angle. For the same flow rate and cone angle, the bigger diameter tubes has higher friction factor than the smaller diameter tubes. This may be due to reduced velocity in the tube increases boundary layer thickness and increase the friction factor. Also, as tube diameter increases friction area increases this increases the friction in the coil. Also, the variation in the friction factor with *Re* is more for large diameter tubes as compared to the small diameter tubes.

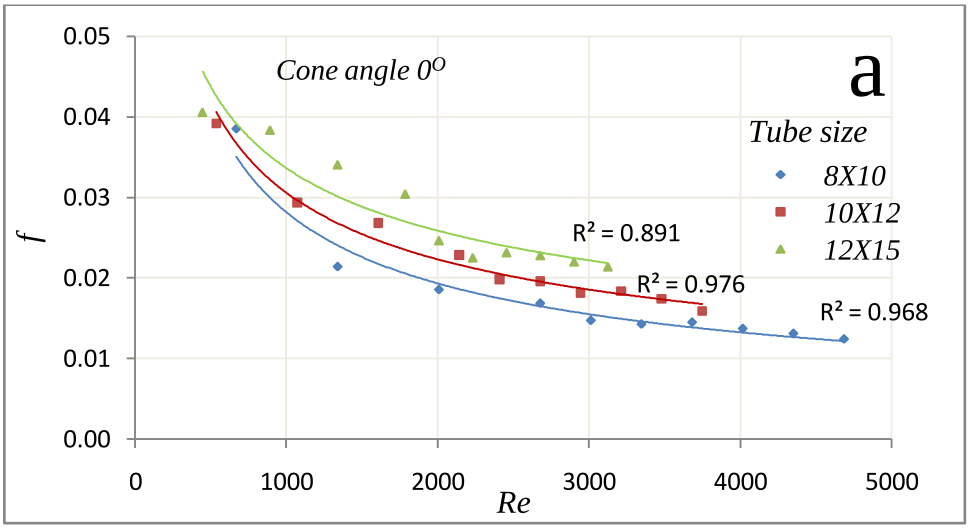

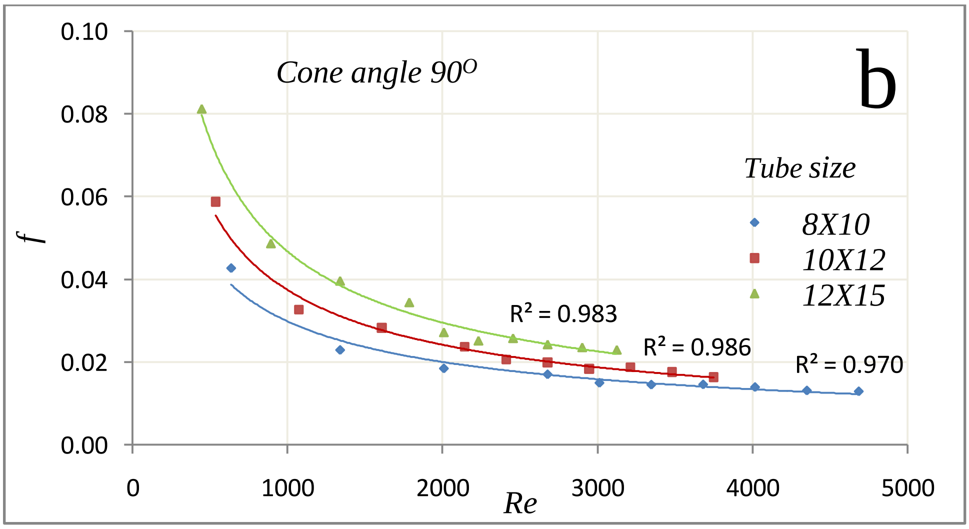

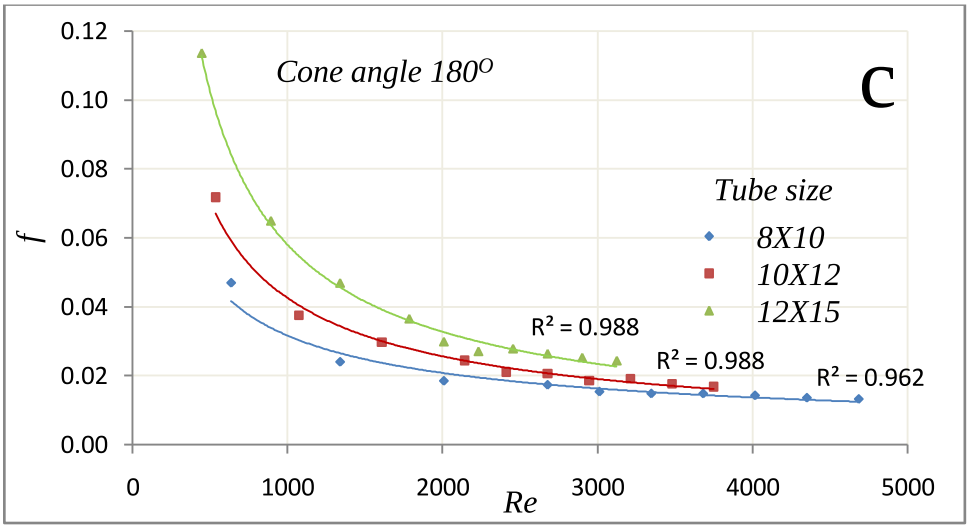

Fig. 5.18 Variation of friction factor (*f*) with *Re* for different tube sizes [(a) cone angle 0^o (b) cone angle 90^o (c) cone angle 180^o]

5.8 Friction factor (*f*) correlation

In the literature, *f* for the helical coil is given as a function of flow parameter (*Re*) and geometry parameter (δ). The correlations for the conical coils at different cone angles (0^O, 45^O, 90^O, 135^O, 180^O) are proposed in the similar form as:

$$f = c_1 \, . Re^{c_2} . \delta^{c_3} \qquad 5.5$$

The constants c_1, c_2 and c_3 are evaluated by regression analysis. The values of c_1, c_2 and c_3 for the conical coils of different cone angles are given in Table 5.4.

Table 5.4 Constants for friction factor (*f*) correlation (Eq. 5.4)

Constants	0^O	45^O	90^O	135^O	Spiral (180^O)
c_1	6.67	31.70	85.36	237.00	556.24
c_2	-0.40	-0.54	-0.62	-0.70	-0.77
c_3	0.88	1.03	1.15	1.28	1.39
R^2	0.86	0.96	0.97	0.98	0.98
RMS error	0.02226	0.01838	0.01909	0.02018	0.02430

Number of data points for each cone angle: 75

There are many studies available in literature for helical coil heat exchangers. A comparison of *f* values predicted in present work and those reported in literature [186] is given in fig 5.18. This figure shows a very close agreement between the predicted values and the values reported by Raman Rao [186]. Parity charts for friction factor are given in figure (5.19 (a - c))

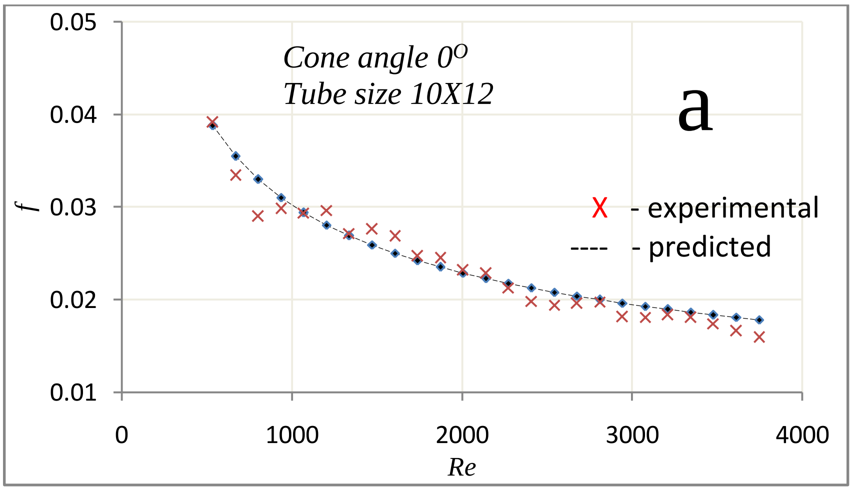

Fig. 5.19(a) Parity plots for friction factor (*f*) correlation

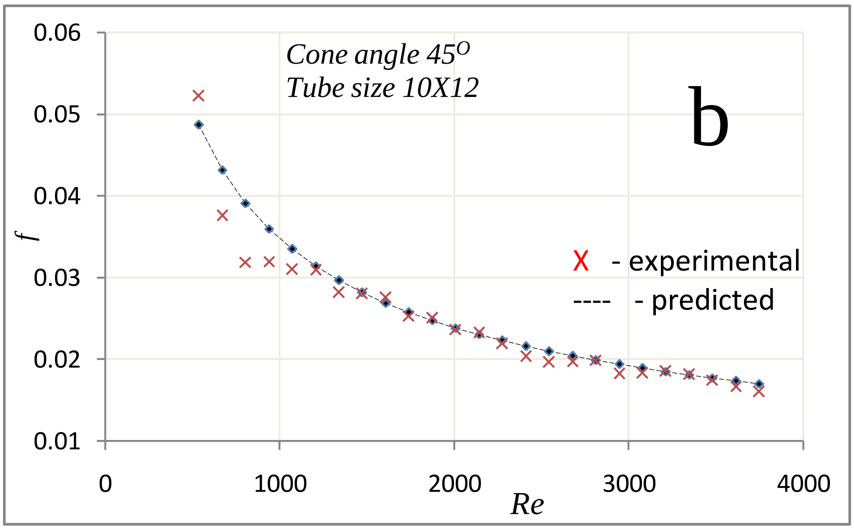

Fig. 5.19(b) Parity plots for friction factor (*f*) correlation

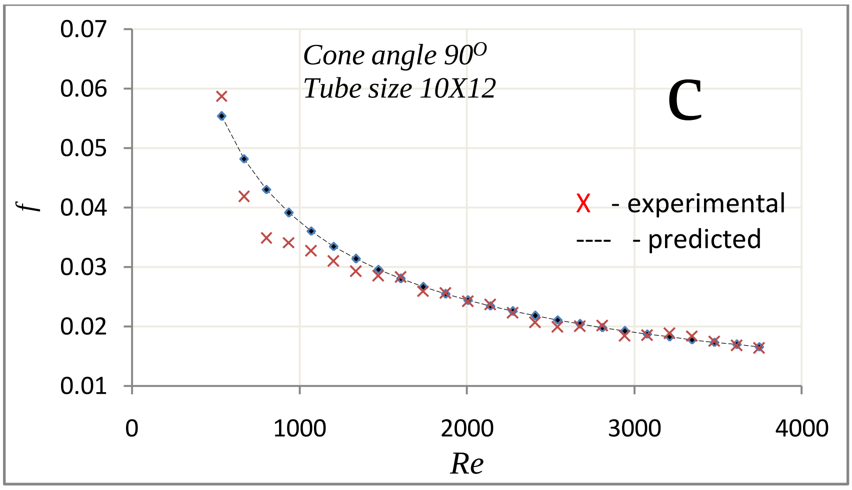

Fig. 5.19(c) Parity plots for friction factor (*f*) correlation

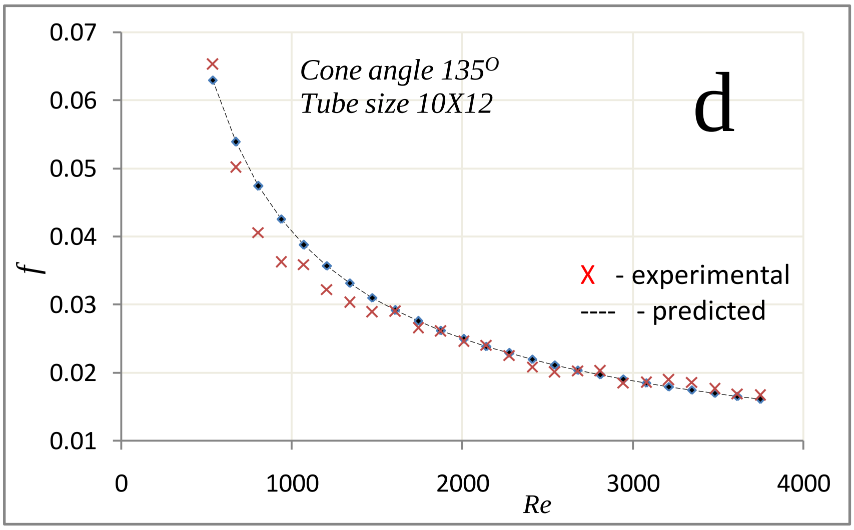

Fig. 5.19(c) Parity plots for friction factor (*f*) correlation

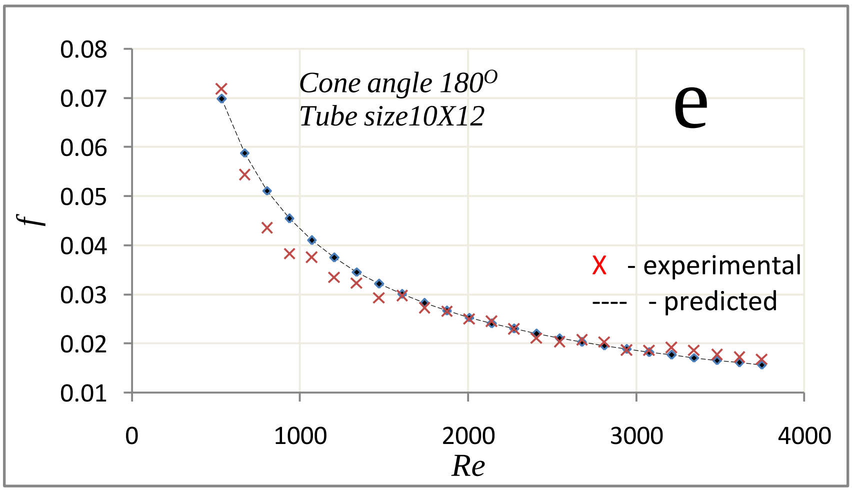

Fig. 5.19(c) Parity plots for friction factor (*f*) correlation

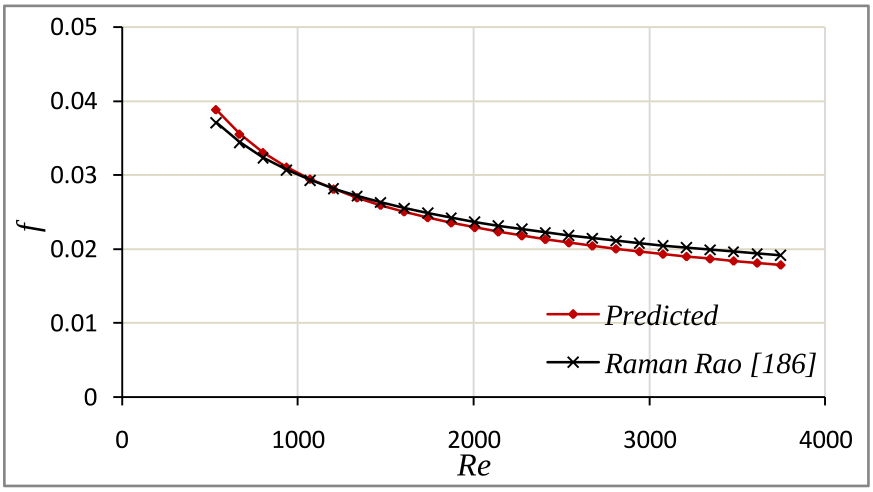

Fig. 5.20 Friction factor (*f*) predicted (correlation) and Raman Rao [186] with *Re*

5.9 Heat transfer enhancement

The heat transfer enhancement in spiral and helical coil heat exchangers is compared with straight tube heat exchanger for laminar flow region (Re < 2100) (Figure 5.20) and for turbulent flow region (Re > 2100) (Figure 5.21). For the straight tubes, the Sieder and Tate correlation [187] in the laminar flow region and Nusselts [188] correlation in turbulent flow region are used for the comparison.

The figures shows that in both flow regions (laminar and turbulent), *Nu* for coiled tubes is higher than that for straight tubes. In laminar region, the heat transfer enhancement is less (Nu_c/Nu_{st} is 1.8 to 2.85 for helical coil and 1.25 to 3.8 for spiral coil) as compared to the enhancement in turbulent region (Nu_c/Nu_{st} is 2.40 to 3.85 for helical coil and 1.78 to 1.93). However, the enhance in heat transfer is obtained at the expense of pumping power as the value of *fc/fs* is 1.2 to 3.0 for helical coil and 2.4 to 3.25 for spiral coil.

The heat transfer enhancement is also studied with variation of *Nu/f* (represents non dimensional form of $Q/\Delta p$) with *Re* at different cone angle (θ) as shown in Figure 5.22. The analysis show that *Nu/f* is a function of *Re* for all cone angles and it increases with increase in tube side *Re*. It also shows that the heat transfer enhancement is high in case of helical coil (0^o), and as cone angle increases the enhancement decreases.

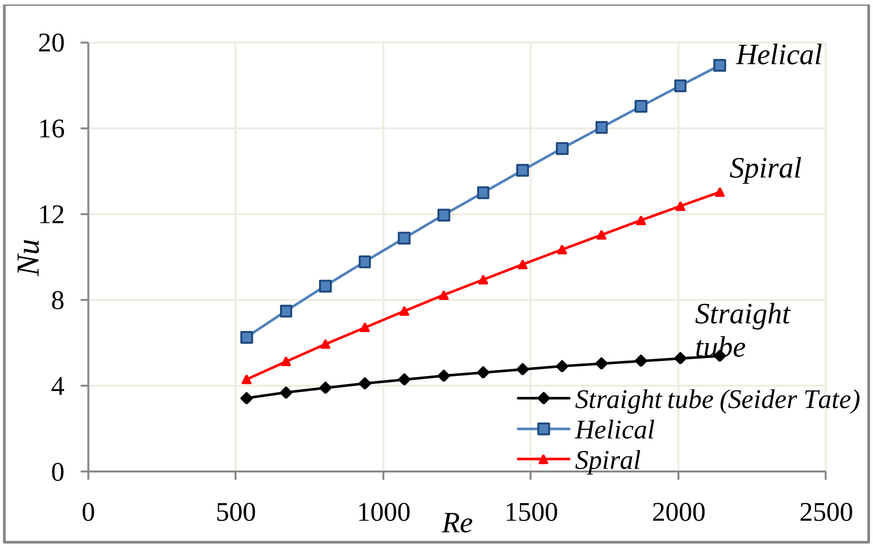

Fig 5.21 Variation of *Nu* with *Re* (Laminar region)

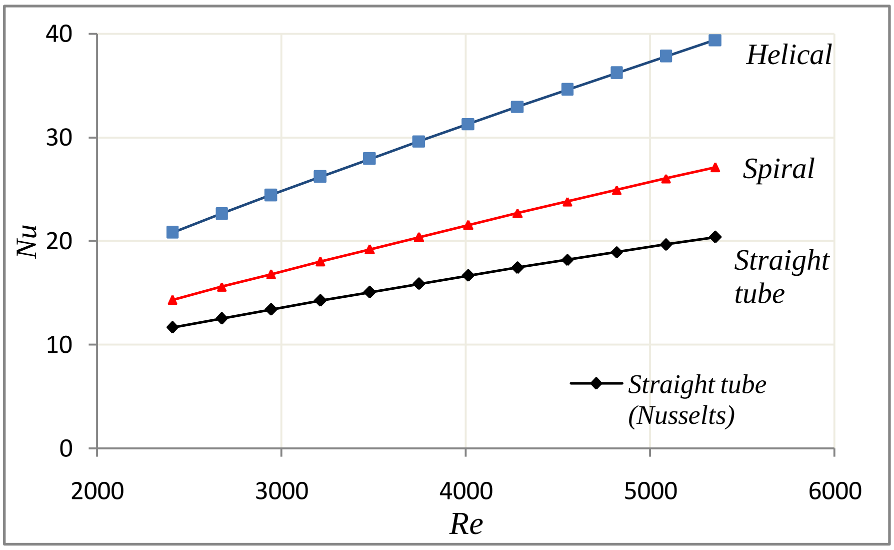

Fig. 5.22 Variation of *Nu* with *Re* (Turbulent region)

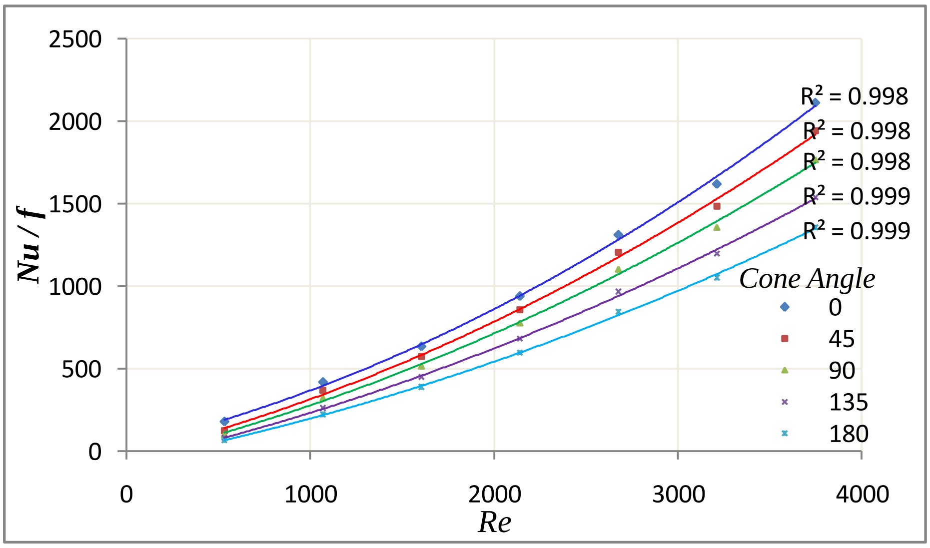

Fig. 5.23 Variation of *Nu/f* with respect to *Re*

Chapter 6

Conclusions and Recommendations

In this work the conical coils of three different tube diameters (8X10, 10X12, 12X15) and five different cone angles (0^O, 45^O, 90^O, 135^O, 180^O) were fabricated and used for the study of heat transfer and pressure drop characteristics. The data for coil heat exchangers is generated using hot water (tube side) and cold water (shell side).

6.1 Conclusions

The specific conclusions drawn from the present work are:

1. *Nu* increases with increase in tube side flow (Q_h) for the coils of all cone angles and tube diameter studied in the present work. However, *Nu* decreases with increase in tube side flow if the cone angle is increased.
2. *Nu* decreases with increase in shell side flow (Q_c) due to fluid stagnation in the turns of the coil. The stagnation of the fluid increases with increase in shell side flow, thus higher values of *Nu* are obtained at low values of shell side flow.
3. *Nu* increases with increase in flow ratio (Q_h/Q_c) indicating that the effect of secondary flow in the coil on heat transfer is more as compared to the effect of fluid stagnation. Cone angle (θ) increases from 0^O to 180^O, the *Nu* decreases for the same value of flow ratio.
4. The tube diameter (d_i) has significant effect on the performance of coil tube heat exchanger, as tube diameter (d_i) increases, *Nu* decreases for the same values of flows (Q_h and Q_c).
5. In comparison with straight tube heat exchangers, coiled tube configuration result in high value of *Nu*. This shows that coiled tube configurations are more efficient for heat transfer applications where pressure drops is comparable with straight tube heat exchangers.
6. The effectiveness of the heat exchanger decreases with increase in *Re* for the coils of all angles. At low flow rates the coil tubes promote more heat transfer than at high flow rates.
7. Friction factor (*f*) is the function of *Re* and it decreases with increase in *Re*. However, linear variation in f is not observed at low values of *Re* as is observed in straight tubes.

8. At a given value of Re, the fraction factor increases with increase in cone angle and tube diameter.
9. Tube side pressure drop (Δp) coil tube heat exchangers as compared to the straight tube heat exchangers. The pressure drop increases with the cone angle.

The correlations proposed for conical coil heat exchangers for tube side flow (500 < Re < 5000) are summarized in the following table (Table 6.1):

Table 6.1 Summary of correlations proposed in the present work

Type of Equation	Cone angle	Correlations
Correlation for heat exchanger effectiveness	*Helical* (0^O)	$\varepsilon = 0.5177. (Q_h/Q_c)^{0.4114}$
	45^O	$\varepsilon = 0.5047. (Q_h/Q_c)^{0.4038}$
	90^O	$\varepsilon = 0.4894. (Q_h/Q_c)^{0.3833}$
	135^O	$\varepsilon = 0.4624. (Q_h/Q_c)^{0.3805}$
	Spiral (180^O)	$\varepsilon = 0.4466. (Q_h/Q_c)^{0.3804}$
***Nu-Pr* correlation based on *Re* as flow parameter and *δ* as coil geometry**	*Helical* (0^O)	$Nu=0.57. Re^{0.8}.Pr^{0.63}.\delta^{1.16}$
	45^O	$Nu=0.56. Re^{0.8}.Pr^{0.60}.\delta^{1.16}$
	90^O	$Nu=0.54. Re^{0.8}.Pr^{0.59}.\delta^{1.18}$
	135^O	$Nu=0.52. Re^{0.8}.Pr^{0.56}.\delta^{1.18}$
	Spiral (180^O)	$Nu=0.50. Re^{0.8}.Pr^{0.53}.\delta^{1.18}$
***Nu-Pr* correlation based on *De* as combination of flow and geometry parameters**	*Helical* (0^O)	$Nu=0.16. De^{0.8}.Pr^{-0.129}$
	45^O	$Nu=0.15. De^{0.8}.Pr^{-0.139}$
	90^O	$Nu=0.141. De^{0.8}.Pr^{-0.184}$
	135^O	$Nu=0.136. De^{0.8}.Pr^{-0.190}$
	Spiral (180^O)	$Nu=0.124. De^{0.8}.Pr^{-0.259}$
Correlation for friction factor (*f*)	*Helical* (0^O)	$f=6.67. Re^{-0.40}. \delta^{0.88}$
	45^O	$f=31.70. Re^{-0.54}. \delta^{1.03}$
	90^O	$f=85.36. Re^{-0.62}. \delta^{1.15}$
	135^O	$f=237. Re^{-0.70}. \delta^{1.28}$
	Spiral (180^O)	$f=556.27. Re^{-0.77}. \delta^{1.39}$

6.2 Recommendations

On the basis of the present work, the following recommendations are made for the future work:

1. The analysis may be carried out for higher tube side and shell side flow rates in conical coils.
2. The fluid of different viscosity may be used to study the heat transfer and pressure drop in coiled tubes.
3. Modular designs are in demand for air cooled heat exchangers. The coiled tubes condenser and evaporators involving air cooling applications may be analysed for their effectiveness.
4. The effectiveness of coiled tubes heat exchangers involving nanofluids as heating and cooling medium may be evaluated.

References

1. Abdalla, M.A., “A four-region, moving-boundary model of a once through, helical coil steam generator”, *Annals of Nuclear Energy*, Volume 21(9), (1994), pp. 541-562.
2. Berger, S.A., Talbot, L, Yao, L.S., “Flow in curved pipes”, *Ann. Rev. Fluid Mech.*, Volume 15, (1983), pp. 461-512.
3. Bai, B., L. Guo, Z. Feng, X. Chen, “Turbulent heat transfer in a horizontally coiled tube”, *Heat Transfer-Asian Research*, Volume 28(5), (1999), pp. 395-403.
4. Rao, B.K., “Turbulent heat transfer to power law fluid in helical passage”, *International Journal of Heat and Mass Transfer*, Volume 15(2), (1994), pp. 142-148.
5. Sandeep, K.P., Palazoglu, T.K., “Secondary flow in coiled tubes”, Presented at the *1999 ASAE, Annual International Meeting. Paper No. 996148. ASAE, 2950*, Niles Rd., St. Joseph, MI 49085-9659 USA, (1999).
6. Genssle, A, Stephan. K, “Analysis of the process characteristics of an absorption heat transformer with compact heat exchangers and the mixture”, TFEE181, *International Journal of Thermal Sciences*, Volume 39, (2000), pp. 30-38.
7. Bergles, A.E., “Handbook of Heat Transfer”, McGraw-Hill, New York, NY, USA, 3rd edition (1998).
8. Bergles, A.E., “The implications and challenges of enhanced heat transfer for the chemical process industries”, *Chemical Engineering Research and Design*, Volume 79, no. 4, (1998), pp. 437–444.
9. Diwan, A., Mahanta, P., Sumitra Raju, K., Suresh Kuamr, P., “Review of passive heat transfer augmentation techniques”, *Proc. Instn. Mech. Engineerss,* Vol. 218, Part A, (2004), pp. 509-527.
10. Jeschke, D, “Heat transfer and pressure loss in coiled pipes”. *Ergaenzungsheft* Z. Ver. Disch. Ing., Volume 68, (1925), pp. 24-28.
11. Seban, R.A., McLaughlin, E.F, “Heat transfer in tube coils with laminar and turbulent flow”, *International Journal of Heat and Mass Transfer,* Volume 6, (1963), pp. 387-395.
12. James, R., Lines, “Helical Coiled heat exchangers Advantages”, *Bulletin by Grahams Manufacturing Co. Inc., Batavia,* NY, (2004).
13. http://www.chicagopipebending.com/products-services/types-of-coils.aspx
14. Dean, W.R, “Note on the motion of fluid in a curved pipe”, *Philosophical Magazine, Series 7,* Volume 4(20), (1927), pp. 208-23.
15. Barua, S.N, “On secondary flow in stationary curved pipes”, *Quarterly Journal of Mechanics and Applied Mathematics,* Volume 16, (1962), pp. 61-77.

16. Dravid, A.N., Smith, K.A., Merrill, E.W., Brian, P.L.T, "Effect of Secondary fluid motion on laminar flow heat transfer in helically coiled tubes", *AIChE Journal*, Volume 17(5), (1971), pp. 1114-1122.
17. Kern, D.Q., Process Heat Transfer, *McGraw hill*, New York, 1986.
18. Acharya, N., Sen, M., Chang, H.C, "Thermal entrance length and Nusselt numbers in coiled tubes", *International Journal of Heat and Mass Transfer*, Volume 37(2), (1993), pp. 36-340.
19. Acharya, N., Sen, M., Chang, H.C., "Analysis of heat transfer enhancement in coiled-tube heat exchangers", *International Journal of Heat and Mass Transfer*, Volume 44, (2001), pp. 3189-3199.
20. Janssen, L.A.M., Hoogendoorn, C.J, "Laminar convective heat transfer in helical coiled tubes", *International Journal of Heat and Mass Transfer*, Volume 21, (1978), pp. 1197-1206.
21. Prabhanjan, D.G., Raghavan, G.S.V., Rennie, T.J, "Comparison of heat transfer rates between a straight tube heat exchanger and a helically coiled heat exchanger", *International Communication in Heat Mass Transfer*, Volume 29 (2), (2002) pp 185–191.
22. Shah, R.K., Joshi, S.D, "Convective heat transfer in curved ducts for a natural circulation system", *Journal of Energy, Heat and Mass Transfer*, Volume 18, (1987), pp. 39–46.
23. a. Eustice, J, "Flow of water in curved pipes", *Proceedings of Royal Society of London, Series A* 84, (1910), pp. 107-18.

    b. Eustice, J, "Experiments of streamline motion in curved pipes", *Proc. R. Soc. London, Ser. A* 85, (1911), pp. 119-31.
24. Dean, W.R., "The streamline motion of fluid in a curved pipe", *Philosophical Magazine, Series 7*, Volume 5(30), (1928), pp. 673-95.
25. White, C.M., "Streamline flow through curved pipes", *Proceedings of the Royal Society of London, Series A,* Volume 123(792), (1928), pp.645-663.
26. Grindley, J.H., Gibson, A.H, "The frictional resistance of air through a pipe", *Proceedings of Royal Society of London Series, A,* 80, (1908) pp. 114-139.
27. Williams, G.S., Hubbell, C.W., Fenkell, G.H., "Experiments at Detroit, Mich., on the effect of curvature upon the flow of water in pipes", Transaction ASCE 47, (1902), pp. 1- 196.
28. Koutsky, J.A., Adler, R.L., "Minimization of axial dispersion by use of secondary flow in helical tubes", *The Canadian Journal of Chemical Engineering*, Volume 42, (1964), pp. 239-245.
29. Mori, Y., Nakayama, S, "Study on forced convective heat transfer in curved pipes (1st report, laminar region)". *International Journal of Heat and Mass Transfer*, Volume 8, (1965), pp. 67-82.

30. Mori, Y., Nakayama, S, “Study on forced convective heat transfer in curved pipes (2nd report, turbulent region)”. *International Journal of Heat and Mass Transfer*, Volume 10, (1967) pp.37-59.

31. McConalogue, D.J., Srivastava, R.S, “Motion of a fluid in a curved tube”, *Proceedings of the Royal Society of London, Series A, Mathematical and Physical Sciences*, Volume 307(1488), (1968), pp. 37-53.

32. Topakoglu, H.C, “Steady laminar flows of an incompressible viscous fluid in curved pipes”, *Journal of Mathematics and Mechanics*, Volume 16(12), (1967), pp.1321-1337.

33. Sreenivasan, K.R., Strykowski, P.J, “Stabilization effects in flow through helically coiled pipes”, *Experiments in Fluids*, Volume 1, (1967), pp. 31-36.

34. Truesdell, L.C., Adler, R.J, “Numerical treatment of fully developed laminar flow in helically coiled tubes”, *AIChE Journal*, Volume 16(6), (1970), pp. 1010-1015.

35. Joseph, B., Adler, R.J, “Numerical treatment of laminar flow in helically coiled tubes of square cross section – Part II. Oscillating helically coiled tubes”. *AIChE Journal*, Volume 21(5), (1970), pp. 974-979.

36. Masliyah, J.H., “Laminar flow in curved semicircular ducts”, *Journal of Fluid Mechanics*, Volume 99(3), (1980), pp. 469-479.

37. Dennis, S.C.R., Ng, M., “Dual solutions for steady laminar flow through a curved tube”, *Journal of Mechanics and Applied Mathematics*, Volume 35(3), (1982), pp.305-324.

38. Smith, F.T, “Steady motion within a curved pipe”, *Proceedings of Royal Society of London, Series A*, Volume 347, (1976), pp. 345-370.

39. Anwer, M., So, R.M.C., Lai, Y.G., “Perturbation by and recovery from bend curvature of a fully developed turbulent pipe flow”, *Physics of Fluids*, Volume 1(8), (1989), pp. 1387-1397.

40. Dennis, S.C.R., Riley, N., “Fully developed flow in a curved pipe at large Dean number”, *Proc. R. Soc. London Ser. A*, 434, (1991), pp. 473-478.

41. Boersma, B.J., Nieuwstadt, F.T.M., “Large-eddy simulation of turbulent flow in a curved pipe”, *International Journal of Fluid Engineering*, Transactions of the ASME, Volume 118(2), (1996), pp. 248-254.

42. Park, H., Moore, J.A., Trass, O., Ojha M., “Laser photochromic velocimetry estimation of the vorticity and pressure field–two-dimensional flow in a curved vessel”, *Experiments in Fluids*, Volume 26, (1999), pp. 55-62.

43. Hüttl, T. J., Friedrich, R, “Influence of curvature and torsion on turbulent flow in helically coiled pipes”, *International Journal of Heat and Fluid Flow*, Volume 21(3), (2000), pp.345-353.

44. Hüttl, T.J., Friedrich, R, “Direct numerical simulation of turbulent flows in curved and helically coiled pipes”, *Computers and Fluids*, Volume 30, (2001), pp. 591-605.

45. Yamamoto, K., Akita, T., Ikeuchi, H., Kita, Y, “Experimental study of the flow in a helical circular tube”, *Fluid Dynamics Research*, Volume 16, (1995), pp.237-249.
46. Yamamoto, K., Yanase, S., Jiang, R, “Stability of the flow in a helical tube”, *Fluid Dynamics Research*, Volume 22, (1998), pp.153-170.
47. Eason, R. M., Bayazitoglu, Y, Meade, A, “Enhancement of heat transfer in square helical ducts”, *International Journal of Heat and Mass Transfer*, Volume 37(14), (1994), pp. 2077-2087.
48. Bolinder, C.J., Sunden, B., “Numerical prediction of laminar flow and forced convective heat transfer in a helical square duct with finite pitch”, *International Journal of Heat and Mass Transfer*, Volume 39(15), (1996), pp. 3101-3115.
49. Silva, R.J., Valle, R.M., Ziviani, M, “Numerical hydrodynamic and thermal analysis of laminar flow in curved elliptic and rectangular channels”. *International Journal of Thermal Sciences*, Volume 38, (1999), pp.585-594.
50. Gammack, D., Hydon, P.E, “Flow in pipes with non-uniform curvature and torsion”, *Journal of Fluid Mechanics*, Volume 433, (2001), pp. 357-382.
51. Thomson, D.L., Bayazitoglu, Y., Meade, A.J, “Series solution of low Dean and Germano number flows in helical rectangular ducts”, *International Journal of Thermal Sciences*, Volume 40, (2001), pp. 937-948.
52. Chandratilleke, T.T., Nursubyakto, “Numerical prediction of secondary flow and convective heat transfer in externally heated curved rectangular ducts”, *International Journal of Thermal Sciences*, Volume 42, (2003), pp.187-198.
53. Eagles, P.M., “The evolution of the time-dependent localized disturbances to Dean flow in a channel with slowly varying curvature and Gap width”, *Journal of Mechanics and Applied Mathematics*, Volume 56(1), (2003), pp. 93-104.
54. Rennie, T.J., “Numerical and experimental studies of a double-pipe helical heat exchanger”, *Ph.D. Thesis, McGill University*, Montreal, Canada, (2004).
55. Rennie, T.J. and Raghavan, V.G.S., “Experimental studies of a double-pipe helical heat exchanger”, *Experimental Thermal Fluid Science*, Volume 29, (2005), pp. 919–924.
56. Rennie, T.J. and Raghavan, V.G.S., “Effect of fluid thermal properties on heat transfer characteristics in a double pipe helical heat exchanger”, *International Journal of Thermal Science*, Volume 45, (2006), pp. 1158–1165.
57. Rennie, T.J., Raghavan, V.G.S., “Numerical studies of a double-pipe helical heat exchanger”, *Applied Thermal Engineering*, Volume 26, (2006), pp. 1266–1273.

58. Patil, R.K., Shende, B.W., Ghosh, P.K, “Designing a helical-coil heat exchanger”, *Chemical Engineering*, Volume 92(24), (2006), pp. 85-88.

59. Haraburda, S, “Considerations on helical-coil heat exchangers”, *Chemical Engineering*, Vol. 102(7), (1995), pp.149-151.

60. Prabhanjan, D.G., Rennie, T.J., Vijay Raghavan, G.S., “Natural convection heat transfer from helical coiled tubes”, *International Journal of Thermal Sciences*, Volume 43(4), (2004), pp. 359-365.

61. Coronel, P., Sandeep, K.P., “Heat transfer coefficient in helical heat exchangers under turbulent flow conditions”, *International journal of food engineering*, Volume 4, Issue 1, art. 4, (2008), pp. 1-12.

62. Rogers, G.F.C., Mayhew, Y.R., “Heat transfer and pressure loss in helically coiled tubes with turbulent flow”, *International Journal of Heat and Mass Transfer*, Volume 7, (1968), pp. 1207-1216.

63. Kubair, V., Kuloor, N.R., “Heat transfer to Newtonian fluids in coiled pipes in laminar flow”, *International Journal of Heat and Mass Transfer*, Volume 9, (1966), pp. 63-75.

64. Berg, R.R., Bonilla, C. F, *Transaction of New York. Academy of Science*, Volume 13, (1950) pp. 12 (as cited in Kubair and Kuloor, 1966).

65. Mori, Y., Nakayama, S., “Study on forced convective heat transfer in curved pipes (3rd report, theoretical analysis under the condition of uniform wall temperature and practical formulae)”, *International Journal of Heat and Mass Transfer*, Volume 10, (1967), pp. 681-695.

66. Ozisik, M.N., Topakoglu, H.C., “Heat transfer for laminar flow in a curved pipe”, *Journal of Heat Transfer*, Volume 90, (1967), pp. 313-318.

67. Akiyama, M., Cheng, K.C., “Boundary vorticity method for laminar forced convection heat transfer in curved pipes”. *International Journal of Heat and Mass Transfer*, Volume 14, (1971), pp. 1659-1975.

68. Kalb, C.E., Seader, J.D., “Heat and mass transfer phenomena for viscous flow in curved circular tubes”, *International Journal of Heat and Mass Transfer*, Volume 15, (1972) , pp. 801-817.

69. Kalb, C.E., Seader, J.D., “Fully developed viscous-flow heat transfer in curved circular tubes with uniform wall temperature”, *AIChE Journal*, Volume 20(2), (1974), pp. 340-346.

70. Austin, L.R., Seader, J.D., “Fully developed viscous flow in coiled circular pipes”, *AIChE Journal*, Volume 19(1), (1973), pp. 85-94.

71. Zapryanov, Z., Christov, C. Toshev, E., “Fully developed laminar flow and heat transfer in curved tubes”, *International Journal of Heat and Mass Transfer*, Volume 23, (1980), pp. 873-880.

72. Kumar, V., Faizee, B., Mridha, M., Nigam, K.D.P., “Numerical studies of a tube-in-tube helically coiled heat exchanger”, *Chemical Engineering Process*, Volume 01, (2008), pp. 01- 20.

73. Moawed, M., "Experimental investigation of natural convection from vertical and horizontal helicoidal pipes in HVAC applications", *Energy Conversion and Management*, Volume 46, (2005), pp. 2996–3013.

74. Ko, T.H., "Thermodynamic analysis of optimal curvature ratio for fully developed laminar forced convection in a helical coiled tube with uniform heat flux", *International Journal of Thermal Sciences*, Volume 45, (2006), pp 729–737.

75. Jayakumar, J.S., Mahajani, S.M., Mandal, J.C., Iyer, K.N., Vijayan, P.K., "CFD analysis of motion on laminar-flow heat-transfer in helically-coiled tubes", *AICHE Journal*, Volume 17, (2008), pp. 1142–1222.

76. Conte, I., Peng, X.F., "Numerical investigations of laminar flow in coiled pipes", *Applied Thermal Engineering*, Volume 28, (2008), pp 423–432.

77. Ferng Y.M., Lin, W.C., Chieng, C.C., "Numerically investigated effects of different Dean Number and pitch size on flow and heat transfer characteristics in a helically coil-tube heat exchanger", *Applied Thermal Engineering*, Volume 36, (2012), pp. 378-385.

78. Singh, M. P, "Entry flow in a curved pipe", *Journal of Fluid mechanics*, Volume 65(3), (1974), pp. 517-539.

79. Shokouhmand, H., Salimpour, M.R., Akhavan-Behabadi, M.A., "Optimal Reynolds number of laminar forced convection in a helical tube subjected to uniform wall temperature", *International Communications in Heat and Mass Transfer*, Volume 34, (2008), pp 753–761.

80. Patankar, S.V., Pratap, V.S., Spalding, D.B., "Prediction of laminar flow and heat transfer in helically coiled pipes". *Journal of Fluid Mechanics*, Volume 62(3), (1974), pp. 539-551.

81. Kalb, C.E., Seader, J.D., "Entrance region heat transfer in a uniform wall temperature helical coil with transition from turbulent to laminar flow", *International Journal of Heat and Mass Transfer*, Volume 26(1), (1983), pp. 23-32.

82. Li, L.J., Lin, C.X., Ebadian, M.A, "Turbulent mixed convective heat transfer in the entrance region of a curved pipe with uniform wall-temperature", *International Journal of Heat and Mass Transfer*, Volume 41(23), (1997), pp. 3793-3805.

83. Li, L.J., Lin, C.X., Ebadian, M. A., "Turbulent heat transfer to near-critical water in a heated curved pipe under the conditions of mixed convection", *International Journal of Heat and Mass Transfer*, Volume 42(16), (1998), pp. 3147-3158.

84. Lin, C.X., Zhang, P., Ebadian, M.A., "Laminar forced convection in the entrance region of helical pipes", *International Journal of Heat and Mass Transfer*, Volume 40(14), (1999), pp. 3293-3304.

85. Rindt, C.C.M., Sillekens, J.J.M., Van Steenhoven A.A., "The influence of the wall temperature on the development of heat transfer and secondary flow

in a coiled heat exchanger", *International Communications in Heat and Mass Transfer*, Volume 26(2), (1999), pp. 187-198.

86. Saffari Hamid, Rouhollah Moosavi, Nourooz Mohammad Nouri, Cheng-Xian Lin, "Prediction of hydrodynamic entrance length for single and two-phase flow in helical coils", *Chemical Engineering and Processing: Process Intensification*, Volume 86, (2014), pp. 9-21.
87. Xin, R.C., Ebadian, M.A., "Natural convection heat transfer from helicoidal pipes". *Journal of Thermophysics and Heat Transfer*, Volume 10, No. 2, (1996), pp. 297-302.
88. Xin, R.C., Ebadian, M.A., "The effects of Prandtl numbers on local and average convective heat transfer characteristic in helical pipes", *Journal of Heat Transfer*, Volume 119, (1997), pp. 467-473.
89. Andrade, Clhudia R., Zaparoli, Edson L., "Effects of Temperature dependant viscosity on pulley developed Laminar and forced convection in curved duct", *International Communications in Heat Mass Transfer*, Volume 28, Issue 2, (2001), pp. 21l-220.
90. Lemenand, T., Peerhossaini H., "A thermal model for prediction of the Nusselt number in a pipe with chaotic flow", *Applied Thermal Engineering*, Vol. 22, (2002), pp.1717- 1730.
91. Aravind, G.S., Arun, Y, Sunder, R S, Subrahmaniyam S., "Natural Convective Heat Transfer in Helical Coiled Heat Exchanger", *IE (I) Journal CH*, Volume 84 (2003).
92. Naphon, P, "Thermal performance and pressure drop of the helical-coil heat exchangers with and without helically crimped fins", *International Communication in Heat Mass Transfer*, Volume 34 (3), (2007), pp 321–330.
93. Salimpour M.R., "Heat transfer characteristics of a Temperature-dependent property fluid of shell and coiled tube Heat exchangers", *International Communication of Heat Mass Transfer*, Volume 35, (2008), pp. 1190–1195.
94. Kharat, Rahul, Bhardwaj, Nitin, Jha, R.S., "Development of heat transfer coefficient correlation for concentric helical coil heat exchanger", *International Journal of Thermal Sciences*, Volume 48, (2009), pp. 2300–2308.
95. Nasser Ghorbani, Hessam Taherian, Mofid Gorji, Hessam Mirgolbabaei, "An experimental study of thermal performance of shell-and-coil heat exchangers", *International Communication of Heat Mass Transfer*, Volume 37, Issue 7, (2010), pp. 775-781.
96. Jung-Yang San, Chih-Hsiang Hsu, Shih-Hao Chen, "Heat transfer characteristics of a helical heat exchanger", *Applied Thermal Engineering*, Volume 39, (2012), pp. 114-120.
97. José Fernández-Seara, Carolina Piñeiro-Pontevedra, J. Alberto Dopazo, "The performance of a vertical helical coil heat exchanger, Numerical model

and experimental validation", *Applied Thermal Engineering*, Volume 62, Issue 2, (2014), pp. 680-689.

98. Yao, L.S., Berger, S.A., "Flow in heated curved pipes", *Journal of Fluid Mechanics*, Volume 88(2), (1978), pp. 339-354.

99. Lee, J. B., Simon, H. A, Chow J. C. F., "Buoyancy in developed laminar curved tube flows", *International Journal of Heat and Mass Transfer,* Volume 28(2), (1985), pp. 631-640.

100. Padmanabhan, N., "Entry flow in heated curved pipes", *International Journal of Heat and Mass Transfer*, Vol. 30(7), (1987), pp. 1453-1463.

101. Futagami, K., Aoyama, Y., "Laminar heat transfer in a helically coiled tube", *International Journal of Heat and Mass Transfer*, Volume 31(2), (1988), pp 387-396.

102. Goering, D.J., Humphrey, J.A.C., Greif, R., "The dual influence of curvature and buoyancy in fully developed tube flows", *International Journal of Heat and Mass Transfer,* Volume 40(9), (1997), pp. 2187-2199.

103. Shokouhmand, H., Salimpour, M.R., Akhavan-Behabadi, M.A, "Experimental investigation of shell and coiled tube heat exchangers using Wilson plots", *International Communications in Heat and Mass Transfer*, Volume 35, (2006), pp. 84–92.

104. Inagaki, Y., Koiso, H., Takumi, H., Ioka, I., Miyamoto, Y., "Thermal hydraulic study on a high-temperature gas-gas heat exchanger with helically coiled tube bundles", *Nuclear Engineering and Design,* Volume 185, (1998), pp.141-151.

105. Zachár, A., "Investigation of natural convection induced outer side heat transfer rate of coiled-tube heat exchangers", *International Journal of Heat and Mass Transfer*, Volume 55, Issues 25–26, (2012), pp. 7892-7901.

106. Park Hyunku, Seung-Rae Lee, Seok Yoon, Hosung Shin, Dae-Soo Lee, "Case study of heat transfer behavior of helical ground heat exchanger", *Energy and Buildings,* Volume 53, (2012), pp. 137-144.

107. Neshat, E, Hassainpour, S, Bahiraee, F, "Experimental and Numerical study on unsteady natural convection heat transfer in helically coiled tube heat exchangers", *Heat and Mass Transfer*, Volume 50, (2014), pp. 877-885.

108. Je-Young Moon, Jeong-Hwan Heo, Bum-Jim Chung, "Natural convection experiments on the outer surface of an inclined helical coil", *Heat and Mass Transfer*, (2015), DOI: 10.1007/s00231-015-1495-5.

109. Vimal Kumar, Supreet Saini, Manish Sharma, Nigam, K.D.P., "Pressure drop and heat transfer study in tube-in-tube helical heat exchanger", *Chemical Engineering Science,* Volume 61, Issue 13, (2006), pp. 4403-4416.

110. Abdalla, Gomaa, Wael, I. A., Aly, M., Omara, Mahmoud, Abdelmagied, "Correlations for heat transfer coefficient and pressure drop in the annulus of concentric helical coils", *Heat Mass Transfer,* Volume 50, (2014), pp. 583–586 DOI 10.1007/s00231-013-1258-0.

111. Mandal, M.M, Nigam, K.D.P., “Experimental Study on Pressure Drop and Heat Transfer of Turbulent Flow in Tube in Tube Helical Heat Exchanger”, *Industrial and Engineering Chemistry Research*, Volume. 48(20), (2009), pp. 9318–9324.

112. Pawar, S.S., Sunnapwar, V. K., “Experimental studies on heat transfer to Newtonian and non-Newtonian fluids in helical coils with laminar and turbulent flow”, *Experimental Thermal and Fluid Science*, Volume 44, (2013), pp. 792-804.

113. Nada, S.A, Shaer, E.I., Huzayyain, W.G., “Performance of Multi tube in helical coil as compact heat exchanger”, *Heat and Mass Transfer,* (online 2014), DOI 10.1007/s00231-014-1469-z.

114. Naphon, Paisarn, Jamnean Suwagrai, “Effect of curvature ratios on the heat transfer and flow developments in the horizontal spirally coiled tubes”, *International Journal of Heat and Mass Transfer*, Volume 50, (2007), pp 444–451.

115. Naphon, Paisarn, and Wongwises, Somachi, “An Experimental study on the in tube convective heat transfer coefficient in a spiral coil heat exchanger”, *International Communications in Heat and Mass Transfer*, Volume 29(6), (2002), pp 797-809.

116. Naphon, Paisarn, Wongwises, Somachi, “Heat transfer coefficients under dry-and-wet surface conditions for a spirally coiled finned tube heat exchanger”, *International Communications in Heat and Mass Transfer*, Volume 32, (2005), pp 371–385.

117. Naphon, P, Wongwises, S, “A review of flow and heat transfer characteristics in curved tubes”, *Renewable and Sustainable Energy Reviews*, 10, (2006), pp. 463–490.

118. Duc-Khuyen Nguyen, Jung-Yang San, “Effect of solid heat conduction on heat transfer performance of a spiral heat exchanger”, *Applied Thermal Engineering*, (2014), In Press.

119. Ho, J.C., Wijeysundera N.E., Rajasekar S, “Study of a compact spiral-coil cooling and dehumidifying heat exchanger unit”, *Applied Thermal Engineering*, Volume 16, (1996), pp. *777–790.*

120. Xing Lu, Xueping Du, Min Zeng, Sen Zhang, Qiuwang Wang, “Shell-side thermal-hydraulic performances of multilayer spiral-wound heat exchangers under different wall thermal boundary conditions”, *Applied Thermal Engineering*, Volume 70, (2014), pp.1216-1227

121. Pongsoi Parinya, Santi Pikulkajorn, Somchai Wongwises, “Heat transfer and flow characteristics of spiral fin-and-tube heat exchangers: A review”, *International Journal of Heat and Mass Transfer*, Volume 79, (2014), pp. 417-431.

122. Piazza, Ivan Di, Ciofalo, Michele, “Numerical prediction of turbulent flow and heat transfer in helically coiled pipes”, *International Journal of Thermal Sciences*, Volume 49, (2008), pp 653–663.

123. Patankar, S.V., Pratap, V.S., Spalding, D.B., “Prediction of turbulent flow in curved pipes”, *Journal of Fluid Mechanics*, Volume 67(3), (1975), pp 583-595.

124. Wang Hui, Ajay K. Prasad, Suresh G. Advani, “Hydrogen storage system based on hydride materials incorporating a helical-coil heat exchanger”, *International Journal of Hydrogen Energy*, Volume 37, Issue 19, (2012), pp. 14292-14299.

125. Jamshidi N., Farhadi M., Ganji D.D., Sedighi K., “Experimental analysis of heat transfer enhancement in shell and helical tube heat exchangers”, *Applied Thermal Engineering*, Volume 51, Issues 1–2, (2013), pp. 644-652.

126. Xing Lu, Xueping Du, Min Zeng, Sen Zhang, Qiuwang Wang, “Shell-side thermal-hydraulic performances of multilayer spiral-wound heat exchangers under different wall thermal boundary conditions”, *Applied Thermal Engineering*, Volume 70, Issue 2, (2014), pp. 1216-1227.

127. Prasad,, P.R., Sujatha, V., Sarma, C.B., Raju, G.J.V.J, “Studies on ionic mass transfer in the presence of spiral coil turbulence promoters in batch fluidized beds”, *Chemical Engineering and Processing*, Volume 43, (2004), pp. 1055–1062.

128. Neeraas, B.O., Fredheim, A.O., Aunan, B, “Experimental shell-side heat transfer and pressure drop in gas flow for spiral-wound LNG heat exchanger”, *International Journal of Heat and Mass Transfer*, Volume 47, (2004), pp. 353–361.

129. Seok Yoon, Seung-Rae Lee, Gyu-Hyun Go, Skhan Park, “An experimental and numerical approach to derive ground thermal conductivity in spiral coil type ground heat exchanger”, *Journal of the Energy Institute*, In Press, (2014), online.

130. Srbislav B. Genić, Branislav M. Jaćimović, Marko S. Jarić, Nikola J. Budimir, Mirko M. Dobrnjac, “Research on the shell-side thermal performances of heat exchangers with helical tube coils”, *International Journal of Heat and Mass Transfer*, Volume 55, Issues 15–16, (2012), pp. 4295-4300.

131. Ito, H., “Friction factors for turbulent flow in curved pipes”, *Journal of Basic Engineering*, Transactions of the ASME, Volume 81, (1959), pp. 123-134.

132. Nunge, R.J., Lin., T.S, “Laminar flow in strongly curved tubes”, *AIChE Journal*, Volume 19(6), (1973), pp.1280-1281.

133. Sarin, V.B., "The steady laminar flow of an elastico-viscous liquid in a curved pipe of varying elliptic cross section", *Mathematical and Computer Modeling,* Volume 26(3), (1997), pp. 109-121.

134. Akagawa, K., Sakaguchi, T, Ueda M., "Study on a gas-liquid two-phase flow in helically coiled tubes", *Bulletin of the JSME,* Volume 14(72), (1971), pp. 564-571.

135. Kasturi, G., Stepanek. J.B., "Pressure drop and void fraction measurements in concurrent gas-liquid flow in a coil", *Chemical Engineering Science*, Volume 27, (1972), pp. 1871-1880.

136. Rangacharyulu, K., Davies, G.S., "Pressure drop and holdup studies of air liquid flow in helical coils", *Chemical Engineering*, Volume 29, (1984), pp 41-46.

137. Tarbell, J. M., Samuels, M. R., "Momentum and heat transfer in helical coils", *Chemical Engineering*, Vol. 5, (1973), pp. 117-127

138. Grundmann, R., "Friction diagram of the helically coiled tube", *Chemical Engineering Process*, Volume 19, (1985), pp. 113-115.

139. Hart, J., Ellenberger, J., Hamersma, P.J., "Single and two-phase flow through helically coiled tubes", *Chemical Engineering Science,* Volume 45(4), (1988), pp. 775-783.

140. Guo, L., Feng, Z., Chen, X., "An experimental investigation of the frictional pressure drop of steam-water two-phase flow in helical coils", *International Journal of Heat and Mass Transfer,* Volume 44, (2002), pp. 2601-2610.

141. Guo, L., Feng, Z., and X. Chen, "Pressure drop oscillations of steam-water two phase flow in helically coiled tube", *International Journal of Heat and Mass Transfer,* Volume 44, (2002), pp. 1555-1564.

142. Downing, R. S., Kojaysoy, G., "Single and two-phase pressure drop characteristics in miniature helical channels", *Experimental Thermal and Fluid Science*, Volume 26, (2002), pp. 535-546.

143. Jayanti, S. Hewitt, G.F., "On the Paradox concerning friction factor ratio in laminar flow in coils", *Proceedings: Mathematical and Physical Sciences*, Volume 432(1885), (1991), pp. 291-299.

144. Van Dyke, M., "Extended Stokes series: laminar flow through a loosely coiled pipe", *Journal of Fluid Mechanics*, Volume 86, (1978), pp. 129-145.

145. Ali S., "Pressure drop correlations for flow through regular helical coil tubes", *Fluid Dynamics Research,* Volume 28, (2001), pp. 295–310.

146. Pimenta, T.A., Campos, J.B.L.M., "Friction losses of Newtonian and non-Newtonian fluids flowing in laminar regime in a helical coil", *Experimental Thermal and Fluid Science,* Volume 36, (2012), pp. 194–204.

147. Soeberg, K., "Viscous flow in curved tubes, Velocity profiles", *Chemical Engineering Science*, Volume 43(4), (1988), pp. 855-862.

148. Webster, D. R., Humphrey, J.A.C., “Experimental observations of flow stability in a helical coil”, *Transactions of the ASME, Journal of Fluids Engineering*, Volume 15(3), (1993), pp. 436-443.

149. Webster, D. R., Humphrey, J.A.C., “Traveling wave instability in helical coil flow”, *Physics of Fluids*, Vol. 9(2), (1997), pp. 407-418.

150. Taylor, G.I., “The criteria for turbulence in curved pipes”, *Proceedings of the Royal Society of London, Series A*, Volume *124*, (1929), *pp. 243-249.*

151. Hon, R., Humphrey J. A. C., Champagne, F., “Transition to turbulence of the flow in a straight pipe downstream of a helical coil”, *Physics of Fluids*, Vol. 11(10), (1999), pp. 2993-3002.

152. Austen, D. S, Soliman H.M., “Laminar flow and heat transfer in helically coiled tubes with substantial pitch”, *Experimental Thermal and Fluid Science*, Volume 1, (1988), pp. 183-194.

153. Xie, D.G., “Torsion effect on secondary flow in a helical pipe”, *International Journal of Heat and Mass Transfer*, Volume 11(2), (2001), pp. 114-119.

154. Liu, S., Masliyah, J.H., “Axially invariant laminar flow in helical pipes with a finite pitch”, *Journal of Fluid Mechanics*, Volume 251, (1993), pp. 315-353.

155. Liu, S., Masliyah J. H., “Developing convective heat transfer in helical pipes with finite pitch”, *International Journal of Heat and Fluid Flow*, Volume 15(1), (1994), pp. 66-74.

156. Yang, G., Dong, F., Ebadian, M.A., “Laminar forced convection in a helicoidal pipe with finite pitch”, *International Journal of Heat and Mass Transfer*, Vol. 38(5), (1995), pp.853-862.

157. Wang, J.W., Andrews,J.R.G., “Numerical Simulation of Flow in Helical Ducts”, *AIChE Journal*, Volume 41(5), (1995), pp. 1071-1080.

158. Jayakumar, J.S., Mahajani, S.M., Mandal, J.C., Iyer, K.N., Vijayan, P.K., “CFD analysis of single phase flow inside helically coiled tube”, *Computers and Chemical Engineering*, Volume 34, (2010), pp. 430-446.

159. Mihail, R., Straja, S., “The behavior of the helically coiled tube as a polymerization reactor”, *Chemical Engineering Science*, Volume 36, (1981), pp.1296-1266.

160. Sedahmed, G.H., Shemilt, L.W., Wong, F., “Natural convection mass transfer characteristics of rings and helical coils in relation to their use in electrochemical reactor design”, *Chemical Engineering Science*, Volume 40(7), (1985), pp.1109-1114.

161. Prasad, B.V.S.S.S., Das, D.H., Prabhakar, A.K., “Pressure drop, heat transfer and performance of a helically coiled tubular exchanger”, *Heat Recovery Systems & CHP*, Volume 9(3), (1989), pp. 249-256.

162. Allen, P.L., Ajele, O.J., "Optimum configuration of natural convection shell and coil heat exchanger with respect to thermal performance", *Proceedings of the 1994 Annual conference*, June 27-30, San Jose, California, *American Solar Energy Society*, (1994), pp. 292-297.

163. Taherian, H., Allen P.L., "Natural convection from vertical helical coils in a cylindrical enclosure", *Proceedings of the ASME Heat Transfer Division, HTD*, Volume 353, (1997), pp. 135-142.

164. Taherian, H., Allen, P.L., "Experimental study of natural convection shell-and coil heat exchangers", *ASME Proceedings of the 7th AIAA/ASME, Joint Thermo physics and Heat Transfer Conference, HTD* - Volume 357-2 (1998).

165. Klunge, T., Kalra, A., Belfort, G., "Viscosity effects on Dean vortex membrane microfiltration", *AIChE Journal*, Volume 45(9), (1966), pp. 1913-1926.

166. Fleming, W.H., Khan, J.A., Rhodes, C.A., "Effective heat transfer in a etalhydride-based hydrogen separation process", *International Journal of Hydrogen Energy*, Volume 26, (2001), pp. 711-724.

167. Sahoo, P.K., Md., I., Ansari, A., Datta, A.K., "Computer-aided design and performance of an indirect type helical tube ultra-high temperature (UHT) milk sterilizer", *Journal of Food Engineering*, Volume 51, (2002), pp.13-19.

168. Sahoo, P.K., Md., I., Ansari, A., Datta, A.K., "A computer based iterative solution for accurate estimation of heat transfer coefficients in a helical tube heat exchanger", *Journal of Food Engineering*, Volume 58, (2004), pp. 211-214.

169. Yi, J., Liu, Z.H., Wang, J., "Heat transfer characteristics of the evaporator section using small helical coiled pipe in a looped heat pipe", *Applied Thermal Engineering*, Volume 23, (2003), pp. 89-99.

170. Hameed, M.S. Muhammed M.S., "Mass transfer into liquid falling tubes in straight and helically coiled tubes", *International Journal of Heat and Mass Transfer*, Volume 46, 2003, pp. 1715-1724.

171. Fernández-Seara, J., Sieres, J, Vazquez, J., "Heat and mass transfer analysis of a helical coil rectifier in an ammonia-water absorption system". *International Journal of Thermal Sciences*, Volume 42, (2003), pp. 783-794.

172. Yu, B, Han, J.T., Kang, H.J., Lin, C.X., Awwad, A. Ebadian, M.A., "Condensation heat transfer of R-134a flow inside helical pipes at different orientations", *International Communications in Heat and Mass Transfer*, Volume 30(6), (2003), pp.745-754.

173. Xiaowen, Yi, Lee, W.L., "The use of helical heat exchanger for heat recovery domestic water-cooled air-conditioners", *Energy Conversion and Management*, Volume 50, (2009), pp. 240–246.

174. El-Sayed Mosaad, M., Al-Hajeri, M., Al-Ajmi Abo, R., Koliub, M., “Heat transfer and pressure drop of R-134a condensation in a coiled, double tube”, *Heat and Mass Transfer*, Volume 45, (2009), pp. 1107-1115.
175. Zhao Zhenxing, Xiangyu Wang, Defu Che , Zidong Cao, “Numerical studies on flow and heat transfer in membrane helical-coil heat exchanger and membrane serpentine-tube heat exchanger”, *International Communications in Heat and Mass Transfer*, Volume 38, (2011), pp. 1189–1194.
176. Yang Zhen, Zhenxing Zhao, Yinhe Liu, Yongqiang Chang, Zidong Cao, “Convective heat transfer characteristics of high-pressure gas in heat exchanger with membrane helical coils and membrane serpentine tubes”, *Experimental Thermal and Fluid Science*, Volume 35, (2011), pp. 1427–1434.
177. Kumbhare, B P, Purandare, P.S., Mali, K.V., “Experimental analysis of square and circular coil for the heat recovery system”, *International journal Engineering and science,* Volume 2(5), (2012), pp. 318–327.
178. Bazargan Hassanzadeh, Ali Keshavarz, Masood Ebrahimi, “Heat transfer simulation in a helically coiled tube steam generator”, *Heat Mass Transfer*, Volume 50, (2014), pp. 13–21, DOI 10.1007/s00231-013-1215-y.
179. Ghorbani, N., Taherian, H., Gorji,M, Mirgolbabaei, H., “An Experimental study of thermal performance of shell and coil heat exchangers”, *International Communication of Heat and Mass Transfer*, Volume 37, (2010), pp. 775-781.
180. Ghorbani, N., Taherian, H., Gorji,M, Mirgolbabaei, H., “Experimental study of mixed convection heat transfer in vertical helically coiled tube heat exchangers”, *Experimental* Thermal and Fluid Science, Volume 34, Issue 7, (2010), pp. 900-905.
181. Salimpour M.R., “Heat transfer coefficients of shell and coiled tube heat exchangers”, *Experimental Thermal and Fluid Science*, Volume 33, (2009), pp. 203–207.
182. Abdalla Gomaa, Wael I. A. Aly, M. Omara, Mahmoud Abdelmagied, “Correlations for heat transfer coefficient and pressure drop in the annulus of concentric helical coils”, *Heat Mass Transfer,* Volume 50, (2014), pp. 583–586, DOI 10.1007/s00231-013-1258-0
183. Korne, A.B., Mali, K.V., “Heat Transfer analysis of helical coil heat exchanger with circular and square coiled pattern”, *International Journal of Engineering and Sciences*, Volume 2(6), (2012), pp. 413-423.
184. Cengiz Y, Yasar B, Dursun P., “Heat transfer and pressure drops in rotating helical pipes”, *Applied Energy,* Volume 50, (1995), pp.185-195.
185. Ramana Rao, M.V., Sadasivudu, D., “Pressure drop studies in helical coils”, *Indian J. Technology*, Volume 12, (1974), pp. 473.

186. Sieder, E.N., Tate, C.E., “Heat transfer and pressure drop of liquid in straight tube”, *Industrial Engineering Chemistry*, Volume 28, (1931), pp. 1429 (As in J.P. Halman, Heat and mass Transfer, Wielly Publications).

187. Nusselt, W., “Der warmeaustausch zwishche wand und wasser in Rohr”, *Forsh Geb. Ingenieurwes*, Volume 2, (1931), pp. 309 (As in J.P. Halman, Heat and mass Transfer, Wielly Publications).

188. Coleman, H.W., Steele, W.G., “Experimental Uncertainty Analysis for Engineers”, *Wiley,* New York, 1989.

189. ANSI/ASME, “Measurement uncertainty”, *PTC 19*, (1986), pp. 1–1985.

190. Kannadasan, N., Ramanathan, K., Suresh, S., “Comparison of heat transfer and pressure drop in horizontal and vertical helically coiled heat exchanger with CuO / water based nano fluids”, *Experimental Thermal and Fluid Science*, Volume 42, (2012), pp 64–70.

Appendix A

Figures for results of thermal analysis

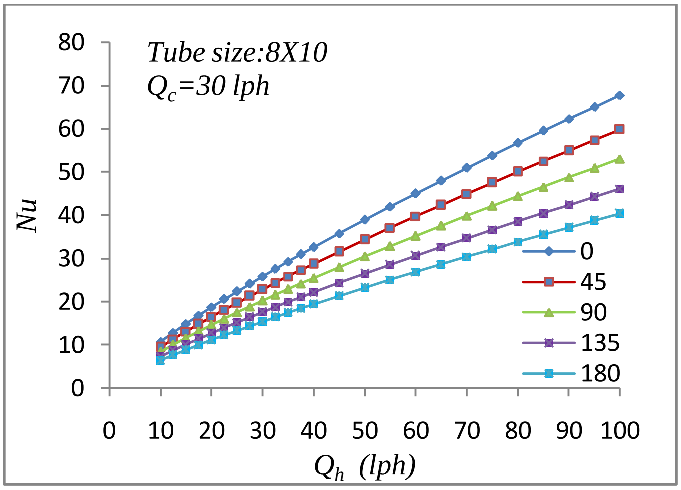

Fig. A.1 Nu vs Q_h (Tube size 8X10 (Q_c = 30 lph))

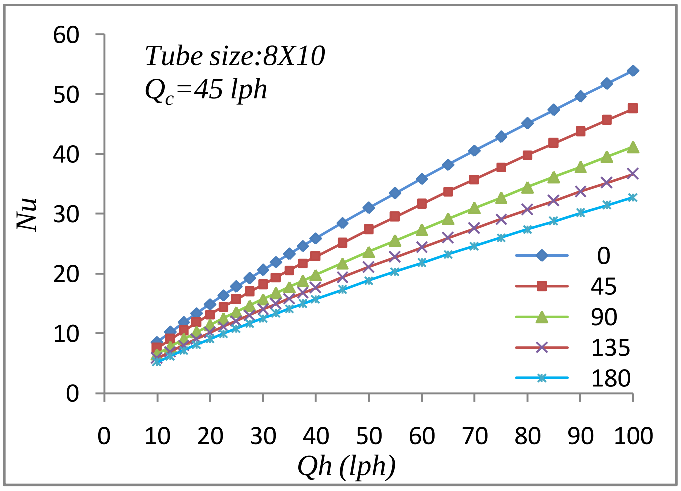

Fig. A.2 Nu vs Q_h (Tube size 8X10 (Q_c = 45 lph))

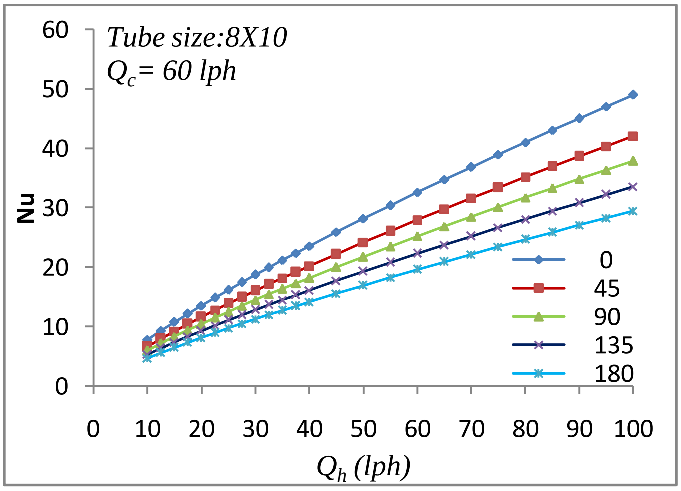

Fig. A.3 Nu vs Q_h (Tube size 8X10 (Q_c = 60 lph))

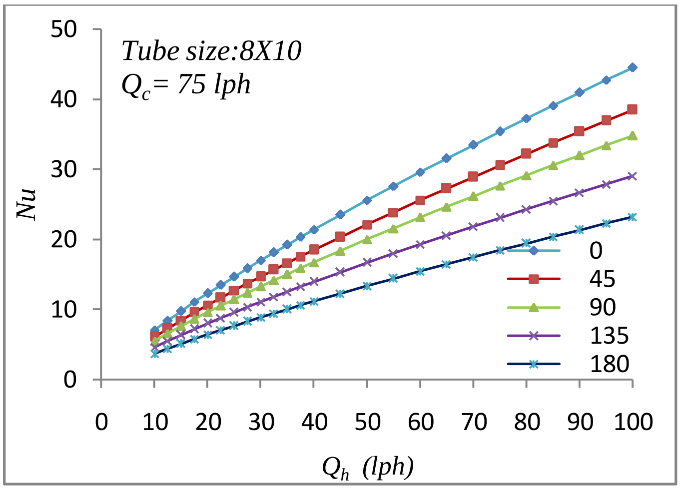

Fig. A.4 Nu vs Q_h (Tube size 8X10 (Q_c = 75 lph))

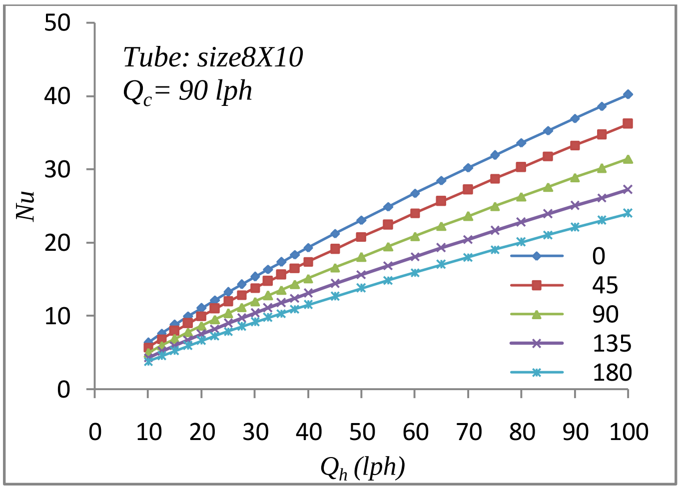

Fig. A.5 Nu vs Q_h (Tube size 8X10 (Q_c = 90 lph))

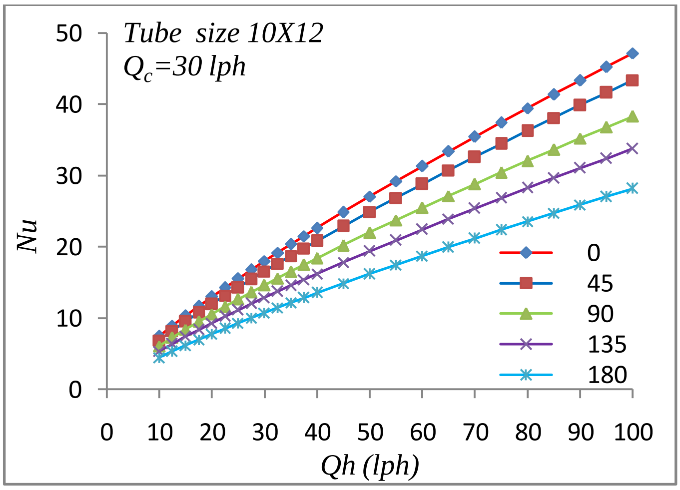

Fig. A.6 Nu vs Q_h (Tube size 10X12 (Q_c = 30 lph))

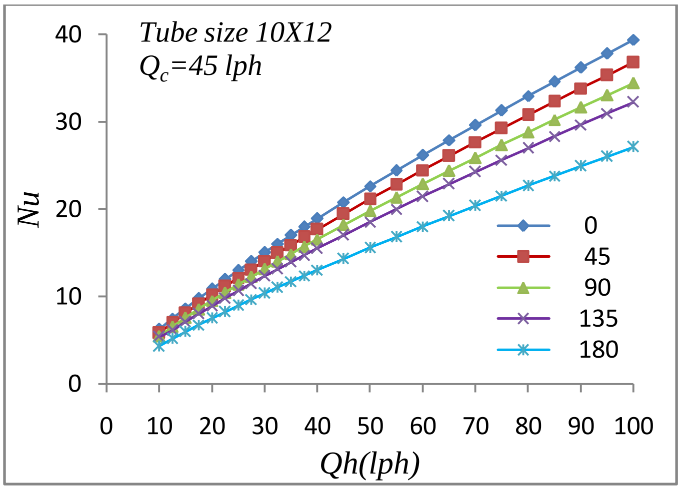

Fig. A.7 Nu vs Q_h (Tube size 10X12 (Q_c = 45 lph))

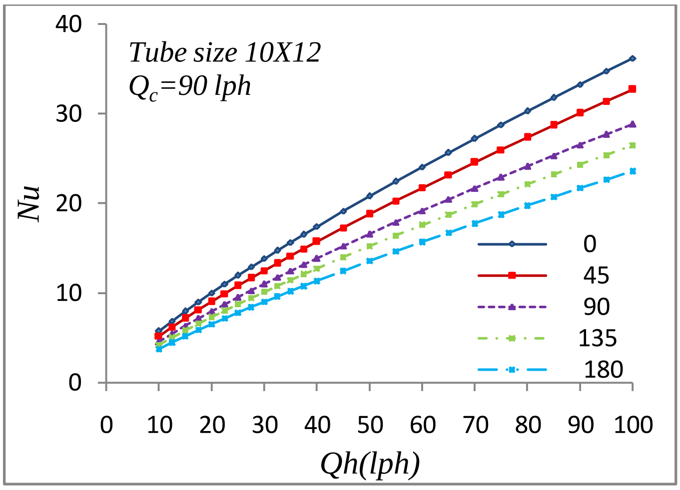

Fig. A 10 Nu vs Q_h (Tube size 10X12 (Q_c = 90 lph))

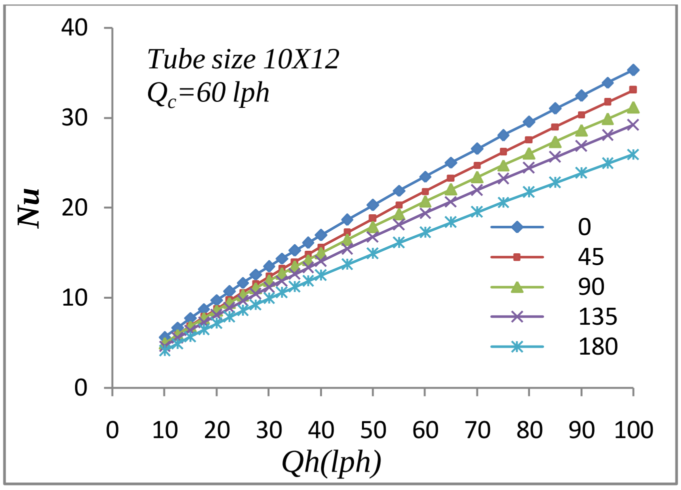

Fig. A.8 Nu vs Q_h (Tube size 10X12 (Q_c = 60 lph))

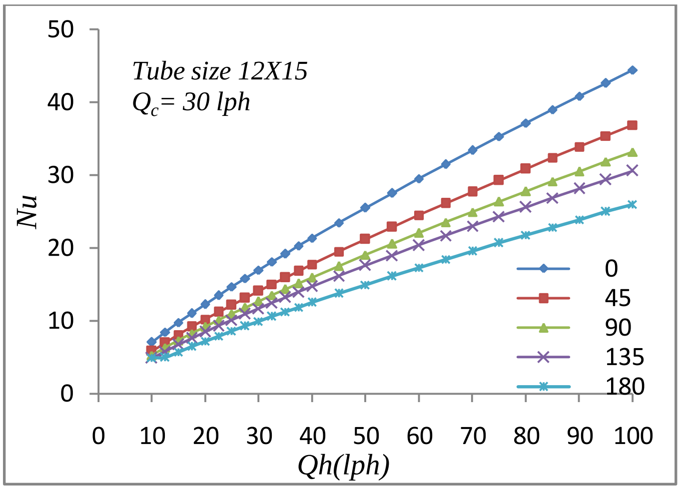

Fig. A.11 Nu vs Q_h (Tube size 12X15 (Q_c = 30 lph))

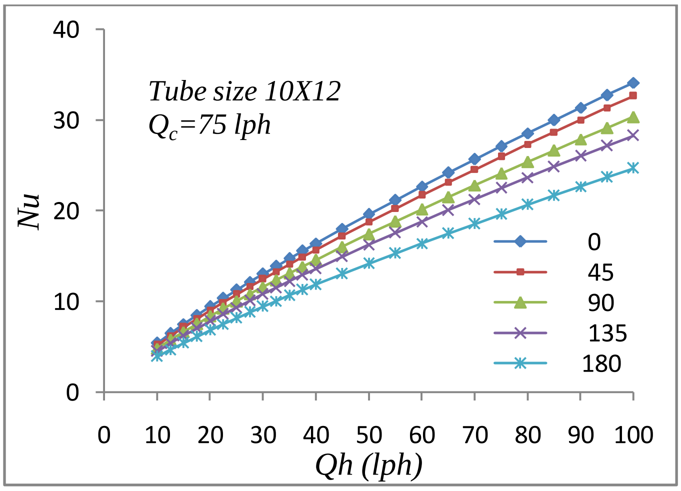

Fig. A.9 Nu vs Q_h (Tube size 10X12 (Q_c = 75 lph))

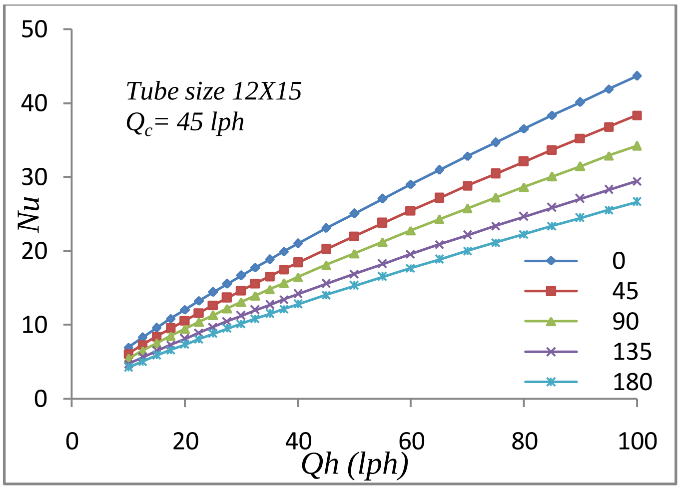

Fig. A.12 Nu vs Q_h (Tube size 12X15 (Q_c = 45 lph))

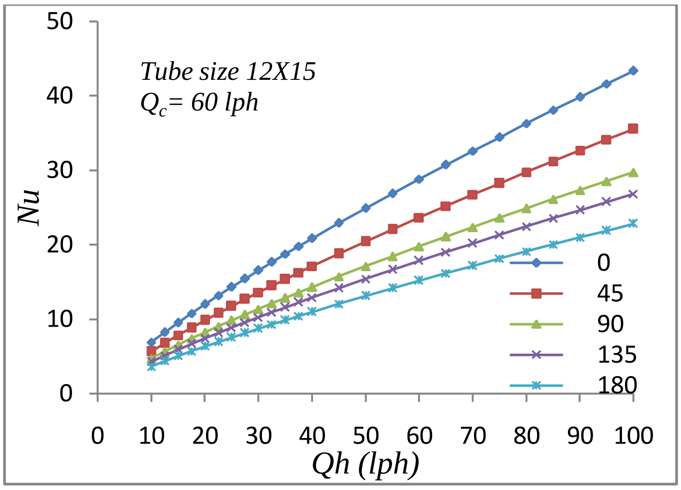

Fig. A.13 Nu vs Q_h (Tube size 12X15 (Q_c = 60 lph)

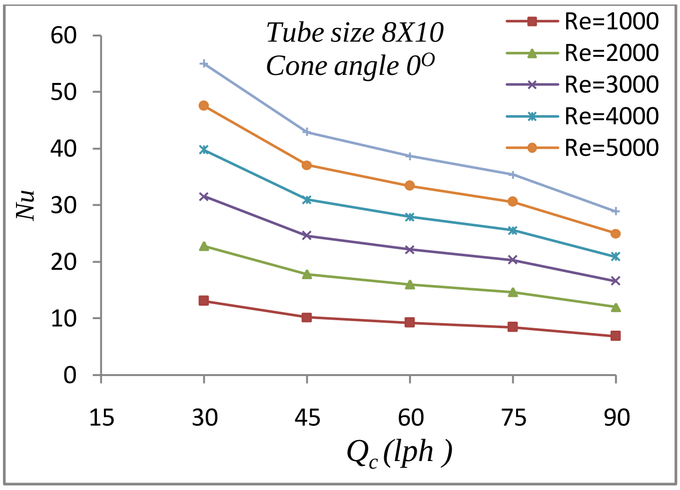

Fig. A.16 Nu vs Q_c (Tube size 8X10 Cone angle:0)

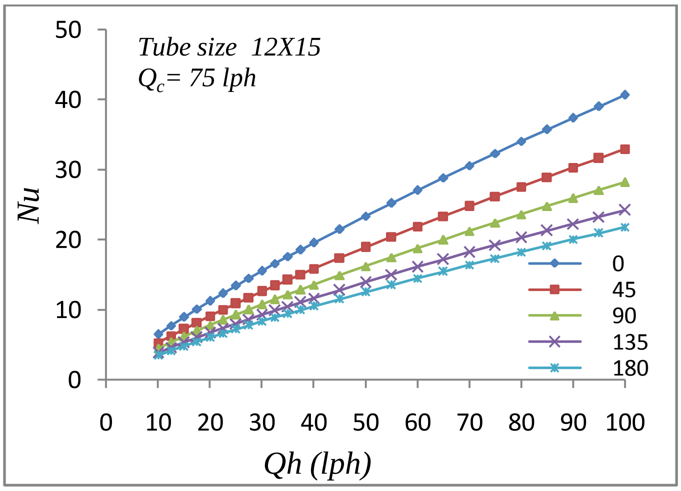

Fig. A.14 Nu vs Q_h (Tube size 12X15 (Q_c = 75 lph))

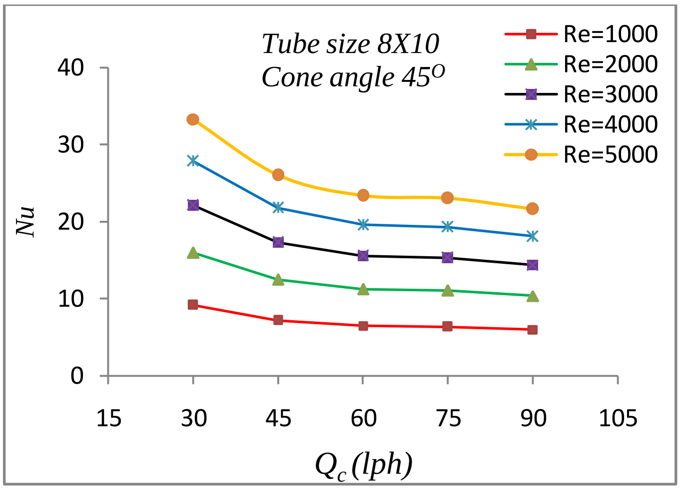

Fig. A.17 Nu vs Q_c (Tube size 8X10 Cone angle:45)

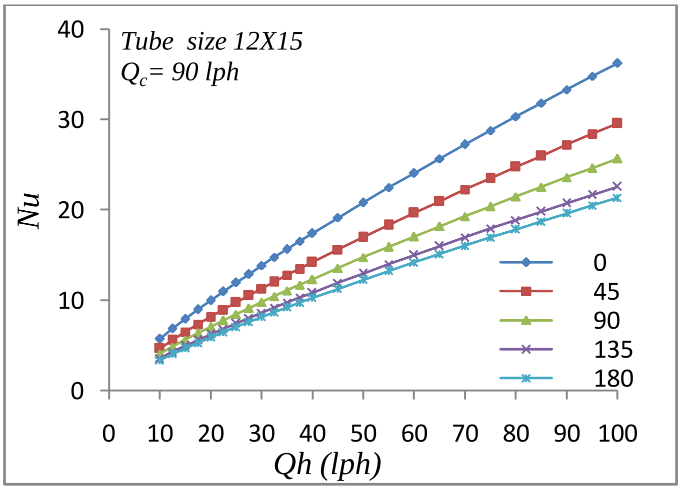

Fig. A.15 Nu vs Q_h (Tube size 12X15 (Q_c = 90 lph))

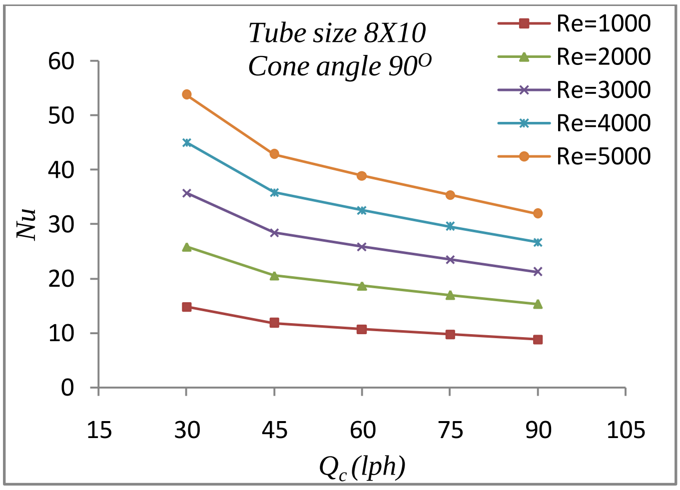

Fig.A.18 Nu vs Q_c (Tube size 8X10 Cone angle: 90^O)

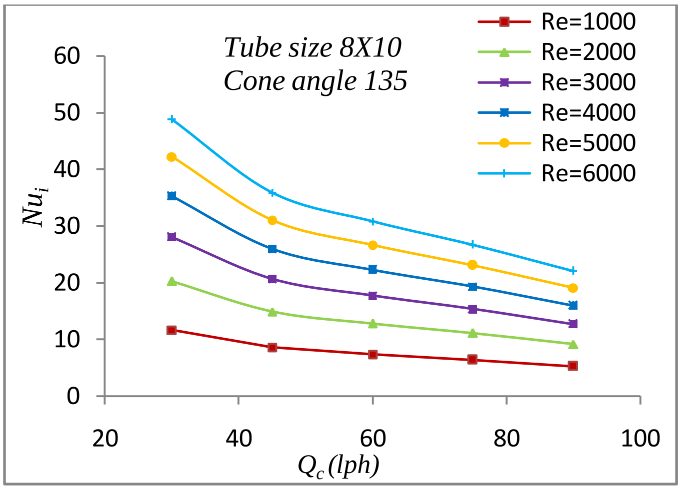

Fig. A.19 Nu vs Q_c (Tube size 8X10 Cone angle: 135^O)

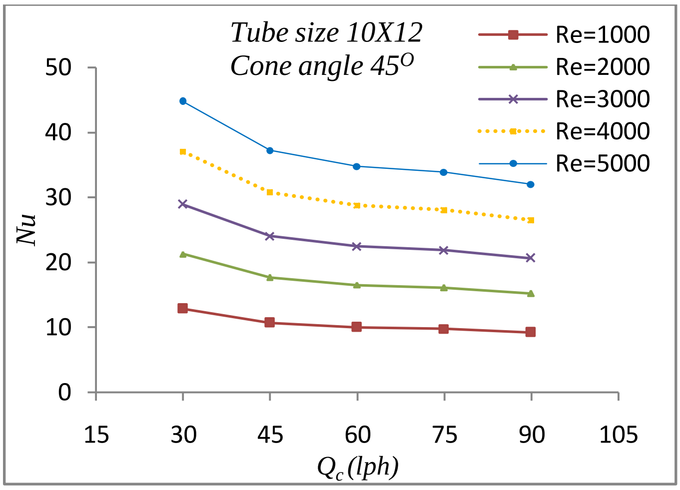

Fig. A.22 Nu vs Q_c (Tube size 10X12 Cone angle: 45^O)

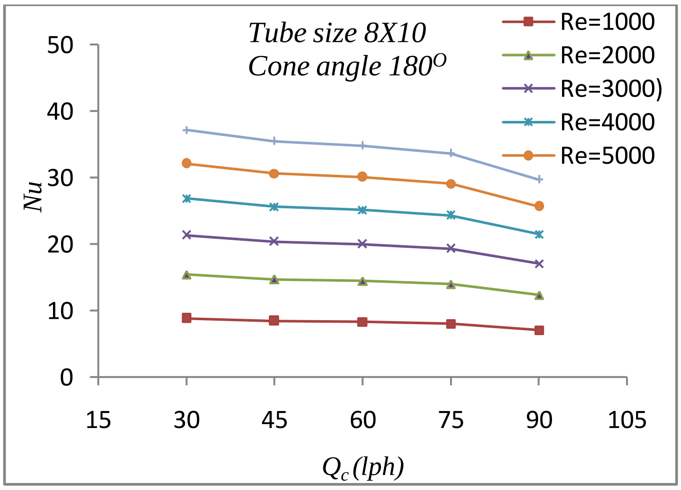

Fig. A. 20 Nu vs Q_c (Tube size 8X10 Cone angle: 180^O)

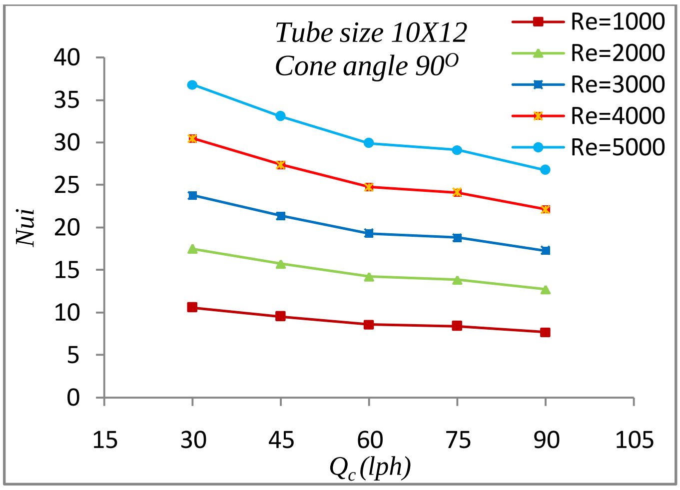

Fig. A.23 Nu vs Q_c (Tube size 10X12 Cone angle: 90^O)

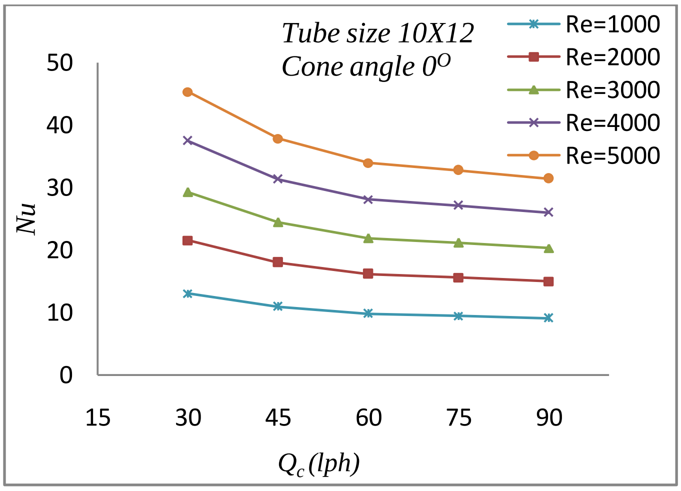

Fig. A.21 Nu vs Q_c (Tube size 10X12 Cone angle: 0^O)

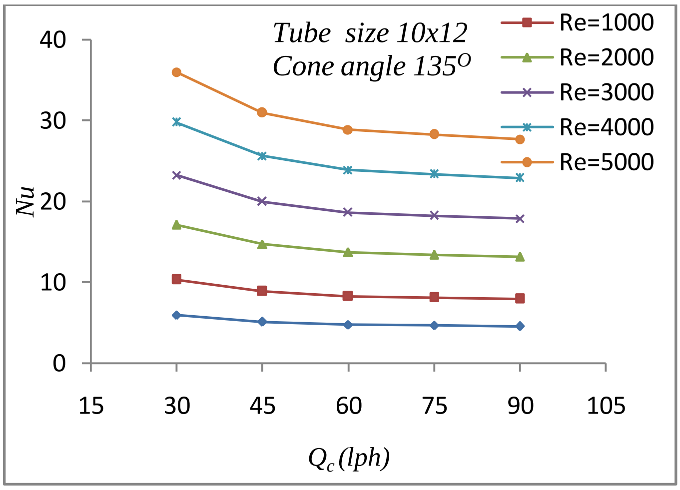

Fig.A.24 Nu vs Q_c (Tube size 10X12 Cone angle: 135^O)

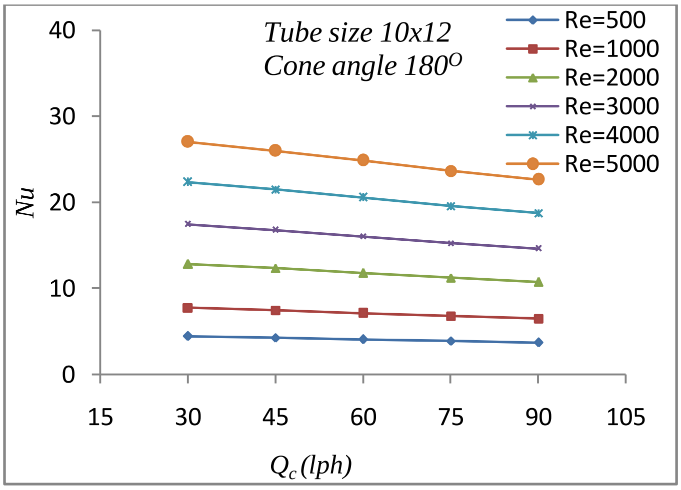

Fig. A.25 Nu vs Q_c (Tube size 10X12 Cone angle: 180^O)

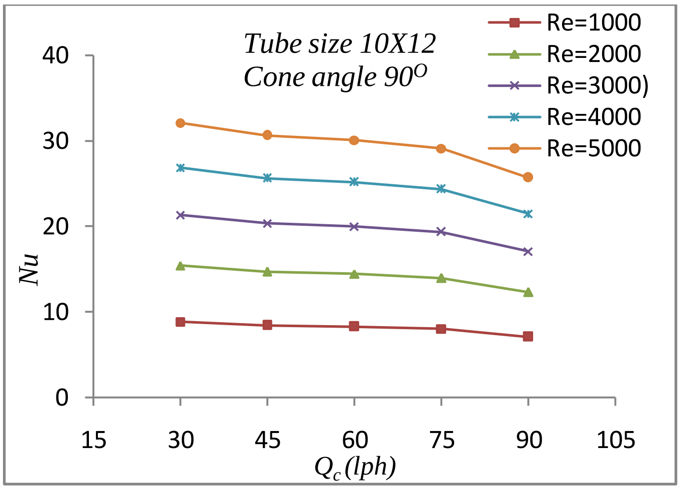

Fig. A.28 Nu vs Q_c (Tube size 12X15 Cone angle: 90^O)

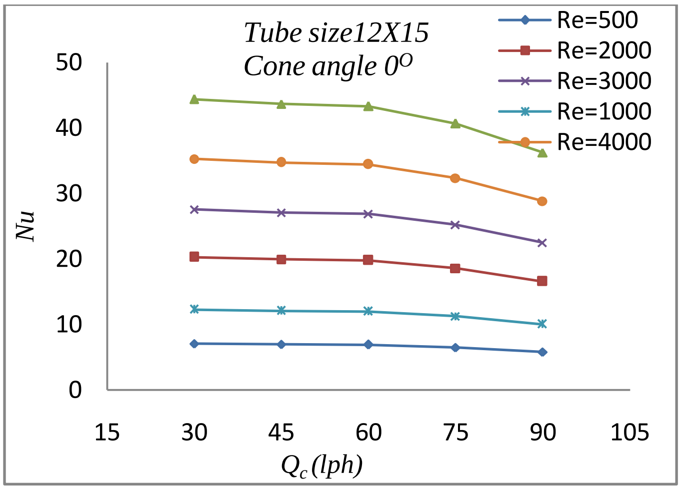

Fig. A.26 Nu vs Q_c (Tube size 12X15 Cone angle: 0^O)

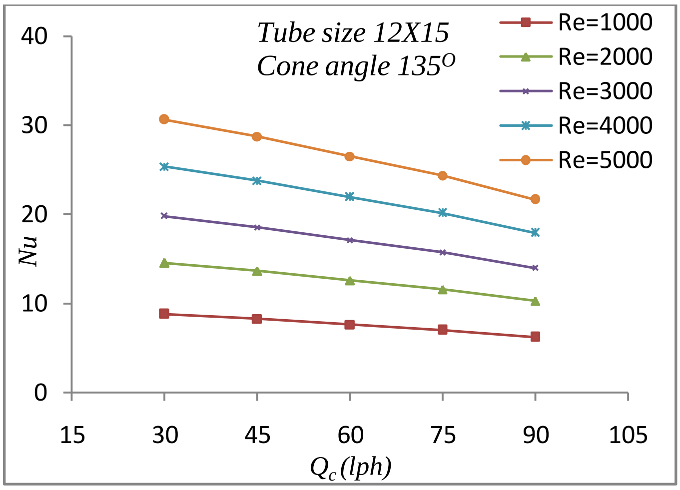

Fig. A.29 Nu vs Q_c (Tube size 12X15 Cone angle: 135^O)

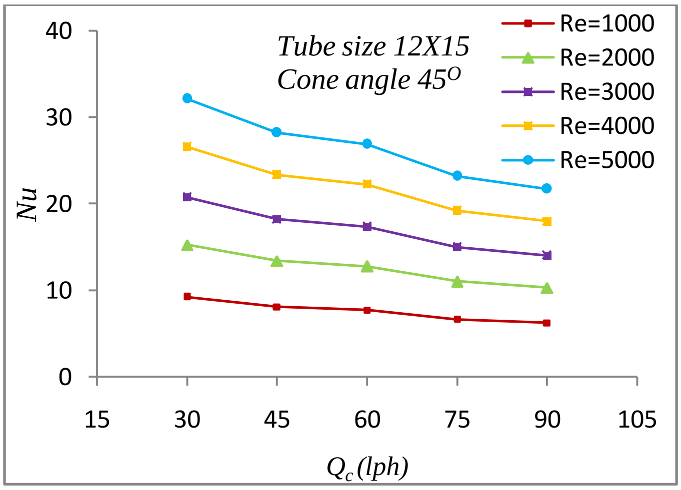

Fig. A.27 Nu vs s Q_c (Tube size 12X15 Cone angle: 45^O)

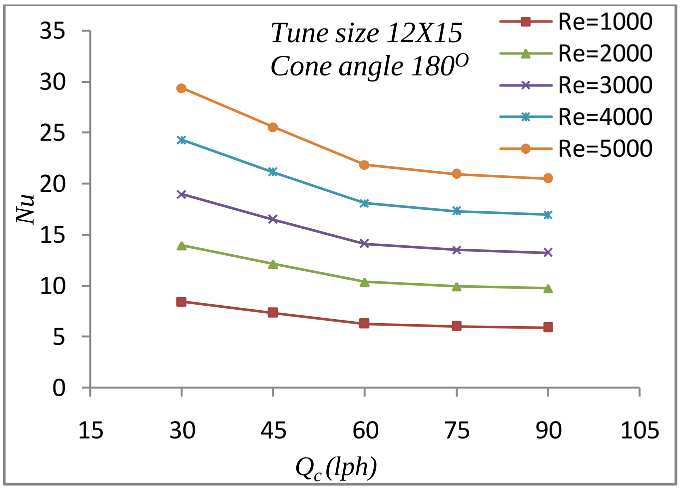

Fig. A.30 Nu vs Q_c (Tube size 12X15 Cone angle: 180^O)

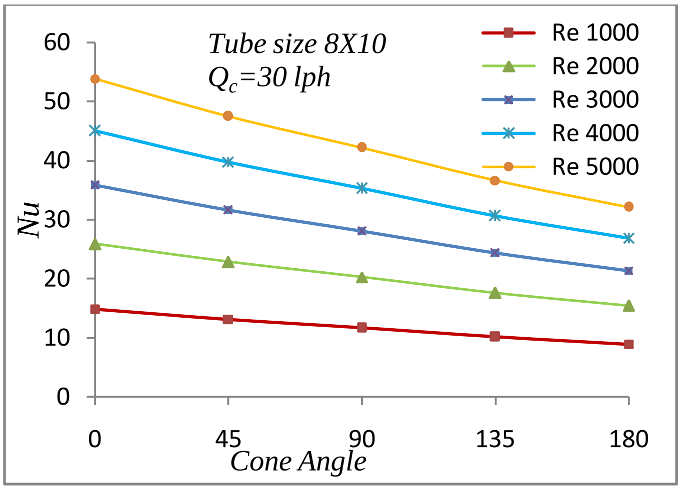

Fig. A.31 Nu vs Cone angle (Tube size 8X10, Q_c = 30 lph)

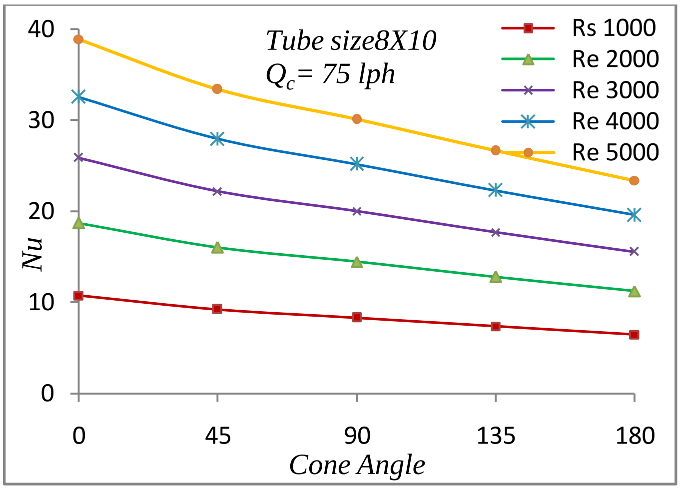

Fig. A.34 Nu vs Cone angle (Tube size 8X10, Qc = 75 ph)

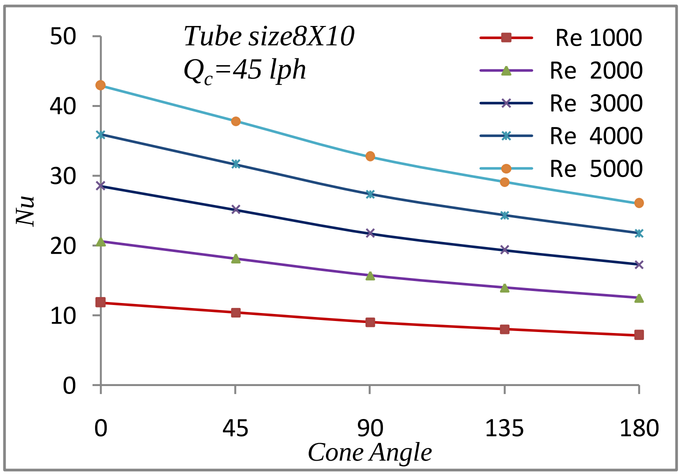

Fig. A.32 Nu vs Cone angle (Tube size 8X10, Qc = 45 lph)

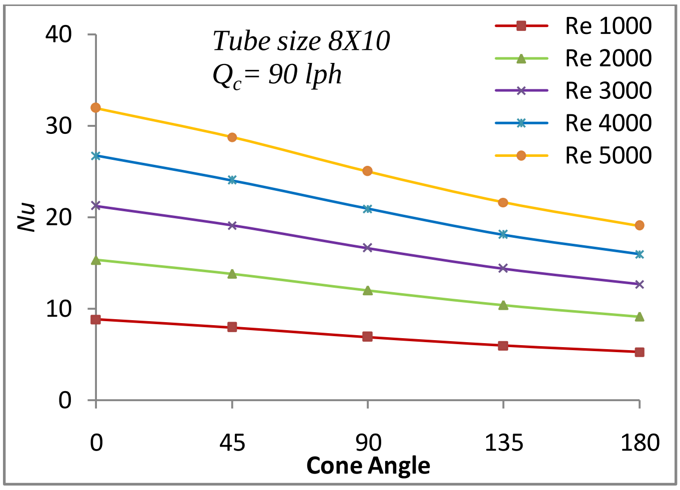

Fig. A. 35 Nu vs Cone angle (Tube size 8X10 (Q_c = 90 lph))

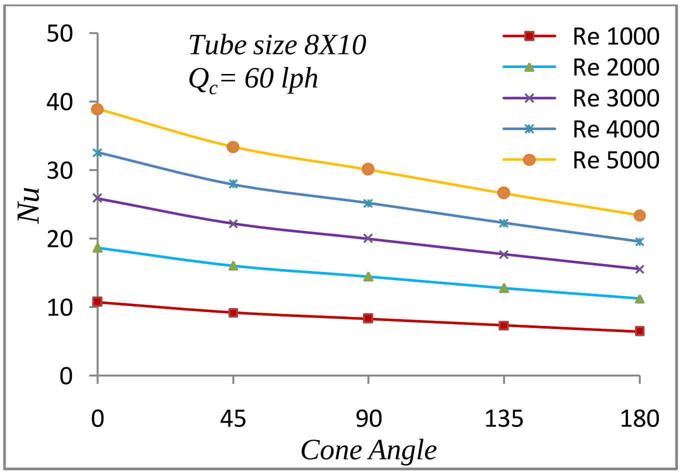

Fig. A.33 Nu vs Cone angle (Tube size 8X10, Q_c = 60 lph))

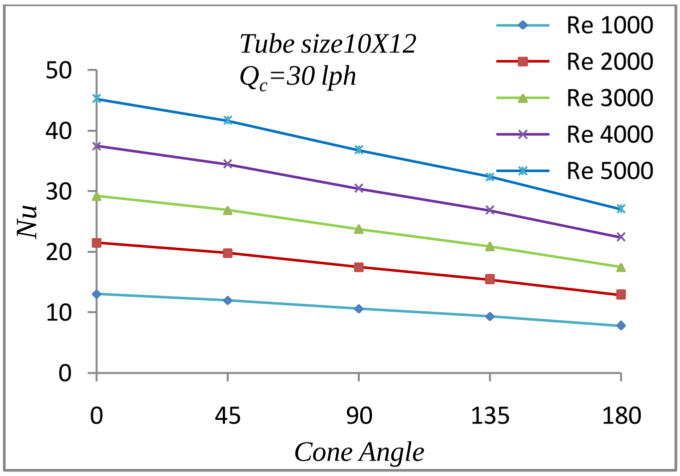

Fig. A.36 Nu vs Cone angle (Tube size 10X12, Q_c = 30 lph)

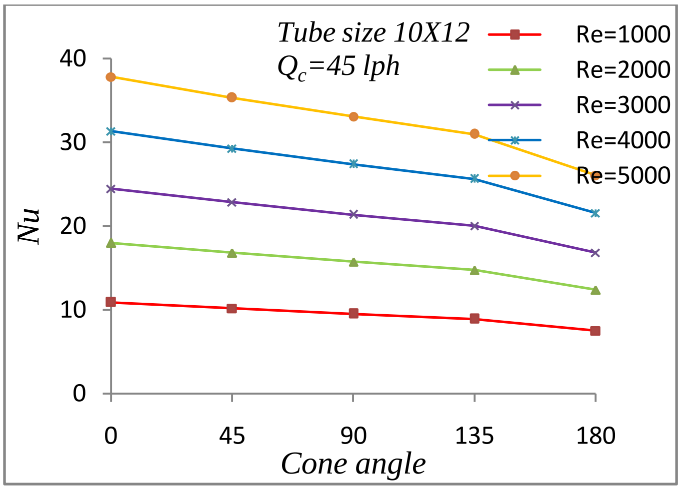

Fig. A.37 Nu vs Cone angle (Tube size 10X12, Q_c = 45 lph)

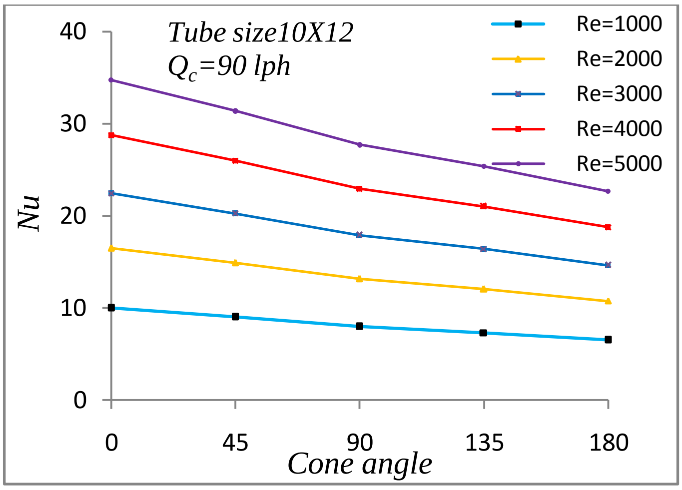

Fig. A.40 Nu vs Cone angle (Tube size 10X12, Q_c = 90 lph)

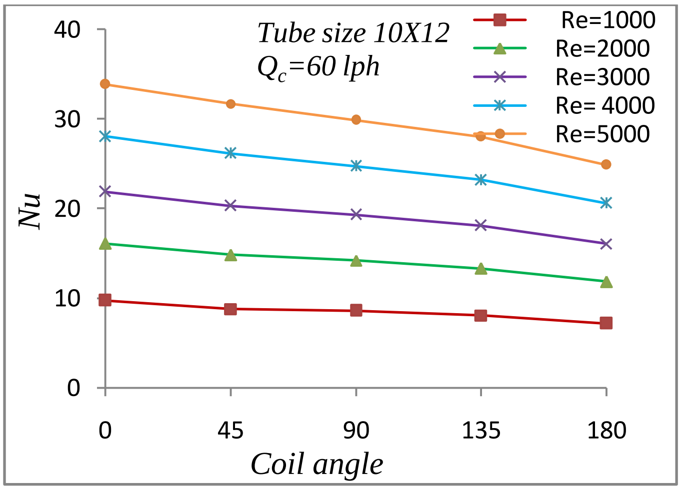

Fig. A.38 Nu vs Cone angle (Tube size 10X12, (Q_c =60 lph)

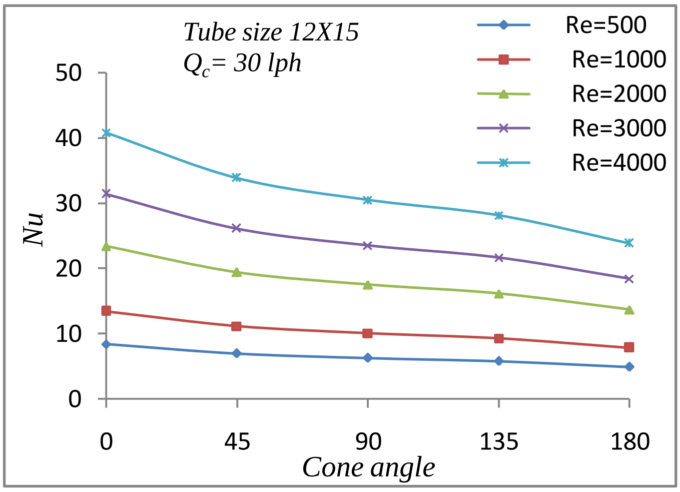

Fig. A.41 Nu vs Cone angle (Tube size 12X15, Q_c = 30 lph)

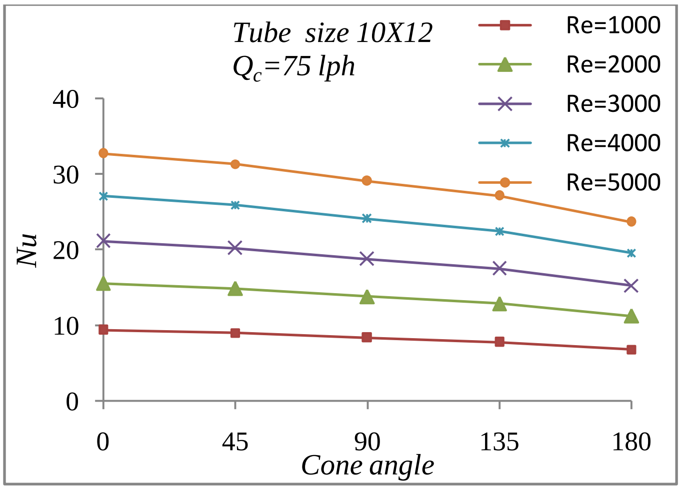

Fig. A.39 Nu vs Cone angle (Tube size 10X12, Q_c = 75 lph)

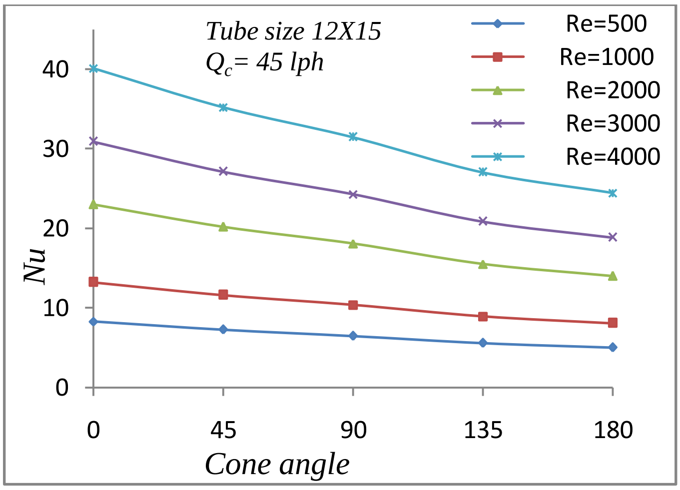

Fig. A.42 Nu vs Cone angle (Tube size 12X15, Q_c = 30 lph)

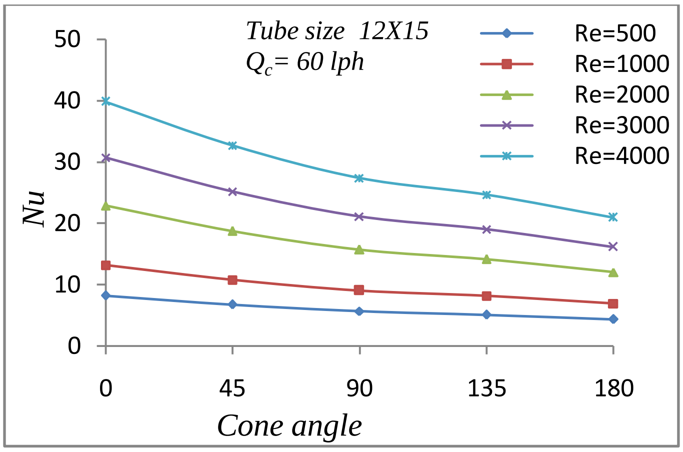

Fig. A.43 Nu vs Cone angle (Tube size 12X15, Q_c = 60 lph)

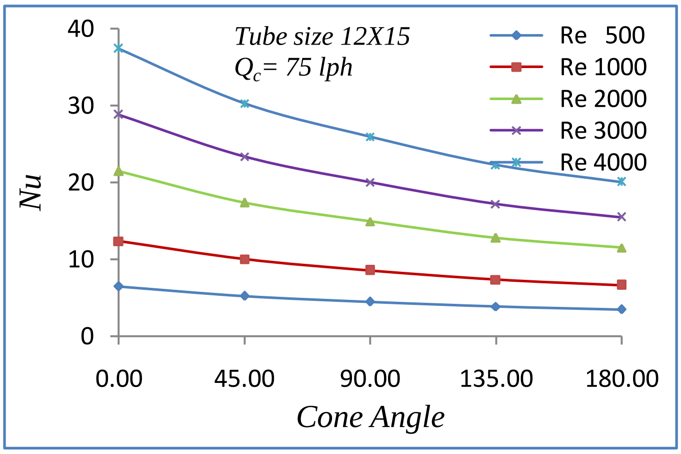

Fig. A.44 Nu vs Cone angle (Tube size 12X15, Q_c = 75 lph)

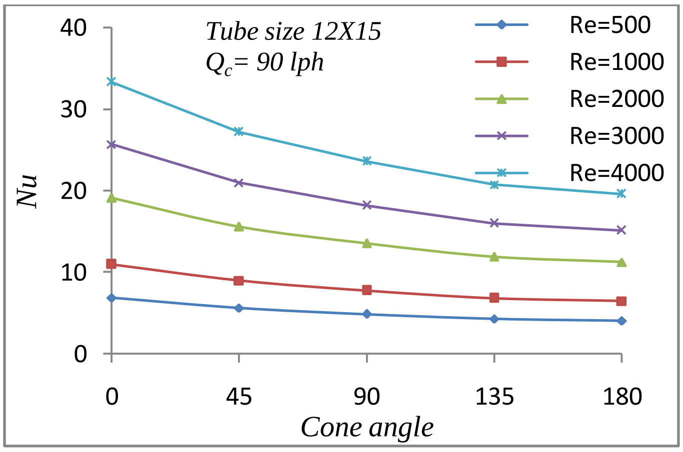

Fig. A. 45 Nu vs Cone angle (Tube size 12×15, Q_c=90 lph)

Appendix B

Sample observation tables
(one of each coil)

Table B.1. Observation table (Tube size: 8X10, Cone angle - *0*^{O})

Tube size: 8X10 Cone angle -0^{O}			T1=Cold Water In T2=Cold Water Out T3=Hot Water in T4=Hot Water out			
Sr. No.	Flow Rate(*lph*)		Temperature (^{O}C)			
	Cold	Hot	T1	T2	T3	T4
1	60	10	26.6	33.6	65.4	31.2
2	60	12.5	26.6	34.4	66.5	32.1
3	60	15	26.6	35.5	67.9	33
4	60	17.5	26.6	36.6	68.4	34.5
5	60	20	26.6	37.5	69.5	35.4
6	60	22.5	26.6	38.6	70.2	36.8
7	60	25	26.6	39.6	70.4	38.1
8	60	27.5	26.6	40.7	70.9	39
9	60	30	26.6	42.1	71.9	40.2
10	60	32.5	26.6	42.8	72.3	40.9
11	60	35	26.6	43.7	72.3	42.3
12	60	37.5	26.6	44.4	72.3	43.2
13	60	40	26.6	45.3	71.8	44.4
14	60	45	26.6	46.3	71.6	45.8
15	60	50	26.6	47.2	72.7	47.2
16	60	55	26.6	48.6	73.1	49
17	60	60	26.6	49.8	73.4	50.6
18	60	65	26.6	51	73.8	51.7
19	60	70	26.6	52.2	72.7	53.5
20	60	75	26.6	53.8	72.7	54.6
21	60	80	26.6	53.5	73.1	54.7
22	60	85	26.6	54.1	73.9	55.7
23	60	90	26.6	55.3	72.2	57
24	60	95	26.6	55.9	72.7	58
25	60	100	26.6	57	72.8	59

Table B.2.Observation table (Tube size: 8X10, Cone angle - *45* ^{O})

Tube size : 8X10 Cone angle 45^{0}			T1=Cold Water In T2=Cold Water Out T3=Hot Water in T4=Hot Water out			
Sr. No	Flow Rate (*lph*)		Temperature (^{O}C)			
	Cold	HOT	T1	T2	T3	T4
1	45	10	28.1	36.9	64.8	33.1
2	45	12.5	28.1	37.1	66.9	34.3
3	45	15	28.1	38	67.5	35.3
4	45	17.5	28.1	39	67.9	36.9
5	45	20	28.1	40	67.9	38
6	45	22.5	28.1	41.4	67.6	39.1
7	45	25	28.1	42.4	67.2	40.2
8	45	27.5	28.1	43.2	66.8	41
9	45	30	28.1	44.2	66.5	41.6
10	45	32.5	28.1	44.7	66.8	42.1
11	45	35	28.1	45.4	67.4	43.2
12	45	37.5	28.1	46.3	68.6	44.6
13	45	40	28.1	47	69.4	46.7
14	45	45	28.1	48.2	70.2	47.9
15	45	50	28.1	49.2	71.8	49.2
16	45	55	28.1	50.2	72.3	51.2
17	45	60	28.1	50.4	72.5	52.6
18	45	65	28.1	50.6	73	54.3
19	45	70	28.1	52.4	73.5	56.4
20	45	75	28.1	53.7	73.7	57.5
21	45	80	28.1	54.6	73	58.2
22	45	85	28.1	55.9	72.5	59.4
23	45	90	28.1	57.2	72.1	59.9
24	45	95	28.1	58.9	72.3	60.4
25	45	100	28.1	59.8	72.5	61.3

Table B.3Observation table(Tube size : 8X10, Cone angle - *90^{O}*)

Tube size : 8X10 Cone angle 90^{O}			T1=Cold Water In T3=Hot Water in		T2=Cold Water Out T4=Hot Water out	
Sr. No	Flow Rate (*lph*)		Temperature(^{O}C)			
	Cold	HOT	T1	T2	T3	T4
1	30	10	28.7	41	62.3	34.6
2	30	12.5	28.7	41.8	63.4	35.8
3	30	15	28.7	42.2	64.5	37
4	30	17.5	28.7	43.6	65	38.3
5	30	20	28.7	45	65.4	39.8
6	30	22.5	28.7	46.3	65.9	40.7
7	30	25	28.7	47.3	66	42.1
8	30	27.5	28.7	48.4	65.2	43.2
9	30	30	28.7	49.6	66	44.7
10	30	32.5	28.7	50.2	66.1	45.3
11	30	35	28.7	51.3	66.5	46.2
12	30	37.5	28.7	52.1	66.6	47.4
13	30	40	28.7	53.3	67	48.3
14	30	45	28.7	53.8	66.9	50.4
15	30	50	28.7	54.8	67.2	51
16	30	55	28.7	55.6	67.5	53.4
17	30	60	28.7	56.6	67.9	54.6
18	30	65	28.7	57.3	68.5	56.4
19	30	70	28.7	58.5	69.5	57.6
20	30	75	28.7	58.9	70	58.3
21	30	80	28.7	59.6	70.5	59
22	30	85	28.7	60.5	70.3	60.7
23	30	90	28.7	61.5	70.2	60.9
24	30	95	28.7	62.2	70.5	61.2
25	30	100	28.7	62.8	70.5	61.9

Table B.4 Observation table (Tube size 8X10, Cone angle- *135^{O}*)

Tube size : 8X10, Cone angle 135^{O}			T1=Cold Water In T3=Hot Water in		T2=Cold Water Out T4=Hot Water out	
Sr. No	Flow Rate (*lph*)		Temperature (^{O}C)			
	Cold	HOT	T1	T2	T3	T4
1	60	10	26.2	34.5	65.2	32.5
2	60	12.5	26.2	35.3	65.9	32.6
3	60	15	26.2	34.8	66.9	33.5
4	60	17.5	26.2	35.6	67.2	34.9
5	60	20	26.2	36.4	67.5	35.8
6	60	22.5	26.2	37.3	68	36.8
7	60	25	26.2	38	68.2	37.9
8	60	27.5	26.2	39.2	68.5	39
9	60	30	26.2	39.5	68.7	40.3
10	60	32.5	26.2	40.5	68.9	41.1
11	60	35	26.2	41.9	69	42.4
12	60	37.5	26.2	42.4	69.1	43
13	60	40	26.2	43	69.4	44.5
14	60	45	26.2	45	69.5	45.8
15	60	50	26.2	45.2	69.9	47.8
16	60	55	26.3	46.7	69.6	48.6
17	60	60	26.3	47	69.7	50.2
18	60	65	26.3	48.4	69.3	52
19	60	70	26.3	49	69	51.7
20	60	75	26.3	49.7	69.3	52.7
21	60	80	26.3	50.4	69.3	53.4
22	60	85	26.3	51	69.4	54.3
23	60	90	26.3	51.5	68.7	54.9
24	60	95	26.3	52.1	68.9	55.3
25	60	100	26.3	52.7	68.8	56.1

Table B.5 Observation table (Tube 8X10, Cone angle *180^{O}*)

Tube size : 8X10 Cone angle -180^{O}			T1=Cold Water In T3=Hot Water in		T2=Cold Water Out T4=Hot Water out	
Sr. No	Flow Rate (*lph*)		Temperature (^{O}C)			
	Cold	HOT	T1	T2	T3	T4
1	60	10	25.9	33	65.5	32.3
2	60	12.5	25.9	33.7	66.1	33.2
3	60	15	25.9	34.3	67.3	34.1
4	60	17.5	25.9	35.2	68.3	35.3
5	60	20	25.9	36.1	68.7	36.4
6	60	22.5	25.9	37.1	68.5	37.5
7	60	25	25.9	37.9	68.7	38.5
8	60	27.5	25.9	38.8	69.5	39.7
9	60	30	25.9	39.6	69.8	40.7
10	60	32.5	25.9	40.5	69.9	41.5
11	60	35	25.9	41.3	70.6	42.8
12	60	37.5	25.9	42.2	70.7	43.9
13	60	40	25.9	42.9	70.9	44.9
14	60	45	25.9	44.1	70.7	46.3
15	60	50	25.9	45.1	72.3	47.9
16	60	55	25.9	45.9	71.4	48.7
17	60	60	25.9	46.8	72.1	50.3
18	60	65	25.9	48	72.9	51.8
19	60	70	25.9	49	72.3	52.6
20	60	75	25.9	50	71.9	53.4
21	60	80	25.9	50.8	73.3	54.7
22	60	85	25.9	51.6	72.1	55.1
23	60	90	25.9	52.3	73	56.4
24	60	95	25.9	53.2	73.6	57.7
25	60	100	25.9	53.6	72.3	57.8

Table B.6 Observation table (Tube 10X12, Cone angle *0^{O}*)

Tube size : 10X12 Cone angle – 0^{O}			T1=Cold Water In T3=Hot Water in		T2=Cold Water Out T4=Hot Water out	
Sr. No	Flow Rate (*lph*)		Temperature (^{O}C)			
	Cold	HOT	T1	T2	T3	T4
1	60	10	25.4	34.7	65.9	29.9
2	60	12.5	25.4	35.5	66.3	30.9
3	60	15	25.4	36.7	67.9	31.8
4	60	17.5	25.4	37.6	68.4	32.9
5	60	20	25.4	39	69	34.4
6	60	22.5	25.4	39.8	69.1	35.5
7	60	25	25.4	40.6	69.5	36.8
8	60	27.5	25.4	42	70.1	38.1
9	60	30	25.4	42.4	69.9	38.5
10	60	32.5	25.4	42.9	69.6	39.4
11	60	35	25.4	43.9	71	41.1
12	60	37.5	25.4	45.1	71.2	42.7
13	60	40	25.4	46.3	71.7	43.4
14	60	45	25.4	46.8	71.4	45
15	60	50	25.4	47.5	70.7	46.2
16	60	55	25.4	48.4	70.6	47.7
17	60	60	25.4	50.1	71.9	49.6
18	60	65	25.4	51.1	71	50.6
19	60	70	25.4	52.5	71.7	51.4
20	60	75	25.4	52.9	71.9	52.5
21	60	80	25.4	53.9	72.3	53.7
22	60	85	25.4	54.4	70.9	54
23	60	90	25.4	54.7	71	54.3
24	60	95	25.4	55	71.1	55.1
25	60	100	25.4	55.3	70.6	55.5

Table B.7. Observation table for (Tube size 10X12, Cone angle *44* ^{O})

Tube size : 10X12 Cone angle: 45^{0}			T1=Cold Water In T2=Cold Water Out T3=Hot Water in T4=Hot Water out			
	Flow Rate (*lph*)		Temperature (^{O}C)			
Sr. No	Cold	HOT	T1	T2	T3	T4
1	60	10	26.2	34.2	66.6	30
2	60	12.5	26.2	35.4	67.7	31.1
3	60	15	26.2	36.7	68.6	32.3
4	60	17.5	26.2	38.4	69.7	34.2
5	60	20	26.2	39.5	70.3	34.9
6	60	22.5	26.2	40.7	71.3	36.3
7	60	25	26.2	41.6	71.4	37.5
8	60	27.5	26.2	42.7	72	39.2
9	60	30	26.2	43.5	72	40
10	60	32.5	26.2	44.2	72.1	41.1
11	60	35	26.2	44.7	72.3	41.9
12	60	37.5	26.2	45	71.7	42.4
13	60	40	26.2	45.8	72.4	43.5
14	60	45	26.2	46.6	72	45.4
15	60	50	26.2	47.6	72.2	46.8
16	60	55	26.2	48.4	71.8	48.3
17	60	60	26.2	49.3	71.7	49.5
18	60	65	26.2	51.4	72.9	51.5
19	60	70	26.2	52	72.1	52.3
20	60	75	26.2	53.1	72.7	53.2
21	60	80	26.2	53.5	72.7	54
22	60	85	26.2	54.2	71.8	54.8
23	60	90	26.2	55.4	72.1	55.9
24	60	95	26.2	55.7	72.4	56.2
25	60	100	26.2	56.1	72.7	57.1

Table B.8 Observation table (Tube size 10X12, Cone angle *90* ^{O})

Tube size : 10X12 Cone angle 90^{0}			T1=Cold Water In T2=Cold Water Out T3=Hot Water in T4=Hot Water out			
	Flow Rate (*lph)*		Temperature (^{O}C)			
Sr. No	Cold	HOT	T1	T2	T3	T4
1	75	10	24.7	30.6	67.2	28
2	75	12.5	24.7	31.1	68.6	29.2
3	75	15	24.7	32.1	69.7	30.3
4	75	17.5	24.7	33.5	70.2	31.6
5	75	20	24.7	34.5	71	32.8
6	75	22.5	24.7	35.4	71.7	34
7	75	25	24.7	36.4	72.4	35.6
8	75	27.5	24.7	37.3	72.6	36.7
9	75	30	24.7	38.6	73.4	38.5
10	75	32.5	24.7	39.5	73.5	39.8
11	75	35	24.7	39.7	72.4	40.2
12	75	37.5	24.7	40.1	72.8	41.2
13	75	40	24.7	41.1	72.2	42.4
14	75	45	24.7	42	72.5	44
15	75	50	24.7	42.9	73.3	46.1
16	75	55	24.7	43.8	73	47.4
17	75	60	24.7	45.8	73.4	48.6
18	75	65	24.7	46.5	72.5	49.8
19	75	70	24.7	46.6	72.5	50.7
20	75	75	24.7	47	71.9	51.5
21	75	80	24.7	47.6	71.9	52.2
22	75	85	24.7	48.9	73.6	54.1
23	75	90	24.7	50.5	74.7	55.7
24	75	95	24.7	52	74.4	56.2
25	75	100	24.7	52.3	74.4	57.2

Table B.9. Observation table (Tube size 10X12, Cone angle *135* ^{O})

Tube size : 10X12 Cone angle 135^{O}			T1=Cold Water In T3=Hot Water in		T2=Cold Water Out T4=Hot Water out	
	Flow Rate (*lph*)		Temperature (^{O}C)			
Sr. No	Cold	HOT	T1	T2	T3	T4
1	90	10	25.6	30.2	66.2	28.6
2	90	12.5	25.6	31.2	67.9	30.2
3	90	15	25.6	32.2	69.1	31.4
4	90	17.5	25.6	33	70.3	32.4
5	90	20	25.6	34.1	70.6	33.5
6	90	22.5	25.6	34.8	70.6	34.4
7	90	25	25.6	35.4	71.4	35.9
8	90	27.5	25.6	36.4	71	36.8
9	90	30	25.6	36.9	70.6	37.9
10	90	32.5	25.6	37.3	70.4	38.6
11	90	35	25.6	38.1	71.2	39.9
12	90	37.5	25.6	39	70.6	40.4
13	90	40	25.6	39.7	71.1	42.1
14	90	45	25.6	40.2	71.3	43.2
15	90	50	25.6	41.7	72.7	45.1
16	90	55	25.6	42.5	70.5	46.1
17	90	60	25.6	42.6	70.3	47.3
18	90	65	25.6	43.3	70.2	48.6
19	90	70	25.6	44.2	71.2	49.9
20	90	75	25.6	45.5	71.4	51
21	90	80	25.6	45.7	70.9	51.5
22	90	85	25.6	46.2	71	52.7
23	90	90	25.6	46.9	71	53
24	90	95	25.6	47.4	70.8	53.4
25	90	100	25.6	47.8	70.8	53.9

Table B.10. Observation table (Tube size 10X12, Cone angle *180*^{O})

Tube size : 10X12 Cone angle: 180^{O}			T1=Cold Water In T3=Hot Water in		T2=Cold Water Out T4=Hot Water out	
	Flow Rate (*lph*)		Temperature (^{O}C)			
Sr. No	Cold	HOT	T1	T2	T3	T4
1	60	10	26.3	32.4	67.8	33
2	60	12.5	26.3	34.2	68.4	34.2
3	60	15	26.3	35.5	69.6	35.7
4	60	17.5	26.3	36.1	69.7	36.8
5	60	20	26.3	37.2	70.3	37.9
6	60	22.5	26.3	37.8	70.1	38.5
7	60	25	26.3	38	70.5	39.8
8	60	27.5	26.3	39.4	70.8	41
9	60	30	26.3	40.1	71.5	42.2
10	60	32.5	26.3	40.4	71.5	43.1
11	60	35	26.3	40.9	71.2	44.3
12	60	37.5	26.3	41.6	71.3	45.4
13	60	40	26.3	42.6	71	46.4
14	60	45	26.3	43.6	71.1	47.6
15	60	50	26.3	44.2	71	48.7
16	60	55	26.3	45.2	70.8	50.1
17	60	60	26.3	46	70.5	51.5
18	60	65	26.3	47.4	70	52.3
19	60	70	26.3	47.6	70.9	53.9
20	60	75	26.3	48.3	70.6	54.6
21	60	80	26.3	48.7	70	54.9
22	60	85	26.3	49.3	69.3	55.2
23	60	90	26.3	49.9	70.3	56.7
24	60	95	26.3	50.4	70.5	57.1
25	60	100	26.3	51	70.8	57.7

Table B.11Observation table(Tube size 12X15,Cone angle 0^O)

Tube size : 12X15 Cone angle O^O			T1=Cold Water In T3=Hot Water in	T2=Cold Water T4=Hot Water out		
Sr. No	Flow Rate (*lph*)		Temperature (^OC)			
	Cold	HOT	T1	T2	T3	T4
1	60	10	29.4	38	65.2	33.1
2	60	12.5	29.4	38.5	65.5	33.3
3	60	15	29.4	39.2	66.9	33.9
4	60	17.5	29.4	39.9	67.3	34.5
5	60	20	29.4	40.7	67.1	35.5
6	60	22.5	29.4	41.5	67.5	36.3
7	60	25	29.4	42.8	68.9	37.2
8	60	27.5	29.4	43	68.5	37.8
9	60	30	29.4	44.1	69.1	39
10	60	32.5	29.4	45.2	67.7	39.8
11	60	35	29.4	45.8	69.9	40.5
12	60	37.5	29.4	46.7	70	41.5
13	60	40	29.4	47	69.4	42.5
14	60	45	29.4	48.8	69.9	44.5
15	60	50	29.4	49.4	69.8	45.8
16	60	55	29.4	51.4	71.3	47.2
17	60	60	29.4	52	71.3	48.2
18	60	65	29.4	53.3	72.8	49.9
19	60	70	29.4	54	71.7	51.1
20	60	75	29.4	54.7	73.2	52.2
21	60	80	29.4	56.1	73.8	53.6
22	60	85	29.4	56.4	72.7	54.3
23	60	90	29.4	57.1	73.6	55.1
24	60	95	29.4	57.5	73.8	55.8
25	60	100	29.4	58.2	73.1	56.6

Table B.12 Observation table (Tube size 12X15, Cone angle 45^O)

Tube size : 12X15 Cone angle 45^O			T1=Cold Water In T3=Hot Water in	T2=Cold Water Out T4=Hot Water out		
Sr. No.	Flow Rate (*lph*)		Temperature (^OC)			
	Cold	HOT	T1	T2	T3	T4
1	60	10	27.8	36.6	64.2	31.9
2	60	12.5	27.8	37.2	65	32.5
3	60	15	27.8	38.3	66.4	33.2
4	60	17.5	27.8	39.8	67.1	34.4
5	60	20	27.8	41.4	67.3	35.4
6	60	22.5	27.8	43	67.8	37
7	60	25	27.8	44.2	67.7	37.9
8	60	27.5	27.8	45.3	68.3	39.1
9	60	30	27.8	46.2	68.4	40.2
10	60	32.5	27.8	47.3	68.4	41.4
11	60	35	27.8	48.3	69.6	42.5
12	60	37.5	27.8	48.9	69.7	43.2
13	60	40	27.8	49.7	69.9	44.6
14	60	45	27.8	50.8	70.6	46
15	60	50	27.8	52.3	71	47.7
16	60	55	27.8	53.3	70.1	48.8
17	60	60	27.8	53.8	70.2	50.1
18	60	65	27.8	54.9	70.3	51.6
19	60	70	27.8	55.8	70	52.8
20	60	75	27.8	56.5	71.4	54
21	60	80	27.8	58.4	72.4	56
22	60	85	27.8	59	71.7	56.5
23	60	90	27.8	59.6	72.9	57.6
24	60	95	27.8	59.9	72.5	57.8
25	60	100	27.8	60.2	72.9	58

Table B.13 Observation table (Tube size 12X15, Cone angle *90°*)

Tube size : 12X15 Cone angle 90^0			T1=Cold Water In T3=Hot Water in		T2=Cold Water Out T4=Hot Water out	
Sr. No.	Flow Rate *lph*		Temperature (°*C*)			
	Cold	HOT	T1	T2	T3	T4
1	45	10.0	29.8	39.2	65.1	34.6
2	45	12.5	29.8	39.7	65.5	35.3
3	45	15.0	29.8	40.5	66.2	36.1
4	45	17.5	29.8	41.3	67	36.8
5	45	20.0	29.8	42.6	67.2	38.2
6	45	22.5	29.8	44.1	67.5	39.5
7	45	25.0	29.8	45.2	68.1	40.5
8	45	27.5	29.8	46.5	68.3	41.6
9	45	30.0	29.8	47.7	68.1	42.7
10	45	32.5	29.8	48.7	68.2	43.8
11	45	35.0	29.8	49.8	68.6	45.0
12	45	37.5	29.8	51.0	69.3	45.8
13	45	40.0	29.8	52.0	69.4	47.0
14	45	45.0	29.8	53.0	69.6	48.5
15	45	50.0	29.8	54.2	70.0	50.0
16	45	55	29.8	55.2	70.1	51.2
17	45	60	29.8	56.2	69.8	52.2
18	45	65	29.8	57.2	70.9	54.0
19	45	70	29.8	58.1	71.3	55.2
20	45	75	29.8	59.0	71.2	56.2
21	45	80	29.8	59.7	70.5	57.0
22	45	85	29.8	60.6	70.4	58.0
23	45	90	29.8	61.0	71.4	59.0
24	45	95	29.8	61.6	71.1	59.4
25	45	100	29.8	61.9	71.2	59.8

Table B.14 Observation table (Tube size: 12X15, Cone angle *135°)*

Tube size : 12X15 Cone angle 135^0			T1=Cold Water In T3=Hot Water in		T2=Cold Water Out T4=Hot Water out	
Sr. No	Flow Rate (*lph)*		Temperature (°*C*)			
	Cold	HOTH	T1	T2	T3	T4
1	45	10	28.8	39.7	66.2	35
2	45	12.5	28.8	40.2	66.7	35.8
3	45	15	28.8	40.5	67.3	36.6
4	45	17.5	28.8	41.1	68	37.6
5	45	20	28.8	42	68.2	38.9
6	45	22.5	28.8	43.4	68.7	40
7	45	25	28.8	44.9	68.2	41.3
8	45	27.5	28.8	46	68.9	42.3
9	45	30	28.8	47.2	68.9	43.7
10	45	32.5	28.8	48.4	69	44.9
11	45	35	28.8	49.7	69.4	46
12	45	37.5	28.8	50.5	70.4	47.2
13	45	40	28.8	52.4	70.5	48.4
14	45	45	28.8	52.5	70.5	49.8
15	45	50	28.8	54	70.3	51.4
16	45	55	28.8	54.7	71.4	52.8
17	45	60	28.8	55.8	71.3	54.4
18	45	65	28.8	57.2	71.5	55.8
19	45	70	28.8	58.3	71.3	57.1
20	45	75	28.8	59.3	71.4	58
21	45	80	28.8	60.5	73	59.9
22	45	85	28.8	61.1	71.7	60.2
23	45	90	28.8	61.7	72	60.6
24	45	95	28.8	62.2	72.1	61
25	45	100	28.8	62.8	72.7	61.5

Table B.15. Observation table (Tube size: 12X15, Cone angle *180^{O}*)

Tube size : 12X15 Cone angle 180^{O}			T1=Cold Water In T3=Hot Water in		T2=Cold Water Out T4=Hot Water out	
Sr. No	Flow Rate (*lph*)		Temperature (^{O}C)			
	Cold	HOT	T1	T2	T3	T4
1	75	10	29.3	32.8	66	32.4
2	75	12.5	29.3	33.2	65.4	33.8
3	75	15	29.3	34.3	66.1	34.7
4	75	17.5	29.3	34.9	66.8	35.6
5	75	20	29.3	35.8	67.4	36.6
6	75	22.5	29.3	36.6	67.9	37.7
7	75	25	29.3	37.4	68.2	38.8
8	75	27.5	29.3	38.7	69.1	39.7
9	75	30	29.3	39.3	69.3	40.6
10	75	32.5	29.3	40.4	69.5	41.7
11	75	35	29.3	41.3	69.6	42.6
12	75	37.5	29.3	41.8	69.8	43.1
13	75	40	29.3	42.5	69.8	43.6
14	75	45	29.3	43.4	69.7	44.5
15	75	50	29.3	44.6	69.9	45.8
16	75	55	29.3	45.4	69.8	46.8
17	75	60	29.3	46.7	69.5	48.1
18	75	65	29.3	47.9	69.8	49.5
19	75	70	29.3	49	69.9	50.7
20	75	75	29.3	50.4	69.7	52
21	75	80	29.3	51.4	69.9	54.3
22	75	85	29.3	52.4	69.8	55.4
23	75	90	29.3	53.3	69.4	56.3
24	75	95	29.3	54.5	69.6	57.5
25	75	100	29.3	55.2	69.7	58.4